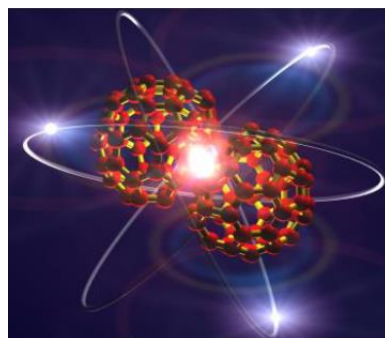


**The Sixth International Conference**  
***"Dynamics of Systems on the Nanoscale"***  
**and**  
**The Tenth International Symposium**  
***"Atomic Cluster Collisions"***



**DySoN-ISACC 2021**

**Regina Elena Hotel**  
**Santa Margherita Ligure, Italy**  
**October 18-22, 2021**



**Book of Abstracts**



# Table of Contents

<b>Preface</b>	<b>4</b>
<b>Conference Venue</b>	<b>6</b>
<b>Conference Reception</b>	<b>6</b>
<b>Conference Dinner</b>	<b>6</b>
<b>Topical Issue of EPJD</b>	<b>6</b>
<b>DySoN-ISACC International Advisory Committee</b>	<b>6</b>
<b>Organizing Committee</b>	<b>7</b>
<b>Contact Information</b>	<b>7</b>
<b>Conference Program</b>	<b>8</b>
<b>Overview of Abstracts</b>	<b>12</b>
<b>List of Participants</b>	<b>78</b>

## Preface

The sixth International Conference “[Dynamics of Systems on the Nanoscale](#)” (DySoN) and the tenth International Symposium “[Atomic Cluster Collisions](#)” (ISACC) are organized jointly under the title “**DySoN-ISACC 2021 Conference**”.

The DySoN-ISACC 2021 Conference will take place on **October 18-22, 2021** in Best Western Hotel Regina Elena (Santa Margherita Ligure, Italy). The conference is co-organized by the [University of Ferrara](#) (Ferrara, Italy), [University of Kent](#) (Canterbury, United Kingdom) and [MBN Research Center](#) (Frankfurt am Main, Germany).

A series of International Symposia “Atomic Cluster Collisions: structure and dynamics from the nuclear to the biological scale” started in 2003, and nine ISACC conferences have been held so far. The ISACC series promotes the growth and exchange of scientific information on the structure, properties and dynamics of complex nuclear, atomic, molecular, cluster, nanoscopic and biological systems studied primarily by means of photonic, electronic and atomic collisions. Most ISACC conferences were satellites of the International Conferences on Photonic Electronic and Atomic Collisions (ICPEAC). In light of the Covid-19 pandemic the XXXIII ICPEAC Conference has been postponed to 2023. Despite this, the ISACC International Advisory Committee decided to organize the Tenth ISACC Symposium in 2021 as a joint meeting with the DySoN 2021 conference.

The “Dynamics of Systems on the Nanoscale” conference has been built upon the ISACC series reflecting a need for an interdisciplinary conference covering a broader range of topics than just atomic cluster collisions, related to the Dynamics of Systems on the Nanoscale. The DySoN conference series was launched in 2010 and five DySoN conferences have been held so far.

The DySoN conferences promote the growth and exchange of interdisciplinary scientific information on the structure formation and dynamics of animate and inanimate matter on the nanometer scale. There are many examples of complex many-body systems of micro- and nanometer scale size exhibiting unique features, properties and functions. These systems may have very different nature and origin, e.g. atomic and molecular clusters, nanostructures, ensembles of nanoparticles, nanomaterials, biomolecules, biomolecular and mesoscopic systems. A detailed understanding of the structure and dynamics of these systems on the nanoscale is a difficult and fundamental task, the solution of which is necessary in nano- and biotechnologies, materials science and medicine.

Although mesoscopic, nano- and biomolecular systems differ in their nature and origin, a number of fundamental problems are common to all of them: What are the underlying principles of self-organization and self-assembly of matter at the micro- and nanoscale? Are these principles classical or quantum? How does function emerge at the nano- and mesoscale in systems of different origin? What criteria govern the stability of these systems? How do their properties change as a function of size and composition? How are their properties altered by their environment? Seeking answers to these questions is at the core of a new interdisciplinary field that lies at the intersection of physics, chemistry and biology, a field entitled Meso-Bio-Nano (MBN) Science.

The joint DySoN-ISACC 2021 Conference will cover experimental, theoretical and applied aspects of all the aforementioned topics. Particular attention will be devoted to dynamical phenomena and many-body effects taking place in various MBN systems on the nanoscale, which include problems of structure formation, fusion and fission, collision and fragmentation, surfaces and interfaces, collective electron excitations, reactivity, nanoscale phase and morphological transitions, irradiation-driven transformations of complex molecular systems, irradiation-induced biodamage, channeling phenomena, construction of novel light sources, and many more. The utilization of advanced computational techniques and high-performance computing for studying the aforementioned phenomena and effects will also be discussed. Links of the DySoN and ISACC topics to novel and emerging technologies will be an important focus of the DySoN-ISACC 2021 Conference.

Finally, DySoN-ISACC 2021 will provide a platform to host discussions about current research, technological challenges and related initiatives within the Topical Areas of DySoN and ISACC Conference Series. The hope is that all participants will be enriched and further motivated by the session topics and the ensuing general discussions. Have a memorable Meeting!

***Topical Areas of DySoN and ISACC:***

- Structure and dynamics of molecules, clusters and nanoparticles
- Cluster and biomolecular ensembles, composite systems
- Clustering, self-organization, phase and morphological transitions on the nanoscale
- Clustering in systems of various degrees of complexity
- Nanostructured materials, surfaces and interfaces
- Cluster structure and dynamics on a surface
- Reactivity and nanocatalysis
- Electron and spin transport in molecular systems
- Collision and radiation processes, fusion, fission, fragmentation
- Electron-, photon- and ion-cluster collisions
- Collision processes with biomolecules
- Radiation-induced chemistry
- Irradiation-driven transformations, damage and fabrication of MesoBioNano systems
- Propagation of particles through media
- Clusters and biomolecules in external fields: electric, magnetic, laser etc.
- Cluster and biomolecular research with Free Electron Lasers
- Biomedical and technological applications of radiation
- Related technologies: novel light sources, controlled nanofabrication, functionalized materials

## Conference Venue

The Conference will be hosted by Best Western Hotel Regina Elena (Santa Margherita Ligure, Italy). The hotel is located on the seafront that connects Santa Margherita Ligure to Portofino, among the Regional Natural Park and the Tigullio Gulf and the Marine Protected Area of Portofino.

Santa Margherita Ligure is a municipality in the Italian region Liguria, located about 35 kilometers southeast of Genoa, in the area traditionally known as Tigullio. The town is known for Castello di Santa Margherita Ligure, built by the Republic of Genoa in 1550 as a defense against the increasing attacks of North African pirates, as well as for Villa Durazzo - a complex that includes two patrician villas, a 16<sup>th</sup>-century castle and a 17<sup>th</sup>-century park.

## Conference Reception

The conference reception will take place on Monday, October 18, from 19<sup>00</sup> to 22<sup>00</sup> and will be located at the Best Western Hotel Regina Elena.

## Conference Dinner

The conference dinner will take place on Wednesday, October 20, from 19<sup>00</sup> to 22<sup>30</sup>.

On Thursday, October 21, the conference participants will have a possibility to take a walk through Santa Margherita Ligure from 14<sup>30</sup> to 16<sup>00</sup>.

## Topical Issue of EPJD

A Topical Issue “**Dynamics of Systems on the Nanoscale (2021)**” will be launched in the **European Physical Journal D: Atomic, Molecular, Optical and Plasma Physics**, <https://epjd.epj.org/>. The main scope of this topical issue will be to present recent advances and perspectives in this highly interdisciplinary field of modern research. It will include regular articles, reviews and colloquium papers.

**This Topical Issue will be opened to the entire research community** working in the DySoN and ISACC topical areas and will not be restricted to the participants of the DySoN-ISACC 2021 Conference. All conference participants are encouraged to submit their novel results to this Topical Issue.

The deadline for manuscript submission is **March 31, 2022**. Guest Editors are Prof. Vincenzo Guidi, Prof. Nigel Mason, Dr. Alexey Verkhovtsev and Prof. Andrey Solov'yov.

## DySoN-ISACC International Advisory Committee

- Andrey V. Solov'yov (MBN Research Center, Frankfurt am Main, Germany) - **IAC Chair**
- Ilko Bald (University of Potsdam, Germany)
- Catherine Bréchnac (Laboratoire Aime Cotton, CNRS, Orsay, France)
- Michel Broyer (University of Lyon, France)
- Jean-Patrick Connerade (Imperial College London, London, UK)
- Franco Gianturco (The University of Innsbruck, Austria)
- Vincenzo Guidi (University of Ferrara, Italy)
- Bernd Huber (Centre Interdisciplinaire de Recherche Ions Lasers, CIRIL - GANIL, Caen, France)
- Julius Jellinek (Argonne National Laboratory, Argonne, Illinois, USA)
- Shiv Khanna (Virginia Commonwealth University, Richmond, USA)
- Nigel Mason (University of Kent, Canterbury, UK)
- Thomas Möller (Institut für Optik und Atomare Physik, TU Berlin, Germany)
- Jefferson Shinpaugh (East Carolina University, Greenville, USA)
- Iliia Solov'yov (Carl von Ossietzky University, Oldenburg, Germany)
- Eric Suraud (Université Paul Sabatier, Toulouse, France)
- Eugene Surdutovich (Oakland University, Rochester, Michigan, USA)

## Organizing Committee

- Vincenzo Guidi (University of Ferrara, Italy) - **Co-Chair**
- Nigel Mason (University of Kent, United Kingdom) - **Co-Chair**
- Andrey Solov'yov (MBN Research Center, Germany) - **Co-Chair**
- Andrei Korol (MBN Research Center, Germany)
- Ilia Solov'yov (Carl von Ossietzky University of Oldenburg, Germany)
- Irina Solovyeva (MBN Research Center, Germany)
- Alexey Verkhovtsev (MBN Research Center, Germany)

## Sponsors

The DySoN-ISACC 2021 conference is held under the auspices of the following sponsors:

- MBN Research Center gGmbH, Frankfurt am Main, Germany
- University of Ferrara, Ferrara, Italy
- University of Kent, Canterbury, United Kingdom
- Sir John and Lady Mason Academic Trust
- Virtual Institute of NanoFilms
- Springer Verlag
- H2020-MSCA-RISE project "N-Light"
- H2020-MSCA-RISE project "RADON"

## Contact Information

### **Professor Vincenzo Guidi**

DySoN-ISACC 2021 Co-Chair

Dept. of Physics and Earth Sciences,  
University of Ferrara  
Via Saragat 1  
44122 Ferrara, Italy  
Phone: +39 0532 974284  
E-mail: [vincenzo.guidi@unife.it](mailto:vincenzo.guidi@unife.it)  
Website:  
[docente.unife.it/vincenzo.guidi-en](http://docente.unife.it/vincenzo.guidi-en)

### **Professor Nigel J. Mason, OBE**

DySoN-ISACC 2021 Co-Chair

School of Physical Sciences  
University of Kent  
Canterbury, CT2 7NH  
United Kingdom  
Phone: +44 (0)1227 823321  
E-mail: [N.J.Mason@kent.ac.uk](mailto:N.J.Mason@kent.ac.uk)  
Website:  
[kent.ac.uk/physical-sciences](http://kent.ac.uk/physical-sciences)

### **Prof. Dr. Andrey V. Solov'yov**

DySoN-ISACC 2021 Co-Chair

MBN Research Center gGmbH  
Altenhöferallee 3  
60438 Frankfurt am Main,  
Germany  
Phone: +49 (0)69 34875600  
E-mail: [solovyov@mbnresearch.com](mailto:solovyov@mbnresearch.com)  
Website:  
[www.mbnresearch.com](http://www.mbnresearch.com)

## DySoN-ISACC Conference Web Page

Updated information on the DySoN-ISACC 2021 conference is available at [www.dyson-conference.org](http://www.dyson-conference.org).  
General information on the DySoN conference series can also be found there.

Relevant information on the ISACC series is available at [www.isacc-portal.org](http://www.isacc-portal.org).

## Conference Program

### Monday, October 18 (DySoN-related sessions)

10 <sup>00</sup> – 14 <sup>00</sup>	Participants registration
14 <sup>00</sup> – 14 <sup>15</sup>	<b>DySoN-ISACC 2021 Opening</b> <b>Vincenzo Guidi, Nigel J. Mason and Andrey V. Solov'yov</b>
14 <sup>15</sup> – 15 <sup>45</sup>	<b><u>Afternoon session I: Dynamics of systems on the nanoscale</u></b> <b>Andrey Solov'yov</b> , MBN Research Center, Frankfurt am Main, Germany <i>Advances and challenges in computational multiscale modelling of MesoBioNano systems</i> <b>Eleanor Campbell</b> , University of Edinburgh, Edinburgh, Scotland <i>Shake, rattle and roll: STM studies of Fullerenes</i> <b>Beata Ziaja-Motyka</b> , Center for Free-Electron Laser Science, DESY, Hamburg, Germany <i>Transitions in matter induced by intense X-ray radiation and their diagnostics</i>
15 <sup>45</sup> – 16 <sup>15</sup>	Coffee break
16 <sup>15</sup> – 17 <sup>45</sup>	<b><u>Afternoon session II: Structure and dynamics of molecules, clusters and nanoparticles</u></b> <b>Riccardo Ferrando</b> , University of Genoa, Italy <i>Symmetry breaking and symmetry recovery in the growth of metal nanoparticles</i> <b>Rodolphe Antoine</b> , Institut Lumière Matière, Université Claude Bernard Lyon1, France <i>Tailoring the optical properties of gold catenane nanoclusters. Surface ligand, silver doping, and self-assembly</i> <b>Stefan Bromley</b> , University of Barcelona, Spain <i>Understanding cosmic nanodust using molecular dynamics</i>
19 <sup>00</sup> – 22 <sup>00</sup>	Welcome reception

### Tuesday, October 19 (DySoN-related sessions)

9 <sup>30</sup> – 11 <sup>00</sup>	<b><u>Morning session I: Cluster and biomolecular ensembles, composite systems</u></b> <b>Ilko Bald</b> , University of Potsdam, Potsdam, Germany <i>Novel nanoarchitectures for the monitoring of single molecules and plasmon induced chemical reactions by surface-enhanced Raman scattering (SERS)</i> <b>Michael Mertig</b> , Kurt-Schwabe-Institut für Mess- und Sensortechnik Meinsberg e.V. and Technische Universität Dresden, Germany <i>Putting DNA origami-based nanostructures in stable motion</i> <b>Ilia Solov'yov</b> , Carl von Ossietzky University of Oldenburg, Oldenburg, Germany <i>Structure and dynamics of cryptochrome photoreceptors</i>
11 <sup>00</sup> – 11 <sup>30</sup>	Coffee break
11 <sup>30</sup> – 13 <sup>00</sup>	<b><u>Morning session II: Irradiation-driven processes and technologies involving Meso-Bio-Nano systems</u></b> <b>Nigel Mason / Perry Hailey</b> , University of Kent, Canterbury, United Kingdom <i>Irradiation-driven transformations of ice deposits under astrochemical conditions</i> <b>Marco Beleggia</b> , Technical University of Denmark, Lyngby, Denmark <i>Organic ice resist lithography</i>



	<b>Harald Plank</b> , Graz University of Technology, Graz, Austria <i>3D nanoprinting via focused electron beams: principles and applications</i>
13 <sup>00</sup> – 14 <sup>30</sup>	Lunch
14 <sup>30</sup> – 16 <sup>00</sup>	<b><u>Afternoon session I: Radiation-induced chemistry</u></b> <b>Pablo de Vera</b> , European Centre for Theoretical Studies in Nuclear Physics and Related Areas (ECT*), Trento, Italy <i>Irradiation driven molecular dynamics interfaced with Monte Carlo for detailed simulations of focused electron beam induced deposition</i> <b>Alexey Prosvetov</b> , MBN Research Center, Frankfurt am Main, Germany <i>Atomistic insights into metal nanostructure growth under focused electron beam irradiation</i> <b>Duncan Mifsud</b> , University of Kent, Canterbury, United Kingdom <i>Sulphur astrochemistry in the laboratory: techniques to understand the formation of interstellar and planetary Sulphur-bearing molecules</i>
16 <sup>00</sup> – 16 <sup>30</sup>	Coffee break
16 <sup>30</sup> – 18 <sup>00</sup>	<b><u>Afternoon session II: Structure and dynamics of molecules, clusters and nanoparticles</u></b> <b>Filipe Ferreira da Silva</b> , Universidade Nova de Lisboa, Caparica, Portugal <i>Electron interactions with HFC (R134a) refrigerant gas</i> <b>Short presentations:</b> <b>Cesare Roncaglia</b> , University of Genoa, Genoa, Italy <i>Structural transitions in metal nanoparticles: equilibrium-driven processes in Au and AuPd</i> <b>Iva Falková</b> , Institute of Biophysics of CAS, Brno, Czech Republic <i>Novel software based on artificial neural networks and deep learning for automatic analysis of ionizing radiation-induced foci (IRIFs) and advanced analysis of their micro-morphological and additional parameters</i> <b>Anders Frederiksen</b> , Carl von Ossietzky University of Oldenburg, Oldenburg, Germany <i>Structural and dynamic traits of avian cryptochromes</i> <b>Gesa Grüning</b> , Carl von Ossietzky University of Oldenburg, Oldenburg, Germany <i>The influence of dynamical degrees of freedom on spin relaxation in the European Robin cryptochrome</i>

**Wednesday, October 20 (DySoN-related sessions)**

9 <sup>30</sup> – 11 <sup>00</sup>	<b><u>Morning session I: Interaction of radiation with biomolecular systems: mechanisms and applications</u></b> <b>Simone Taioli</b> , European Centre for Theoretical Studies in Nuclear Physics and Related Areas (ECT*), Trento, Italy <i>Ab initio informed Monte Carlo simulations of biologically relevant materials excitation spectra</i> <b>Marc Benjamin Hahn</b> , Bundesanstalt für Materialforschung und -prüfung, Berlin, Germany <i>The change of DNA radiation damage upon hydration: In-situ observations by near-ambient-pressure XPS</i> <b>Thomas Schlathölter</b> , Zernike Institute for Advanced Materials, University of Groningen, The Netherlands <i>Multiple valence electron detachment following Auger decay of inner-shell vacancies in gas-phase DNA</i>
------------------------------------	--

11 <sup>00</sup> – 11 <sup>30</sup>	Coffee break
11 <sup>30</sup> – 13 <sup>00</sup>	<p><b><u>Morning session II: Interaction of radiation with bio-systems: mechanisms and applications</u></b></p> <p><b>Martin Falk</b>, Institute of Biophysics of the CAS, Brno, Czech Republic <i>Repair focus micro- and nano architecture in DSB repair efficiency and pathway selection</i></p> <p><b>Alexey Verkhovtsev</b>, MBN Research Center, Frankfurt am Main, Germany <i>Lethal DNA damage caused by heavy ion-induced shock waves in cells</i></p> <p><b>Kate Ricketts</b>, University College London, United Kingdom <i>Realising the potential of particle therapy and nanoparticle enhanced radiotherapy</i></p>
13 <sup>00</sup> – 13 <sup>15</sup>	Conference photo
13 <sup>15</sup> – 14 <sup>30</sup>	Lunch
14 <sup>30</sup> – 16 <sup>00</sup>	<p><b><u>Afternoon session I: Propagation of particles through media</u></b></p> <p><b>Andrei Korol</b>, MBN Research Center, Frankfurt am Main, Germany <i>Crystal-based intensive gamma-ray light sources</i></p> <p><b>Hartmut Backe</b>, Institute of Nuclear Physics, University of Mainz, Germany <i>Considerations on channeling of charged particles in diamond, based on experiments, simulations, and the Fokker-Planck equation</i></p> <p><b>Werner Lauth</b>, Institute of Nuclear Physics, University of Mainz, Germany <i>Characterization of crystalline undulators at the Mainz Microtron MAMI</i></p>
16 <sup>00</sup> – 16 <sup>30</sup>	Coffee break
16 <sup>30</sup> – 18 <sup>00</sup>	<p><b><u>Afternoon session II: Design and practical realization of novel gamma-ray crystal-based light sources</u></b></p> <p><b>Marco Romagnoni</b>, Università degli Studi di Milano, Milan, Italy <i>Advancement of bent crystals technology in high-energy particle accelerators</i></p> <p><b>Davide De Salvador</b>, University of Padova, Italy <i>Pulsed laser melting processes for nanoscale doping and strain control</i></p> <p><b>Thu Nhi Tran Thi</b>, European Synchrotron Radiation Facility, Grenoble, France <i>Revealing single crystal quality by insight Diffraction Imaging technique</i></p>
19 <sup>00</sup> – 22 <sup>30</sup>	Conference Dinner

**Thursday, October 21 (ISACC-related sessions)**

9 <sup>30</sup> – 11 <sup>00</sup>	<p><b><u>Morning session I: Collision and radiation-induced processes</u></b></p> <p><b>Ilya Fabrikant</b>, University of Nebraska-Lincoln, Nebraska, USA <i>Positronium collisions with molecules: Free-electron-gas model</i></p> <p><b>Sadia Bari</b>, Deutsches Elektronen-Synchrotron (DESY), Hamburg, Germany <i>Soft X-ray spectroscopy of peptides and porphyrins</i></p> <p><b>Eric Suraud</b>, Université Paul Sabatier, Toulouse, France <i>Towards the analysis of attosecond dynamics in complex systems</i></p>
11 <sup>00</sup> – 11 <sup>30</sup>	Coffee break
11 <sup>30</sup> – 13 <sup>00</sup>	<p><b><u>Morning session II: Electron and photon cluster collisions</u></b></p> <p><b>Juraj Fedor</b>, J. Heyrovský Institute of Physical Chemistry, Czech Republic <i>Statistical vs. non-statistical emission of electrons from hot anions</i></p> <p><b>Himadri Chakraborty</b>, Northwest Missouri State University, Maryville, USA <i>Ultrafast relaxation of photoexcited “hot” electrons in fullerene materials</i></p>

	<b>Hassan Abdoul-Carime</b> , University of Lyon, France <i>Reaction in selected molecular films induced by low energy electrons</i>
13 <sup>00</sup> – 14 <sup>30</sup>	Lunch
14 <sup>30</sup> – 16 <sup>00</sup>	Free time / Conference walk through the town (optional)
16 <sup>00</sup> – 16 <sup>30</sup>	Coffee break
16 <sup>30</sup> – 18 <sup>00</sup>	<b><u>Afternoon session I: Cluster-molecule interactions, reactivity and nanocatalysis</u></b> <b>Vincenzo Guidi</b> , University of Ferrara, Italy <i>An operando FTIR to monitor the reaction mechanism of adsorbed molecular species in chemoresistive devices</i> <b>Andrew Wheatley</b> , University of Cambridge, United Kingdom <i>On the potential of immobilizing active species for energy and sensing applications</i> <b>Shiv Khanna</b> , Virginia Commonwealth University, Richmond, USA <i>Metal-chalcogenide superatoms for nano p- n- junction with tunable band gaps, adjustable band alignment, and light harvesting</i>

### Friday, October 22 (ISACC-related sessions)

9 <sup>30</sup> – 11 <sup>00</sup>	<b><u>Morning session I: Structure and dynamics of molecules, clusters and nanoparticles</u></b> <b>Sascha Schäfer</b> , Carl von Ossietzky University of Oldenburg, Oldenburg, Germany <i>Probing ultrafast nanoscale dynamics by femtosecond electron imaging</i> <b>Nektarios Papadogiannis</b> , Hellenic Mediterranean University, Heraklion, Greece <i>Laser-generated ultrafast and coherent X-ray sources and their application in nanoscopy</i> <b>Małgorzata Śmiałek</b> , Gdansk University of Technology, Poland <i>What happens if phenol meets toluene?</i>
11 <sup>00</sup> – 11 <sup>30</sup>	Coffee break
11 <sup>30</sup> – 13 <sup>15</sup>	<b><u>Morning session II: Structure and dynamics of nanosystems (short presentations)</u></b> <b>Jonathan Hungerland</b> , Carl von Ossietzky University of Oldenburg, Oldenburg, Germany <i>Phase transition of alanine polypeptides in water</i> <b>Maja Hanić</b> , Carl von Ossietzky University of Oldenburg, Oldenburg, Germany <i>Structural and dynamic characterization of avian cryptochrome 4</i> <b>Diana Nelli</b> , University of Genoa, Genoa, Italy <i>From kinetic trapping to equilibration in the coalescence of elemental and bimetallic nanoparticles</i> <b>Georg Manthey</b> , Carl von Ossietzky University of Oldenburg, Oldenburg, Germany <i>On structure prediction of proteins with alphafold and traditional methods</i> <b>El Yakout El Koraychy</b> , University of Genoa, Genoa, Italy <i>Microscopic formation mechanisms of multiply twinned gold nanoparticles from tetrahedral seed</i> <b>Fabian Schuhmann</b> , Carl von Ossietzky University of Oldenburg, Oldenburg, Germany <i>Computational approach for 3D reconstruction of missing protein fragments</i> <b>Siu Ying Wong</b> , Carl von Ossietzky University of Oldenburg, Oldenburg, Germany <i>Cryptochrome magnetoreception: Four tryptophans could be better than three</i>
13 <sup>15</sup> – 13 <sup>30</sup>	<b>Final Discussion and DySoN-ISACC 2021 Closing</b>

## Overview of Abstracts

<b>Mon-I-1.</b> <i>Advances and challenges in computational multiscale modelling of MesoBioNano systems</i> <b>Andrey Solov'yov</b> .....	15
<b>Mon-I-2.</b> <i>Shake, rattle and roll: STM studies of fullerenes</i> <b>Eleanor Campbell, Renald Schaub, Henry Chandler, Ewan Scougall</b> .....	17
<b>Mon-I-3.</b> <i>Transitions in matter induced by intense X-ray radiation and their diagnostics</i> <b>Beata Ziaja-Motyka</b> .....	18
<b>Mon-II-1.</b> <i>Symmetry breaking and symmetry recovery in the growth of metal nanoparticles</i> <b>Riccardo Ferrando</b> .....	19
<b>Mon-II-2.</b> <i>Tailoring the optical properties of gold catenane nanoclusters. Surface ligand, silver doping, and self-assembly</i> <b>Rodolphe Antoine</b> .....	20
<b>Mon-II-3.</b> <i>Understanding cosmic nanodust using molecular dynamics</i> <b>Stefan Bromley</b> .....	21
<b>Tue-I-1.</b> <i>Novel nanoarchitectures for the monitoring of single molecules and plasmon induced chemical reactions by surface-enhanced Raman scattering (SERS)</i> <b>Ilko Bald, Kosti Tapio, Sergio Kogikoski Jr., Anushree Dutta, Amr Mostafa, Yuya Kanehira</b> ..	22
<b>Tue-I-2.</b> <i>Putting DNA origami-based nanostructures in stable motion</i> <b>Michael Mertig, Felix Kroener, Lukas Traxler, Andreas Heerwig, Alfred Kick, Julia Lenhart, Thomas Welte, Wolfgang Kaiser, Ulrich Rant</b> .....	23
<b>Tue-I-3.</b> <i>Structure and dynamics of cryptochrome photoreceptors</i> <b>Ilia Solov'yov</b> .....	24
<b>Tue-II-1.</b> <i>Irradiation-driven transformations of ice deposits under astrochemical conditions</i> <b>Nigel Mason, Perry Hailey, Duncan Mifsud</b> .....	25
<b>Tue-II-2.</b> <i>Organic ice resist lithography</i> <b>Marco Beleggia</b> .....	26
<b>Tue-II-3.</b> <i>3D nanoprinting via focused electron beams: principles and applications</i> <b>Harald Plank</b> .....	27
<b>Tue-III-1.</b> <i>Irradiation driven molecular dynamics interfaced with Monte Carlo for detailed simulations of focused electron beam induced deposition</i> <b>Pablo de Vera, Martina Azzolini, Gennady Sushko, Isabel Abril, Rafael Garcia-Molina, Maurizio Dapor, Ilia Solov'yov, Andrey Solov'yov</b> .....	29
<b>Tue-III-2.</b> <i>Atomistic insights into the metal nanostructure growth under focused electron beam irradiation</i> <b>Alexey Prosvetov, Alexey Verkhovtsev, Gennady Sushko, Andrey Solov'yov</b> .....	30
<b>Tue-III-3.</b> <i>Sulphur astrochemistry in the laboratory: techniques to understand the formation of interstellar and planetary Sulphur-bearing molecules</i> <b>Duncan Mifsud, Zuzana Kaňuchová, Péter Herczku, Zoltán Juhász, Sándor Kovács, Béla Sulik, Sergio Ioppolo, Robert McCullough, Béla Paripás, Nigel Mason</b> .....	31
<b>Tue-IV-1.</b> <i>Electron interactions with HFC (R134a) refrigerant gas</i> <b>Filipe Ferreira da Silva, J. Pereria-da-Silva, M. Mendes, J. M. M. Araújo, L. M. Cornetta</b> .....	33
<b>Tue-IV-2.</b> <i>Structural transitions in metal nanoparticles: equilibrium-driven processes in Au and AuPd</i> <b>Cesare Roncaglia, Diana Nelli, El Yakout El Koraychy, Chloé Minnai, Riccardo Ferrando</b> .....	34

<b>Tue-IV-3.</b> <i>Novel software based on artificial neural networks and deep learning for automatic analysis of ionizing radiation-induced foci (IRIFs) and advanced analysis of their micro-morphological and additional parameters</i>	
<b>Tomáš Vičar, Martin Falk, Iva Falková, Jaromír Gumulec, Radim Kolář, Olga Kopečná, Eva Pagáčová</b> .....	35
<b>Tue-IV-4.</b> <i>Structural and dynamic traits of avian cryptochromes</i>	
<b>Anders Frederiksen, Maja Hanić, Iliia Solov'yov</b> .....	37
<b>Tue-IV-5.</b> <i>The influence of dynamical degrees of freedom on spin relaxation in the European Robin cryptochrome</i>	
<b>Gesa Grüning, Iliia Solov'yov</b> .....	38
<b>Wed-I-1.</b> <i>Ab initio informed Monte Carlo simulations of biologically relevant materials excitation spectra</i>	
<b>Simone Taioli, Paolo Trevisanutto, Pablo de Vera, Stefano Simonucci, Isabel Abril, Rafael Garcia-Molina, Maurizio Dapor</b> .....	39
<b>Wed-I-2.</b> <i>The change of DNA radiation damage upon hydration: In-situ observations by near-ambient-pressure XPS</i>	
<b>Marc Benjamin Hahn, Paul Dietrich, Jörg Radnik</b> .....	40
<b>Wed-I-3.</b> <i>Multiple valence electron detachment following Auger decay of inner-shell vacancies in gas-phase DNA</i>	
<b>Thomas Schlathölder</b> .....	41
<b>Wed-II-1.</b> <i>Repair focus micro- and nano architecture in DSB repair efficiency and pathway selection</i>	
<b>Elham Persimehr, Lucie Dobesova, Jiri Toufar, Elizaveta Bobkova, Hannes Hahn, Charlotte Neitzel, Ruth Winter, Götz Pilarczyk, Georg Hildenbrand, Olga Kopečna, Eva Pagacova, Iva Falkova, Alena Bacikova, Tatiana Bulanova-Chramko, Mariia Zadneprianetc, Elena Kulikova, Alla Boreyko, Evgeny Krasavin, Dieter Heermann, Harry Scherthan, Martin Falk, Michael Hausmann</b> .....	42
<b>Wed-II-2.</b> <i>Lethal DNA damage caused by heavy ion-induced shock waves in cells</i>	
<b>Alexey Verkhovtsev, Ida Friis, Iliia Solov'yov, Andrey Solov'yov</b> .....	44
<b>Wed-II-3.</b> <i>Realising the potential of particle therapy and nanoparticle enhanced radiotherapy</i>	
<b>Kate Ricketts, Gary Royle</b> .....	45
<b>Wed-III-1.</b> <i>Crystal-based intensive gamma-ray light sources</i>	
<b>Andrei Korol, Andrey Solov'yov</b> .....	46
<b>Wed-III-2.</b> <i>Considerations on channeling of charged particles in diamond, based on experiments, simulations, and the Fokker-Planck equation</i>	
<b>Hartmut Backe</b> .....	47
<b>Wed-III-3.</b> <i>Characterization of crystalline undulators at the Mainz Microtron MAMI</i>	
<b>Werner Lauth, Hartmut Backe</b> .....	49
<b>Wed-IV-1.</b> <i>Advancement of bent crystals technology in high-energy particle accelerators</i>	
<b>Marco Romagnoni, A. Mazzolari, L. Bandiera, A. Sytov, M. Soldani, M. Tamisari, V. Guidi</b> .	50
<b>Wed-IV-2.</b> <i>Pulsed laser melting processes for nanoscale doping and strain control</i>	
<b>Davide De Salvador, E. Napolitani, C. Carraro, F. Sgarbossa, E. Di Russo, G. Maggioni, S.M. Carturan, W. Raniero, S. Bertoldo, D.R. Napoli</b> .....	51
<b>Wed-IV-3.</b> <i>Revealing single crystal quality by insight Diffraction Imaging technique</i>	
<b>Thu Nhi Tran Thi</b> .....	52
<b>Thu-I-1.</b> <i>Positronium collisions with molecules: Free-electron-gas model</i>	
<b>I.I. Fabrikant, R.S. Wilde</b> .....	53

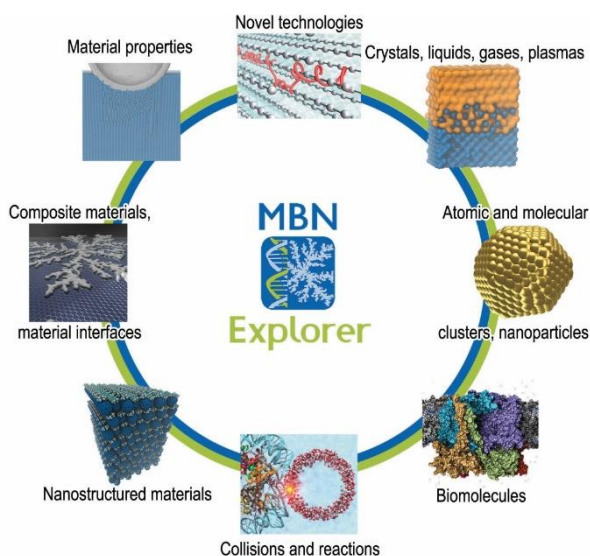
<b>Thu-I-2. <i>Soft X-ray spectroscopy of peptides and porphyrins</i></b> <b>Lucas Schwob, Kaja Schubert, Simon Dörner, Amir Kotobi, <u>Sadia Bari</u></b> .....	54
<b>Thu-I-3. <i>Towards the analysis of attosecond dynamics in complex systems</i></b> <b>P.-G. Reinhard, <u>E. Suraud</u></b> .....	55
<b>Thu-II-1. <i>Statistical vs. non-statistical emission of electrons from hot anions</i></b> <b><u>Juraj Fedor</u></b> .....	56
<b>Thu-II-2. <i>Ultrafast relaxation of photoexcited “hot” electrons in fullerene materials</i></b> <b><u>Himadri Chakraborty</u>, Mohamed Madjet, Esam Ali, Ruma De</b> .....	57
<b>Thu-II-3. <i>Reaction in selected molecular films induced by low energy electrons</i></b> <b><u>Hassan Abdoul-Carime</u></b> .....	58
<b>Thu-III-1. <i>An operando FTIR to monitor the reaction mechanism of adsorbed molecular species in chemoresistive devices</i></b> <b><u>Vincenzo Guidi</u>, Matteo Valt, Michele Della Ciana, Barbara Fabbri, Andrea Gaiardo, Elena Spagnoli</b> .....	59
<b>Thu-III-2. <i>On the potential of immobilizing active species for energy and sensing applications</i></b> <b><u>A.E.H. Wheatley</u>, K.J. Jenkinson, A. Wagner, N. Kornienko, E. Reisner</b> .....	61
<b>Thu-III-3. <i>Metal-chalcogenide superatoms for nano p- n- junction with tunable band gaps, adjustable band alignment, and light harvesting</i></b> <b><u>S.N. Khanna</u>, D. Bista, A.C. Reber, T. Sengupta</b> .....	63
<b>Fri-I-1. <i>Probing ultrafast nanoscale dynamics by femtosecond electron imaging</i></b> <b><u>Sascha Schäfer</u></b> .....	64
<b>Fri-I-2. <i>Laser-generated ultrafast and coherent X-ray sources and their application in nanoscopy</i></b> <b><u>N.A. Papadogiannis</u>, S. Petrakis, A. Grigoriadis, G. Andrianaki, I. Tazes, A. Skoulakis, Y. Orphanos, M. Bakarezos, V. Dimitriou, E.P. Benis, M. Tatarakis.</b> .....	65
<b>Fri-I-3. <i>What happens if phenol meets toluene?</i></b> <b><u>Małgorzata Śmiałek</u></b> .....	67
<b>Fri-II-1. <i>Phase transition of alanine polypeptides in water</i></b> <b><u>Jonathan Hungerland</u>, Iliia Solov'yov</b> .....	69
<b>Fri-II-2. <i>Structural and dynamic characterization of avian cryptochrome 4</i></b> <b><u>Maja Hanić</u>, Anders Frederiksen, Fabian Schuhmann, Corinna Langebrake, Miriam Liedvogel, Jingjing Xu, Henrik Mouritsen, Iliia Solov'yov</b> .....	70
<b>Fri-II-3. <i>From kinetic trapping to equilibration in the coalescence of elemental and bimetallic nanoparticles</i></b> <b><u>Diana Nelli</u>, Giulia Rossi, Zhiwei Wang, Richard Palmer, Manuella Cerbelaud, Chloé Minnai, Riccardo Ferrando</b> .....	72
<b>Fri-II-4. <i>On structure prediction of proteins with alphafold and traditional methods</i></b> <b><u>Georg Manthey</u>, Iliia Solov'yov</b> .....	73
<b>Fri-II-5. <i>Microscopic formation mechanisms of multiply twinned gold nanoparticles from tetrahedral seed</i></b> <b><u>E. El Koraychy</u>, Cesare Roncaglia, Diana Nelli, Manuella Cerbelaud, Riccardo Ferrando</b> .....	74
<b>Fri-II-6. <i>Computational approach for 3D reconstruction of missing protein fragments</i></b> <b><u>Fabian Schuhmann</u>, Iliia Solov'yov</b> .....	75
<b>Fri-II-7. <i>Cryptochrome magnetoreception: Four tryptophans could be better than three</i></b> <b><u>Siu Ying Wong</u>, Yujing Wei, Henrik Mouritsen, Iliia Solov'yov, P.J. Hore</b> .....	77

## Advances and challenges in computational multiscale modelling of MesoBioNano systems

Andrey V. Solov'yov

MBN Research Center, Altenhöferallee 3, 60438 Frankfurt am Main, Germany  
E-mail: solovyov@mbnresearch.com

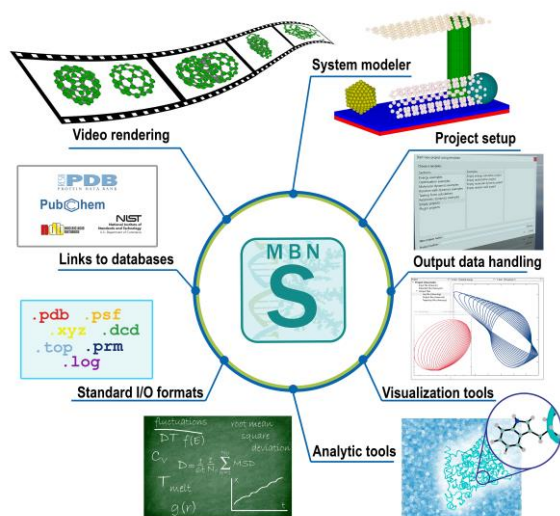
MBN (MesoBioNano) Explorer is a multi-purpose software package developed for advanced multiscale simulations of complex molecular structure and dynamics [1]. It has many unique features and a wide range of applications in Physics, Chemistry, Biology, Material Science, and related industries. A broad variety of



algorithms and interatomic potentials implemented in the program, its parallelization and computational efficiency allow simulations of the structure and dynamics of very different molecular systems with sizes ranging from atomic to mesoscopic [2]. **Fig. 1** illustrates several fields of application of MBN Explorer. The further information about the software package can be found on website: [www.mbnresearch.com/](http://www.mbnresearch.com/), and in the supplementary materials [3].

Most of the existing codes on Molecular Dynamics (MD) are applicable to a particular class of molecular systems and thus have certain unsurmountable limitations. MBN Explorer overcomes such limitations. The main features of the MBN Explorer such as universality, tuneable force fields, unique algorithmic implementations, multiscale modelling methodologies, modular design and computational efficiency are documented in detail in [1-3].

**Figure 1:** Different application areas of MBN Explorer. Adopted from [2]



MBN Explorer is combined with MBN Studio [4] a special multi-task software toolkit with graphical user interface. MBN Studio helps to set up calculations with MBN Explorer, monitoring their progress and examining the calculation results. Such a graphical utility enables the user to visualise selected inputs and outputs. A number of built-in tools allows for the calculation and analysis of specific systems' characteristics. A special modelling plug-in allows the construction of a large variety of molecular systems built of arbitrary atomic and molecular constituents. MBN Studio assists in utilising libraries and databases that provide coordinates and geometries for atomic clusters, nanoparticles, biomolecules, crystals and other MBN systems. The main features of MBN Studio are illustrated in **Fig. 2**.

Together MBN Explorer & Studio is a powerful and universal instrument of computational research capable to simulate a large variety of MBN systems, to visualise and analyse results of their multiscale modelling.

The talk will highlight a number of unique algorithms, such as irradiation driven molecular dynamics [5], reactive CHARMM force fields [6], stochastic [7] and relativistic dynamics [8,9], implemented in the MBN

software, and give examples of their applications in recent case studies. The selected research problems are in

## “Dynamics of systems on the nanoscale”: Mon-I-1

the core of currently running European Research Projects supported within the HORIZON 2020, HORIZON Europe, COST and other Programmes. The examples considered will concern the problems of radiation damage in bimolecular systems, controlled nanofabrication by means of Focused Electron Beam Induced Deposition (FEBID), dynamics of ultrarelativistic charged particles in oriented crystals and related phenomena.

Particular attention in the discussion will be devoted to the development of the novel multiscale methodologies and interlinks of different theoretical and computational frameworks for modelling and the quantitative description of multiscale processes occurring in MBN systems on various temporal, spatial and energy scales. Examples of recent advances in the development of such methodologies for the atomistic modelling of FEBID [10] and crystal-based intensive gamma-ray light sources [11,12] will be given.

- [1] I.A. Solov'yov, A.V. Yakubovich, P.V. Nikolaev, I. Volkovets, and A.V. Solov'yov, *J. Comput. Chem.* **33** (2012) 2412
- [2] I.A. Solov'yov, A.V. Korol, A.V. Solov'yov, *Multiscale Modeling of Complex Molecular Structure and Dynamics with MBN Explorer* (Springer International Publishing, Cham, Switzerland, 2017); 447 p., ISBN: 978-3-319-56085-4, ISBN: 978-3-319-56087-8
- [3] I.A. Solov'yov, G.B. Sushko, A.V. Solov'yov, *MBN Explorer Users' Guide: Version 3.0* (MesoBioNano Science Publishing, Germany, 2017), ISBN: 978-1-975-63904-4; I.A. Solov'yov, G.B. Sushko, A.V. Verkhovtsev, A.V. Korol, A.V. Solov'yov, *MBN Explorer and MBN Studio Tutorials: Version 3.0*, (MesoBioNano Science Publishing, Germany, 2017), ISBN: 978-1-976-46092-0
- [4] G.B. Sushko, I.A. Solov'yov, A.V. Solov'yov, *J. Mol. Graph. Model.* **88** (2019) 247
- [5] G.B. Sushko, I.A. Solov'yov, A.V. Solov'yov, *Eur. Phys. J. D* **70** (2016) 217
- [6] G.B. Sushko, I.A. Solov'yov, A.V. Verkhovtsev, S.N. Volkov, and A.V. Solov'yov, *Eur. Phys. J. D* **70** (2016) 12
- [7] M. Panshenskov, I.A. Solov'yov, and A.V. Solov'yov, Efficient 3D kinetic Monte Carlo method for modeling of molecular structure and dynamics, *J. Comput. Chem.* **35** (2014) 1317
- [8] G.B. Sushko, V.G. Bezchastnov, I.A. Solov'yov, A.V. Korol, W. Greiner, and A.V. Solov'yov, Simulation of ultra-relativistic electrons and positrons channeling in crystals with MBN Explorer, *J. Comput. Phys.* **252** (2013) 404
- [9] A.V. Korol, A.V. Solov'yov, W. Greiner, *Channeling and Radiation in Periodically Bent Crystals*, Springer Series on Atomic, Optical, and Plasma Physics, Vol. 69, 2nd ed., Springer Heidelberg, New York, Dordrecht, London (2014), 284 p., ISBN: 978-3-642-54932-8 (hardcover), ISBN: 978-3-642-54933-5 (e-book)
- [10] P. de Vera, M. Azzolini, G. Sushko, I. Abril, R. Garcia-Molina, M. Dapor, I.A. Solov'yov, and A.V. Solov'yov, Multiscale simulation of the focused electron beam induced deposition process, *Scientific Reports* **10** (2020) 20827
- [11] A.V. Korol and A.V. Solov'yov, Crystal-based intensive gamma-ray light sources (Topical Review), *Eur. Phys. J. D* **74** (2020) 201
- [12] A.V. Korol, G.B. Sushko, and A.V. Solov'yov, All-atom relativistic molecular dynamics simulations of channeling and radiation processes in oriented crystals, *Eur. Phys. J. D* **75** (2021) 107



## Shake, rattle and roll: STM studies of fullerenes

Eleanor E.B. Campbell<sup>1,\*</sup>, Renald Schaub<sup>2,\*\*</sup>, Henry Chandler<sup>2</sup>, Ewan Scougall<sup>2</sup>

<sup>1</sup> EaStCHEM and School of Chemistry, University of Edinburgh, David Brewster Road, Edinburgh EH9 3FJ, Scotland

\*E-mail: eleanor.campbell@d.ac.uk

<sup>2</sup> EaStCHEM and School of Chemistry, University of St. Andrews, North Haugh, St. Andrews KY16 9ST, Scotland

\*\*E-mail: rs51@st-andrews.ac.uk

Ultra-high vacuum, low temperature Scanning Tunneling Microscopy (STM) studies provide exquisite detail concerning the local density of states of molecules deposited on metal substrates. In our recent studies we have applied low temperature STM and Scanning Tunneling Spectroscopy (STS) to study the properties of C<sub>60</sub> and Li@C<sub>60</sub> [1,2]. We were able to show that tunneling current from the STM tip could be used to induce movement of the Li inside the fullerene cage to produce 14 different positions within the cage, each being clearly distinguishable, and leading to different values of tunneling current for a given bias voltage. The switching mechanism for this robust multi-state single molecule switch was shown to be different from any known single-molecule switch mechanisms. Here, we present further work that helps explain the resilience of the molecules under extreme tunneling current conditions and illustrates the important role that diffuse Rydberg-like states (Super-Atom Molecular Orbitals: SAMOs) play in the switching process and in the development of nearly-free electron (NFE) bands within fullerene monolayers. We aim to show the possibility of manipulating fullerenes on the surface to study the build-up of the NFE bands molecule by molecule and explore the potential of these systems as artificial neural networks.

[1] M. Stefanou, H.J. Chandler, R. Schaub, E.E.B. Campbell, *Nanoscale* **11** (2019) 2668

[2] H.J. Chandler, M. Stefanou, E.E.B. Campbell, R. Schaub, *Nature Commun.* **10** (2019) 2283

## Transitions in matter induced by intense X-ray radiation and their diagnostics

Beata Ziaja-Motyka<sup>1,2</sup>

<sup>1</sup>CFEL, DESY, Notkestrasse 85, 22607 Hamburg, Germany

<sup>2</sup>INP, PAS, Radzikowskiego 152, 31-342, Krakow, Poland.

E-mail: ziaja@mail.desy.de

X-ray induced structural transitions in solids are in focus of this talk. Depending on the dose absorbed, an irradiation with a femtosecond X-ray pulse can trigger an ultrafast electronic or structural transition in solid materials. In magnetic materials, an X-ray triggered ultrafast demagnetization can also occur. In this talk, selected study cases [1-8] for these transitions are presented. Dedicated theoretical modeling reveals complex multistage evolution of the irradiated systems, confirmed by experimental measurements performed at FERMI and at other XFEL facilities. Challenges remaining for the modeling and quest for further improvements of the necessary diagnostics tools are discussed.

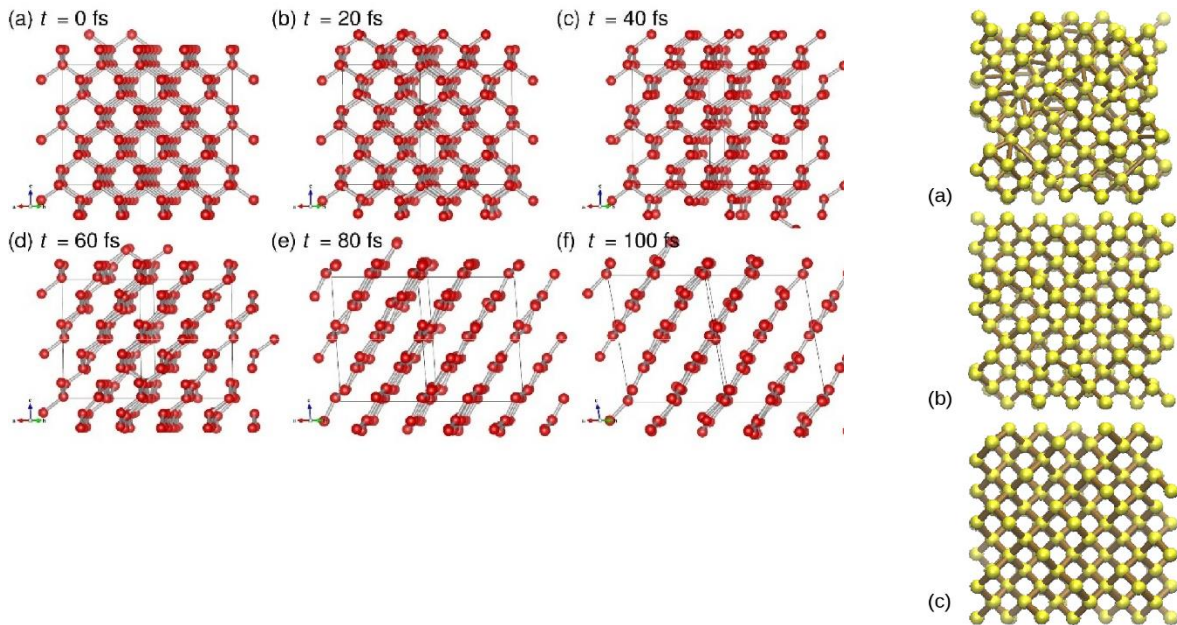


**Figure 1:** Ultrafast graphitization of diamond triggered by soft X-ray pulse of 10 fs duration (left) & dose-dependent structural changes in silicon crystal triggered by hard X-ray pulse of 25 fs duration (right).

- [1] F. Tavella et al., *High Energy Density Physics* **24** (2017) 22
- [2] I. Inoue et al., *PNAS* **113** (2016) 1492
- [3] N. Medvedev, B. Ziaja, *Scientific Reports* **8** (2018) 5284
- [4] P. Finetti et al., *Phys. Rev. X* **7** (2017) 021043
- [5] V. Tkachenko et al., *Scientific Reports* **11** (2021) 5203
- [6] V. Tkachenko et al., *Optics Letters* **45** (2020) 33
- [7] V. Tkachenko et al., *Applied Sciences* **11** (2020) 5157
- [8] K. Nass et al., *Nature Communications* **11** (2020) 1814

## **Symmetry breaking and symmetry recovery in the growth of metal nanoparticles**

Riccardo Ferrando

Department of Physics, University of Genoa  
Via Dodecaneso 33, 16146, Genoa, Italy  
E-mail: ferrando@fisica.unige.it

The properties of metal nanoparticles strongly depend on shape. Nanoparticles with different shapes exhibit different optical response, and the types of facets exposed by the nanoparticles can strongly influence their efficiency in catalysis. Non-crystalline structures can also present strained surfaces, with important effects on molecular adsorption and catalysis. Therefore, the understanding of the basic physical mechanisms of nanoparticle leading to the growth of different nanoparticle shapes is of great importance for applications. This understanding is often achieved by a combination of experiments and computer simulations.

Here we present two examples of nanoparticle growth. The first concerns the growth of tetrahedra (Th) from smaller octahedra (Oh) in Pt nanoparticles [1]. In gas-phase growth experiments, it is found that octahedra are dominant for small sizes, while tetrahedra prevail for larger sizes. This suggests that a Oh→Th transformation is occurring during growth. This transformation is explained neither by the equilibrium Wulff construction nor by the kinetic Wulff construction. Molecular dynamics simulations of the full growth pathway show how the truncated octahedra grow to complete octahedra and how these octahedra further grow to tetrahedra [1,2]. This pathway drives the nanoparticles towards shapes that are progressively less and less compact. The Oh→Th transformation requires a specific form of symmetry breaking which is caused by the formation of metastable defects, namely of atomic islands in hcp stacking.

The second example concerns a growth process which starts from Au tetrahedra and then leads to the formation of multiply twinned particles such as decahedra (Dh) and icosahedra (Ih) [3]. This is studied by molecular dynamics simulations. The first step of the process requires a further symmetry breaking which is achieved by the stabilization of two hcp islands facing the same edge of the tetrahedron. These islands trigger the formation of twin planes and of a fivefold axis between them. The growth around this single fivefold axis leads to the formation of a Dh. In this part of the Th→Dh process, the nanoparticle gradually evolves towards a more compact and symmetric structure. If three hcp islands form on the original Th, three fivefold axes are formed at the same time so that an Ih fragment is grown (direct Th→Ih pathway). Finally, an Ih can grow also from a smaller Dh (Th→Dh→Ih pathway).

[1] Y. Xia, D. Nelli, R. Ferrando, J. Yuan, Z.Y. Li, *Nature Communications* **12** (2021) 3019

[2] D. Nelli, C. Roncaglia, R. Ferrando, C. Minnai, *Catalysts* **11** (2021) 718

[3] E.Y. El Koraychy, C. Roncaglia, D. Nelli, M. Cerbelaud, R. Ferrando, in preparation (2021)

**Tailoring the optical properties of gold catenane nanoclusters. Surface ligand, silver doping, and self-assembly**

Rodolphe Antoine

Institut lumière matière, UMR5306, Université Claude Bernard Lyon1-CNRS,  
Univ. Lyon 69622, Villeurbanne cedex, France.  
E-mail: rodolphe.antoine@univ-lyon1.fr

Ligand protected metal nanoclusters (NCs) are an emerging class of quantum materials connecting the gap between atoms and bulk metallic materials. Owing to their unique electrical, optical and other spectroscopic properties such as luminescence, they are very important in various applications such as sensing and bio-imaging. Concerning optical properties, strongly emissive nanoclusters are highly desirable. Strategies such as aggregation-induced emission, silver doping and ligand-shell rigidifying for increasing the photoluminescence (PL) quantum yield and tuning the PL colors of nanoclusters have been proposed.

During my talk, I will present such strategies applied to Au<sub>10</sub> atomically precision catenane structures of NCs. Deep structural insight from mass spectrometry and ion mobility allow for understanding of the structure-optical properties relationship of NCs to some extent. In the second part of my talk, I will give some recent advances aiming at templating and functionalizing nanoclusters for bio-applications.

- [1] F. Bertorelle et al., *J. Phys. Chem. Lett.* **8** (2017) 1979
- [2] C. Comby-Zerbino, M. Perić, F. Bertorelle, F. Chirot, P. Dugourd, V. Bonačić-Koutecký, R. Antoine, *Nanomaterials* **9** (2019) 457
- [3] R. Antoine, *Nanomaterials* **10** (2020) 377
- [4] S. Basu, M.P. Bakulić, H. Fakhouri, I. Russier-Antoine, C. Moulin, P.-F. Brevet, V. Bonačić-Koutecký, R. Antoine, *J. Phys. Chem. C* **124** (2020) 19368
- [5] S. Basu, H. Fakhouri, C. Moulin, S. Dolai, I. Russier-Antoine, P.-F. Brevet, R. Antoine, *Nanoscale* **13** (2021) 4439
- [6] G.F. Combes et al., *Commun. Chem.* **4** (2021) 69

## Understanding cosmic nanodust using molecular dynamics

Stefan T. Bromley

Department of Materials Science and Physical Chemistry, University of Barcelona,  
08028, Barcelona, Spain  
E-mail: s.bromley@ub.edu

Cosmic dust is found throughout the universe. Formed around aging stars or in supernovae, nascent grains are initially thrown into harsh interstellar space where they reside for millions of years. When eventually finding denser and warmer regions of space, dust becomes the main driver for astrochemistry by providing catalytic sites for reactions while shielding against destructive high energy radiation. Cosmic dust is thereby essential for the formation of a huge range of molecules from water and hydrogen to complex organic molecules. Eventually, these denser regions of space become the birthplace for new stars with orbiting planets largely built from accretion of dust grains.

Our knowledge of the structure and properties of cosmic dust comes mainly from infrared (IR) observations. By comparing observed IR spectra with laboratory spectra, it has been suggested that the majority of dust particles are amorphous magnesium-rich silicates typically with olivine ( $\text{Mg}_2\text{SiO}_4$ ) or pyroxene ( $\text{MgSiO}_3$ ) compositions. By number, it is also likely that nanosized silicate dust grains are the most abundant type of solid species in the universe.

To better understand and interpret the astronomical IR spectra of nanosilicate dust we use ab initio (i.e. quantum mechanical based) and classical molecular dynamics to simulate the temperature dependent IR spectra of realistic nanodust models. We show how our results reveal how the IR spectra of dust particles vary with finite temperatures thus providing us with a tool to estimate the temperature of dust-containing astrophysical environments [1]. Our results also show that IR spectra are not a reliable indicator of the crystallinity of cosmic dust – especially at the nanoscale [2]. Our results will be used in interpreting the high-resolution IR data that the soon-to-be-launched James Webb Space Telescope (JWST) will yield [3].

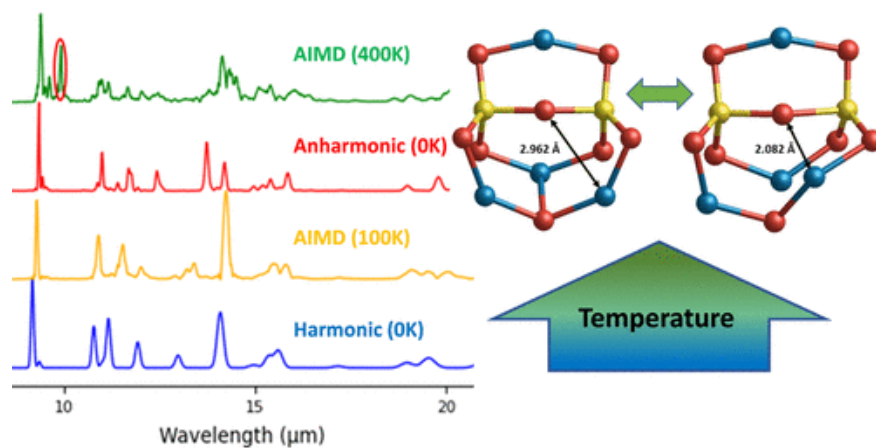


**Figure 1:** Simulated IR spectra of a small nanosilicate cluster with increasing temperature

- [1] J. Mariñoso Guiu, A. Macia Escatller, S. T. Bromley, *ACS Earth and Space Chemistry* **5** (2021) 812  
[2] L. Zamirri, A. Macia Escatller, J. Mariñoso Guiu, P. Ugliengo, S. T. Bromley, *ACS Earth and Space Chemistry* **3** (2019) 2323  
[3] Accepted JWST observational proposal: “Illuminating the Dust Properties in the diffuse ISM with JWST” – led by F. Kemper and S. Zeegers (2021)

## Novel nanoarchitectures for the monitoring of single molecules and plasmon induced chemical reactions by surface-enhanced Raman scattering (SERS)

Ilko Bald<sup>\*</sup>, Kosti Tapio, Sergio Kogikoski Jr., Anushree Dutta, Amr Mostafa, Yuya Kanehira

Institute of Chemistry, University of Potsdam,  
Karl-Liebknecht-Str. 24-25, 14476 Potsdam, Germany

\*E-mail: bald@uni-potsdam.de

DNA is a highly interesting material and can be e.g. used to assemble plasmonic nanoparticles into complex particle arrangement, while the DNA also serves the purpose to place analyte molecules of interest at specific locations. These molecules can then be detected by surface-enhanced Raman scattering (SERS) down to a single-molecule level, and SERS also allows for a monitoring of chemical reactions [1,2].

In the first part of the talk it will be presented how DNA origami technology is used to detect single molecules by SERS. Recently, we have created a versatile DNA origami nanofork antenna (DONA) by assembling Au or Ag nanoparticle dimers with different gap sizes down to 1.17 nm, enabling SERS signal enhancements of up to  $10^{11}$  [3]. This allows for single-molecule SERS measurements, which can even be performed with larger gap sizes to accommodate differently sized molecules, at various excitation wavelengths. A general scheme allows to place single analyte molecules into the SERS hot spots using the DNA origami structure exploiting covalent and noncovalent coupling schemes. By using Au and Ag dimers, single-molecule SERS measurements of a broad range of molecules including proteins is demonstrated.

In the second part of the talk, the monitoring of plasmon induced chemical reactions in single molecules is presented. For this, DNA is used to assemble Ag nanoparticles into superlattices, which provide strong SERS signals of single 8-bromo-adenosine [4,5] modifications introduced into the DNA. Plasmon excitation results in the generation of hot electrons, which can be transferred along the DNA over several nanometers to drive a chemical reaction [6]. The decomposition reaction is tracked by SERS. The results indicate that DNA can provide an attractive platform to study the transfer of hot electrons, leading to the future development of more advanced plasmonic catalysts.

[1] J. Prinz, C. Heck, L. Ellerik, V. Merk, I. Bald, *Nanoscale* **8** (2016) 5612

[2] C. Heck, Y. Kanehira, J. Kneipp, I. Bald, *Angew. Chem. Int. Ed.* **57** (2018) 7444

[3] K. Tapio, A. Mostafa, Y. Kanehira, A. Suma, A. Dutta and I. Bald, *ACS Nano* **15** (2021) 1765

[4] R. Schürmann, I. Bald, *Nanoscale* **9** (2017) 1951

[5] A. Dutta, R. Schürmann, S. Kogikoski Jr., N. S. Mueller, S. Reich, I. Bald, *ACS Catal.* **11** (2021) 8370

[6] S. Kogikoski Jr., A. Dutta, I. Bald, preprint. doi.org/10.26434/chemrxiv.14114306.v2

## Putting DNA origami-based nanostructures in stable motion

Michael Mertig<sup>1,2,\*</sup>, Felix Kroener<sup>1,3</sup>, Lukas Traxler<sup>3</sup>, Andreas Heerwig<sup>2</sup>, Alfred Kick<sup>2</sup>,  
Julia Lenhart<sup>2</sup>, Thomas Welte<sup>3</sup>, Wolfgang Kaiser<sup>3</sup>, Ulrich Rant<sup>3,\*\*</sup>

<sup>1</sup> Institute of Physical Chemistry, Technische Universität Dresden, 01062 Dresden, Germany  
\*E-mail: michael.mertig@tu-dresden.de

<sup>2</sup> Kurt-Schwabe-Institut für Mess- und Sensortechnik Meinsberg e.V., 04736 Waldheim, Germany  
michael.mertig@ksi-meinsberg.de

<sup>3</sup>Dynamic Biosensors GmbH, 82152 Planegg, Germany  
\*\*E-mail: rant@dynamic-biosensors.com

Dynamic methods of biosensing based on electrical actuation of surface-tethered nanolevers require the use of levers whose movement in ionic liquids is well controllable and stable. In particular, mechanical integrity of the nanolevers in a wide range of ionic strengths will enable to meet the chemical conditions of a large variety of applications where the specific binding of biomolecular analytes is analyzed.

We have studied the electrically induced switching behavior of different rod-like DNA origami nanolevers [1-3] and compare that to the actuation of simply double-stranded DNA nanolevers. Figure 1(A) shows a schematic viewgraph of the investigated origami attached to a gold electrode: 100 nm long six-helix bundle and 50 nm long four-helix bundle. (B, C) Electrically induced orientation switching of origami rods. When positive potentials are applied to the electrode, the rods are attracted to the electrode and the fluorescence emission from dyes attached to their top ends is quenched by the metal surface. When negative potentials are applied, the rods are repelled from the surface and the fluorescence emission is high.

The measurements reveal a significantly stronger response of the DNA origami to switching of electrode potential, leading to a smaller potential change necessary to actuate the origami, and subsequently, to a long-term stable movement. The mechanical response time of a 100 nm long origami lever to an applied voltage step is less than 100  $\mu$ s, allowing for a highly dynamic control of the induced motion. Dynamic measurements in buffer solutions with different  $Mg^{2+}$  content show that the levers do not disintegrate even at very low ion concentration and constant switching stress, and thus, provide stable actuation performance. Specific binding of proteins to the origami levers demonstrates that the switching speed correlates with size of protein in a wide dynamic range - from small proteins to ribosomes.

The latter will pave the way for many new applications without largely restricting application-specific environments. In particular, using DNA origami with low concentrations of  $Mg^{2+}$  ions in solution qualifies them for a broad range of biomedical and biophysical applications.

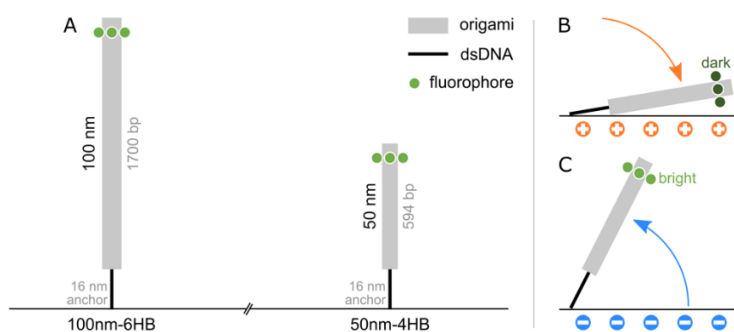


Figure 1

- [1] F. Kroener, A. Heerwig, W. Kaiser, M. Mertig, U. Rant, *J. Am. Chem. Soc.* **139** (2017) 16510  
[2] A. Heerwig, J. Lenhart, F. Kroener, U. Rant, M. Mertig, *Phys. Status Solidi A* **215** (2018) 1700907  
[3] F. Kroener, L. Traxler, A. Heerwig, U. Rant, M. Mertig, *ACS Appl. Mater. Interf.* **11** (2019) 2295



## Structure and dynamics of cryptochrome photoreceptors

Ilia A. Solov'yov

Department of Physics, Carl von Ossietzky University of Oldenburg, Oldenburg, Germany  
Carl-von Ossietzky Str. 9-11, 26129, Oldenburg, Germany  
E-mail: ilia.solovyov@uni-oldenburg.de

Clearly, the laws of physics hold and are exploited in living organisms. Speaking as a physicist, most biological characteristics stem from the laws of classical physics that students learn in their first year. However, crucial characteristics in organisms are governed by quantum physics. The latter characteristics are those in which biological processes involve the jumps of electrons from one state to another. The quantum behavior of electrons covers all chemical transformations, for example it arises in optical transitions induced through light absorption by biomolecules.

The mechanism by which night-migratory songbirds sense the direction of the Earth's magnetic field appears to possibly rely on the quantum spin dynamics of light-induced radical pairs in cryptochrome proteins located in the retina [1-4]. Cryptochrome binds internally the flavin cofactor (FAD), which governs its signaling through light-induced electron transfer involving a chain of four tryptophan residues, TrpA, TrpB, TrpC, TrpD, see Fig. 1. In this presentation I will review the latest experimental findings [3] that demonstrate that the photochemistry of cryptochrome 4 (CRY4) from the night-migratory European robin (*Erithacus rubecula*) is magnetically sensitive *in vitro*, and more so than CRY4 from two non-migratory bird species, chicken (*Gallus gallus*) and pigeon (*Columba livia*). Site-specific mutations of ErCRY4 reveal the roles of four successive flavin–tryptophan radical pairs in generating magnetic field effects and in stabilizing potential signaling states in a way that could enable sensing and signaling functions to be independently optimized in night-migratory birds. The experimental findings will be closely linked to the state-of-the-art computational investigations accomplished by my group in the recent years which help underpin the nature of the electron transfers and explain its unique features in the case of ErCRY4.

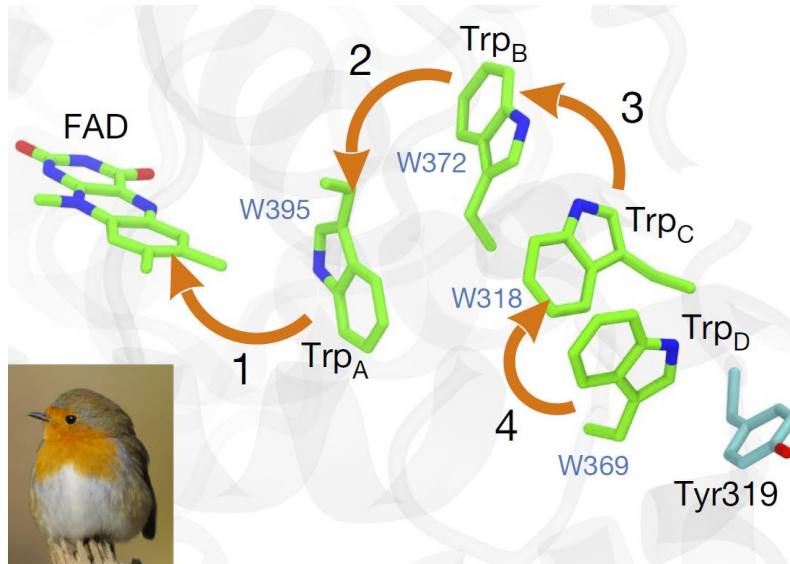


**Figure 1:** Structural homology model of Cryptochrome 4 from European robin showing the flavin group of the FAD chromophore, the Trp-tetrad and Tyr 319. Sequential electron transfers are indicated by arrows. Robin photograph by Thomas Eisenhut (© [www.xeta.at](http://www.xeta.at)). Figure adapted from [2].

- [1] H. Mouritsen, *Nature* **558** (2018) 50
- [2] D.R. Kattnig, J.K. Sowa, I.A. Solov'yov, and P.J. Hore, *New J. Phys.* **18** (2016) 063007
- [3] J. Xu, L.E. Jarocha, T. Zollitsch et al. *Nature* **594** (2021) 535
- [4] E. Sjulstok and I.A. Solov'yov, *J. Phys. Chem. Lett.* **11** (2020) 3866



## **Irradiation-driven transformations of ice deposits under astrochemical conditions**

Nigel J. Mason<sup>\*</sup>, Perry A. Hailey and Duncan V. Mifsud

Centre for Astrophysics and Planetary Science, Physics and Astronomy,  
University of Kent, Canterbury, CT2 7NH, United Kingdom

<sup>\*</sup>E-mail: N.J.Mason@kent.ac.uk

Space is cold, often very cold (<10K), such that ices are common on most surfaces be they large scale planets, moons, comets or micron sized dust grains in the Interstellar Medium (ISM). Such ices are subject to many different types of irradiation including high energy cosmic rays, UV fields from stars and excited hydrogen, and X-rays from compact astronomical objects. In our own solar system, such ices are subject to irradiation by the solar wind and magnetospheric ions. Such irradiation induces both physical and chemical induced changes in the ices which, over time, may significantly alter the properties of the surface of the bodies upon which such ices are present.

Despite the recognition of the importance of astronomical irradiation of ices, our knowledge of the physico-chemical transformations remains scarce and often rather contradictory. This is due to the difficulties in characterising ‘solid-state’ processing compared to the gas phase. In the gas phase, number densities, temperatures and process cross sections are well defined whereas in the solid phase there are many more parameters that need to be characterized: for example, the morphology of the ice (crystalline vs amorphous). In the solid phase ‘simple’ parameters such as ‘cross section’ are not discrete (a cross section depending on ice mixture and structure), indeed some suggest the definition of a cross section in the solid phase has no meaning.

Nevertheless, many experiments have been conducted to study irradiation of ice layers prepared at temperatures compatible with those found on planetary bodies and in the ISM. Such experiments have revealed a myriad of processes that give an insight into the possible processing of astronomical ices and reveal that from very simple ices many complex molecules can be synthesized suggesting possible routes to the prebiotic chemistry necessary for life. However, recent experiments have also shown the sensitivity of such processing as a function of morphology, temperature and type of irradiation. Successive irradiations may determine different routes of formation and destruction dependent upon the order of the irradiations.

Nor is it possible to exactly replicate astronomical conditions. Whilst cryostatic methods can replicate astronomical temperatures, it is hard to achieve pressures compatible with those in space (<10<sup>-12</sup> mbar). Furthermore, in laboratory investigations of the chemistry occurring within interstellar medium, the ices are usually deposited on to flat surfaces used for transmission or reflection spectroscopy (e.g., gold, zinc selenide, magnesium fluoride, etc.) rather than replicate carbon and silicate surfaces on the micron scale. However, the most dramatic difference between laboratory mimics and reality is the time scale over which processing occurs. In the lab higher fluxes are used to allow data to be produced in hours (or maybe over a few days) whereas in space such processing occurs over years!

Accordingly, we are proposing the adoption of a new ‘systems astrochemistry’ approach for experimental studies. Such an approach has already been adopted used for some time now and to great effect in the field of laboratory prebiotic chemistry. We anticipate that its application to experimental astrochemistry will uncover new data hitherto unknown, which could aid in better linking laboratory work to observations and models. Moreover, we propose that experiments be accompanied by a ‘Digital Twin.’ The concept of a digital twin was first adopted in 2010 by NASA in an attempt to improve spacecraft simulation and has since been adopted widely within industrial settings, especially in manufacturing plants.

Developing a digital twin for a laboratory astrochemistry experiment operating under a systems astrochemistry approach would accrue significant scientific benefits, particularly in the areas of sensitivity analysis and scenario planning of changes to experimental parameters and their impact on the emergent chemistry. Examples of such modelling might include assessing the sensitivity of emergent chemical properties to changes in energetic parameters, or the in-silico testing of experiments prior to experimental runs (which would be very useful to research groups with limited access to central research facilities).

In this talk we will present the rationale for such an approach and give some examples of how we plan to adopt it in the near future in studies of irradiation of astronomical ices.

## Organic ice resist lithography

Marco Beleggia

DTU Nanolab, Technical University of Denmark,  
Fisikvej 307, 2800, Kgs. Lyngby, Denmark  
E-mail: mabele@dtu.dk

Organic Ice Resist Lithography (OIRL) is a novel one-step method for patterning nanostructures using a thin frozen layer of beam sensitive organic material [1,2]. Fig. 1 sketches the basic implementation of OIRL. A precursor gas is introduced into the lithography instrument and condenses on a cold sample surface (Fig. 1(a)). After electron-beam (e-beam) patterning (Fig. 1(b)), the unexposed resist is removed by heating up the substrate to room temperature (Fig. 1(c)). The areas exposed to the electron beam become non-volatile and remain on the substrate. This allows bypassing the spinning, baking and development steps required in conventional e-beam lithography. The entire process takes place in a single instrument, does not require cleanroom environment or any additional chemicals and is free of residual resist contamination. In our recently published work [1,2] we have demonstrated the advantages of OIRL over other lithography methods, such as easy handling of fragile and non-planar surfaces and effective fabrication of 3D materials.

The transformation of volatile molecules into a solid pattern stable at ambient conditions is driven by cryo-radiation chemistry: the electron beam, acting as ionizing radiation, progressively de-hydrogenates the organic molecules, creating long-lasting radicals and broken C-H bonds due to the limited mobility of chemical species and molecular fragments at low temperature. Upon warming up, as mobility increases, the system quickly polymerize by cross-linking carbons with dangling bonds. At large irradiation doses C-C bond breaking becomes significant and slows the transformation down. At even larger doses, similarly to conventional resists, we observed a hint of tone reversal from negative to positive, possibly due to knock-on damage/sputtering.

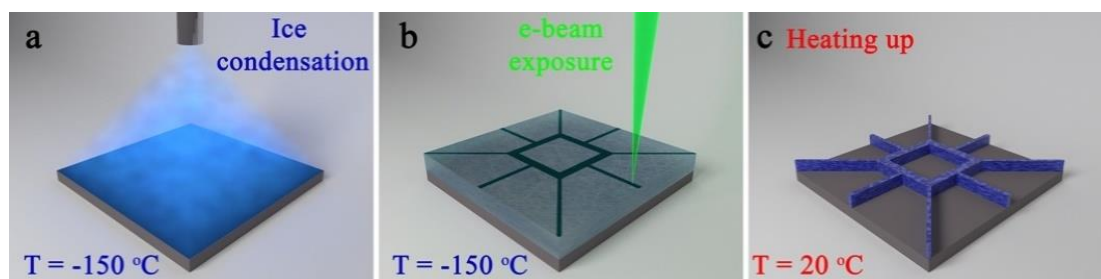


**Figure 1:** Basic steps of OIRL. a) Condensation of organic vapours on a cold substrate; b) e-beam patterning; c) upon heating, the unexposed ice sublimates, while the exposed ice becomes non-volatile and remains on the substrate.

To unveil the mechanism behind the functionality of OIRL we are setting up a computational scheme that follows the chemical and physical steps of the process, from secondary electron generation, to ionization and radical creation, to polymerization. As a result, we can calculate the expected contrast curves of various molecules as a function of their molecular weight and structure. The comparison between simulated and experimental contrast curves sheds light on the origin of relevant parameters such as onset/saturation dose, and provides guidelines in the most optimal choice of molecule for a given target application.

[1] W. Tididi et al., *Nano Letters* **17** (2018) 7886

[2] A. Elsukova et al., *Nano Letters* **18** (2018) 7576

## 3D nanoprinting via focused electron beams: principles and applications

Harald Plank<sup>1,2,3</sup>

<sup>1</sup> Christian Doppler Laboratory - DEFINE, Graz University of Technology

<sup>2</sup> Institute of Electron Microscopy and Nanoanalysis, Graz University of Technology

<sup>3</sup> Graz Centre for Electron Microscopy

Steyrergasse 17, 8010 Graz, Austria

E-mail: harald.plank@felmi-zfe.at

Additive, direct-write manufacturing has become an essential part in research and development during the last decade. While methods down to the microscale have meanwhile entered industrial fabrication, the meso- and in particular the nanoscale are far more challenging with respect to resolution, spatial precision, predictability and reliability. Within the small pool of additive, direct-write technologies for nanoscale fabrication, focused electron beam induced deposition (FEBID), has done tremendous advances in recent years. That technology class relies on the highly localized nano-synthesis of surface adsorbed precursor molecules, which are introduced in the vacuum chamber by a gas injection system. Hence, there are only little demands on substrate materials (vacuum / beam compatibility) and surface morphologies (accessible by the beam), making them true direct-write methods. As a currently unique possibility, FEBID allows for the fabrication of even complex, freestanding 3D nano-objects (Fig. 1a,b) by the controlled movement of the particle beam in combination with defined pulse durations. Together with constantly growing number of precursor materials and improving software packages for a reliable upfront design, 3D FEBID is ready to take on a cutting-edge role in the area of direct-write, additive manufacturing [1].

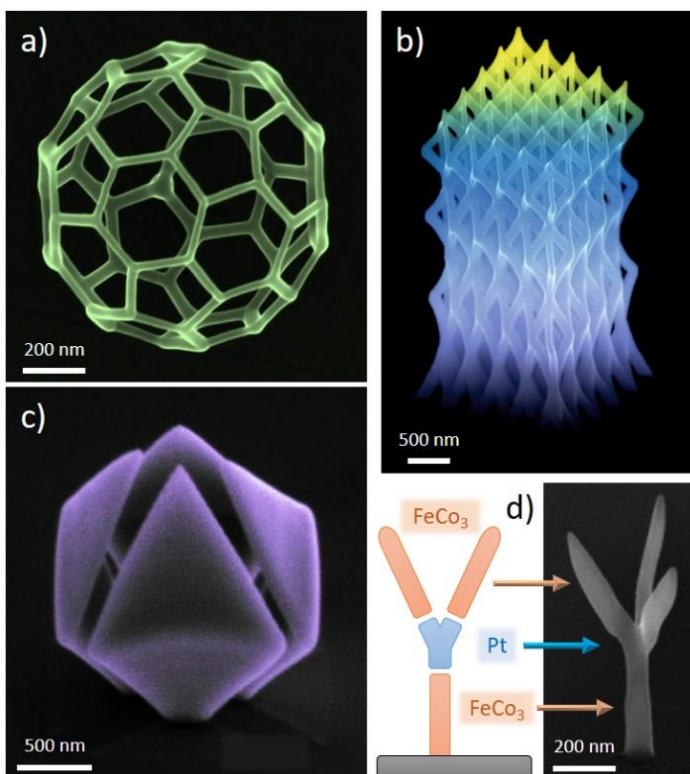


**Figure 1:** 3D nanoprinting via Focused Particle Beam Induced Deposition from the gas phase. While (a) shows the resolution capabilities with individual branches in the sub-50 nm regime, (b) gives an example of a larger 3D structure with branch diameter and apex radii in the sub-100 nm and sub-10 nm regime, respectively, both fabricated in a single step. (c) shows a semi-closed 3D structure, which not only reveal additional challenges during fabrication but in particular open up new application possibilities due to added design flexibility. To expand the latter even further, multi-material 3D fabrication becomes relevant, as representatively shown in (d) by a Pt – FeCo<sub>3</sub> multi-material structure.

In this presentation, we shed light on recent progress of FEBID with emphasis on current fabrication and tuning possibilities in 3D space and start with a basic introduction about the principle. While meshed objects, consisting of individually arranged and interconnected nano-wires (Fig. 1a,b), were mostly used in the past, we here expand the discussion by current activities towards closed 3D designs (Fig. 1c), where new

## **“Irradiation-driven processes and technologies involving Meso-Bio-Nano systems”: Tue-II-3**

effects become relevant. We then turn briefly into materials, their structural and chemical composition and discuss post-processing approaches, which tune or even entirely change the material properties. Those aspects are complemented by several application examples, which strongly benefit from both, the 3D design and the partly unique material properties. That ranges from scientifically oriented nano-applications in the field of resonant optics, magnetics and mechanical sensor concepts towards industrially relevant applications, such as 3D nano-probes for application in scanning probe microscopy [2]. We close the talk with a view on remaining challenges, such as reliable printing of multi-material objects (Fig. 1d) to provide a comprehensive insight in 3D FEBIDs possibilities.

[1] R. Winkler et al., *J. Appl. Phys.* **125** (2019) 210901

[2] H. Plank et al., *Micromachines* **11** (2020) 48

## Irradiation driven molecular dynamics interfaced with Monte Carlo for detailed simulations of focused electron beam induced deposition

Pablo de Vera<sup>1,2,\*</sup>, Martina Azzolini<sup>1</sup>, Gennady Sushko<sup>3</sup>, Isabel Abril<sup>4</sup>,  
Rafael Garcia-Molina<sup>5</sup>, Maurizio Dapor<sup>1,2</sup>, Ilia A. Solov'yov<sup>6</sup>, Andrey V. Solov'yov<sup>3</sup>

<sup>1</sup>European Centre for Theoretical Studies in Nuclear Physics and Related Areas (ECT\*-FBK), Trento, Italy  
\*E-mail: pdeveragomis@ectstar.eu

<sup>2</sup>Trento Institute for Fundamental Physics and Applications (TIFPA-INFN), Trento, Italy

<sup>3</sup>MBN Research Center, Altenhöferallee 3, 60438 Frankfurt am Main, Germany

<sup>4</sup>Departament de Física Aplicada, Universitat d'Alacant, E-03080 Alacant, Spain

<sup>5</sup>Departamento de Física, Universidad de Murcia, 30100 Murcia, Spain

<sup>6</sup>Department of Physics, Carl von Ossietzky Universität, 26129 Oldenburg, Germany

Focused electron beam induced deposition (FEBID) is a cutting-edge technique for the fabrication of complex 3D nanostructures, featuring unique electronic, superconducting, mechanical, optical or magnetic properties [1]. However, as the features resolution falls below  $\sim 10$  nm, even this technique struggles to yield the intended size, shape and composition, primarily due to a lack of molecular-level understanding of the irradiation-driven chemistry (IDC) underlying nanostructure growth. Its further optimization requires a fine control of IDC, which may be accomplished with the help of multiscale computer simulations.

The first atomistic-level simulation of FEBID was achieved in [2] by means of the novel methodology of irradiation driven molecular dynamics (IDMD) implemented in MBN Explorer [3]. IDMD embeds fast, local, random quantum transformations (e.g. rupture-formation of chemical bonds induced by radiation in complex molecular systems) into affordable molecular dynamics simulations. A comprehensive FEBID model requires, as well, a detailed description of the interaction of primary and secondary electrons with the substrate. Here we demonstrate the interface of the Monte Carlo electron transport code SEED [4] with IDMD simulations [5] in MBN Explorer. The SEED program is fed with realistic cross sections for the relevant electron interactions with condensed-phase materials. We obtain accurate predictions of the composition and microstructure of deposits grown by irradiation of  $W(CO)_6$  molecules on  $SiO_2$ , see Fig. 1.

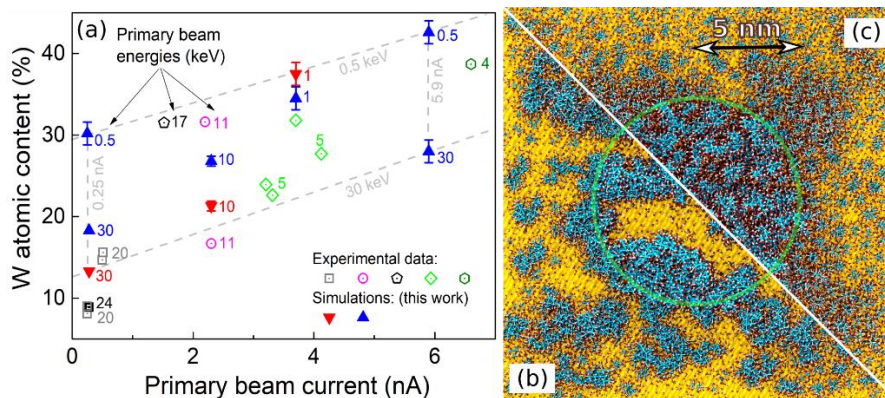


**Figure 1:** (a) W-content in the deposits obtained as a function of electron beam current (abscissa) and energy (numbers next to symbols). (b-c) Top views of simulated deposits for (b) 1 keV and (c) 10 keV beams; the irradiated area is depicted by a green circle; blue/white/red spheres represent W/C/O atoms.

- [1] M. Huth, F. Porrati, O.V. Dobrovolskiy, *Microelectronic Eng.* **18** (2018) 9  
 [2] G.B. Sushko, I.A. Solov'yov, A.V. Solov'yov, *Eur. Phys. J. D* **70** (2016) 217  
 [3] I.A. Solov'yov, A.V. Yakubovich, P.V. Nikolaev, I. Volkovets, A.V. Solov'yov, *J. Comput. Chem.* **33** (2012) 2412  
 [4] M. Dapor, I. Abril, P. de Vera, R. Garcia-Molina, *Phys. Rev. B* **96** (2017) 064113  
 [5] P. de Vera, M. Azzolini, G. Sushko, I. Abril, R. Garcia-Molina, M. Dapor, I.A. Solov'yov, A.V. Solov'yov, *Sci. Rep.* **10** (2020) 20827

## Atomistic insights into the metal nanostructure growth under focused electron beam irradiation

Alexey Prosvetov<sup>\*</sup>, Alexey V. Verkhovtsev, Gennady Sushko, Andrey V. Solov'yov

MBN Research Center,  
Altenhöferallee 3, 60438 Frankfurt am Main, Germany  
<sup>\*</sup>E-mail: prosvetov@mbnexplorer.com

This talk will present the recent results of atomistic irradiation-driven molecular dynamics (IDMD) [1] simulations of the metal nanostructure growth in the process of focused electron beam-induced deposition (FEBID) [2]. These studies have been based on the new multiscale computational methodology [3] that exploits the reactive CHARMM (rCHARMM) force field [4] implemented in the MBN Explorer software package [5], and couples IDMD with Monte Carlo simulations of electron transport. This computational protocol has been applied to model various types of FEBID precursors (particularly Pt(PF<sub>3</sub>)<sub>4</sub>, and Fe(CO)<sub>5</sub>) at different irradiation, replenishment and temperature regimes.

The simulations [6,7] have provided atomistic insights into the initial stage of platinum- and iron-containing FEBID nanostructures growth, including nucleation of metal atoms, formation of small metal clusters on the surface, and their aggregation into larger-size metal structures. The geometrical characteristics (lateral size, height and volume), morphology and metal content of the grown nanostructures have been analyzed at different parameters of the irradiation and precursor replenishment phases. Considering the FEBID of Fe(CO)<sub>5</sub> as a case study, a significant variation of the deposit's morphology and elemental composition has been observed with increasing the electron current from 1 to 4 nA. At low beam current (1 nA) corresponding to a low degree of Fe(CO)<sub>5</sub> fragmentation, the FEBID nanostructures consist of isolated iron clusters embedded into an organic matrix. In this regime, metal clusters do not coalesce with increasing electron fluence, resulting in relatively low nanostructures' metal content. A higher beam current of 4 nA facilitates the precursor fragmentation and the coalescence of metal clusters into a dendrite-like structure with the size corresponding to the size of the primary electron beam.

The analysis of the simulation results [6,7] provides space resolved relative metal content, height and the growth rate of the deposits which represent a valuable reference data for the experimental characterization of the FEBID-grown nanostructures. Further development of the computational model for FEBID may include accounting for multiple channels of electron-induced precursor dissociation and follow-up chemical reactions.

- [1] G.B. Sushko, I.A. Solov'yov, and A.V. Solov'yov, *Eur. Phys. J. D* **70** (2016) 217
- [2] J. M. De Teresa (ed.), *Nanofabrication: Nanolithography Techniques and Their Applications* (IOP Publishing Ltd, 2020)
- [3] P. de Vera, M. Azzolini, G. Sushko, I. Abril, R. Garcia-Molina, M. Dapor, I.A. Solov'yov, A.V. Solov'yov, *Sci. Rep.* **10** (2020) 20827
- [4] G.B. Sushko, I.A. Solov'yov, A.V. Verkhovtsev, S.N. Volkov, and A.V. Solov'yov, *Eur. Phys. J. D* **70** (2016) 12
- [5] I.A. Solov'yov, A.V. Yakubovich, P.V. Nikolaev, I. Volkovets, and A.V. Solov'yov, *J. Comput. Chem.* **33** (2012) 2412
- [6] A. Prosvetov, A.V. Verkhovtsev, G. Sushko, A.V. Solov'yov, Irradiation driven molecular dynamics simulation of the FEBID process for Pt(PF<sub>3</sub>)<sub>4</sub>, *Beilstein J. Nanotechnol.* (in print); arXiv:2105.12206 [physics.chem-ph]
- [7] A. Prosvetov, A.V. Verkhovtsev, G. Sushko, A.V. Solov'yov, Atomistic simulation of the FEBID-driven growth of iron-based nanostructures, arXiv:2109.15191 [cond-mat.mtrl-sci]



## Sulphur astrochemistry in the laboratory: techniques to understand the formation of interstellar and planetary Sulphur-bearing molecules

Duncan V. Mifsud<sup>1,2,\*</sup>, Zuzana Kaňuchová<sup>3,4</sup>, Péter Herczku<sup>2</sup>, Zoltán Juhász<sup>2</sup>, Sándor T. S. Kovács<sup>2</sup>, Béla Sulik<sup>2</sup>, Sergio Ioppolo<sup>5</sup>, Robert W. McCullough<sup>6</sup>, Béla Paripás<sup>7</sup>, and Nigel J. Mason<sup>1</sup>

<sup>1</sup> Centre for Astrophysics and Planetary Science, School of Physical Sciences, University of Kent, Canterbury CT2 7NH, United Kingdom

\*E-mail: duncanvmifsud@gmail.com

<sup>2</sup> Atomic and Molecular Physics Laboratory, Institute for Nuclear Research (Atomki), Debrecen H-4026, Hungary

<sup>3</sup> Astronomical Institute, Slovak Academy of Sciences, Tatranska Lomnicá SK-059 60, Slovak Republic

<sup>4</sup> INAF Osservatorio Astronomico di Roma, Monte Porzio Catone RM-00078, Italy

<sup>5</sup> School of Electronic Engineering and Computer Science, Queen Mary University of London, London E1 4NS, United Kingdom

<sup>6</sup> Department of Physics and Astronomy, School of Mathematics and Physics, Queen’s University Belfast, Belfast BT7 1NN, United Kingdom

<sup>7</sup> Department of Physics, Faculty of Mechanical Engineering and Informatics, University of Miskolc, Miskolc H-3515, Hungary

Despite its relative cosmic ubiquity and its pivotal role in biological and geological systems, the astrochemistry and astrobiology of sulphur is still not well understood [1]. For example, although gas-phase chemistry satisfactorily accounts for the total cosmic abundance of sulphur in diffuse and primitive interstellar media, there is an unexpected and unexplained lack of the element in dense star-forming regions [2]. Within the Solar System, it is known that sulphur ions embedded within giant planetary magnetospheric plasmas may implant into the surfaces of icy moons and result in the formation of sulphur-bearing molecules and minerals. In the context of the Galilean moon system of Jupiter, however, there is some debate as to whether such an exogenic sulphur source plays any role in the formation of SO<sub>2</sub> ice at the surface of Europa, with the literature providing conflicting results [3,4]. Investigating these challenges in sulphur astrochemistry is, generally speaking, made more difficult by the lack of systematicity which often accompanies contemporary laboratory studies, meaning that the results of several studies are often only applicable to very specific astrophysical contexts.

We have thus set out to improve our understanding of sulphur astrochemistry by performing a series of experiments aimed at addressing two questions: (i) can complex organic molecules containing sulphur, which may account for some of the ‘missing’ sulphur in dense molecular clouds, be formed in interstellar ice analogues as a result of processing by galactic cosmic rays? and (ii) can the implantation of Jovian magnetospheric sulphur ions into the icy surface of Europa result in the synthesis of SO<sub>2</sub>? These questions were investigated by (i) irradiating a series of CH<sub>4</sub> and SO<sub>2</sub> ice mixtures with 1 keV electrons at 20 K to decipher if thiols (R–SH) were formed, and (ii) by implanting energetic S<sup>+</sup> ions into a series of oxide ices (CO, CO<sub>2</sub>, and H<sub>2</sub>O) at 20 and 70 K. Experiments were performed using the Ice Chamber for Astrophysics-Astrochemistry; a newly commissioned facility designed for systematic astrochemical experiments involving the ion and electron irradiation of ices [5,6].

Results from our 1 keV electron irradiation of mixed ices containing CH<sub>4</sub> and SO<sub>2</sub> (both known components of interstellar ices) showed no evidence of efficient thiol formation, with other reaction channels such as the formation of C<sub>2</sub>H<sub>6</sub> and SO<sub>3</sub> being preferred irrespective of the original stoichiometric composition of the ice. Our work implanting S<sup>+</sup> ions into planetary ice analogues revealed that, although SO<sub>2</sub> was detected as a radiolytic product when CO or CO<sub>2</sub> ices were used as targets at 20 K, no evidence for its formation could be observed at 70 K (Figure 1). This implies that the implantation of energetic S<sup>+</sup> ions sourced from the Jovian magnetosphere is not the dominant formation mechanism for SO<sub>2</sub>, and that other endogenic sulphur sources

### “Radiation-induced chemistry”: Tue-III-3

should be considered instead. The implantation into H<sub>2</sub>O ices yielded H<sub>2</sub>SO<sub>4</sub> hydrates, in line with previous studies [7].

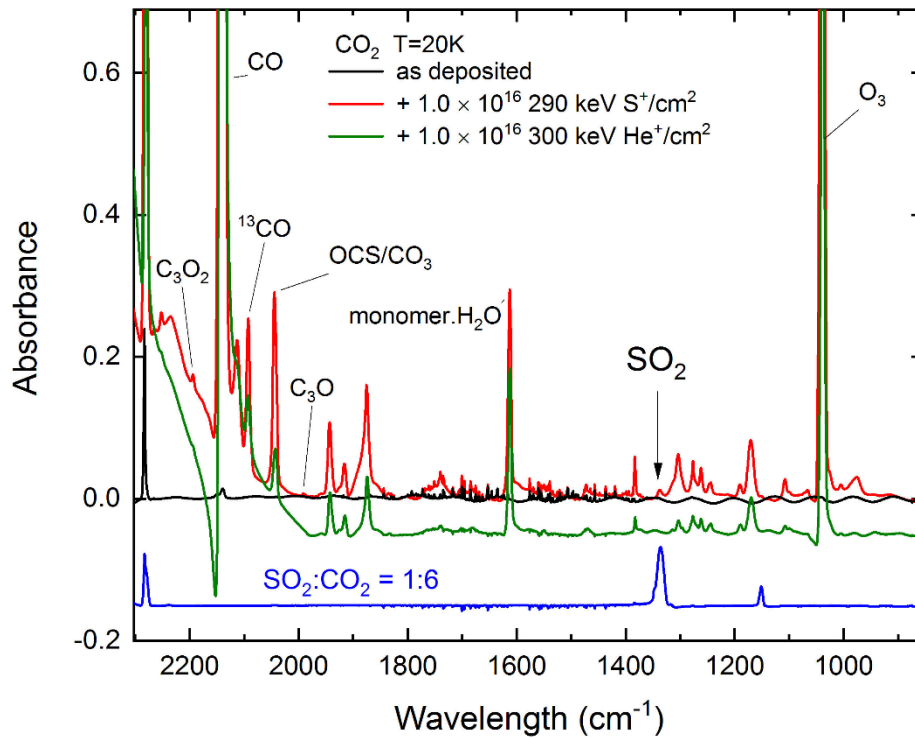


**Figure 1:** Mid-IR spectra for S<sup>+</sup> implantation into CO<sub>2</sub> ice at 20 K. He<sup>+</sup> implantation was performed as a control experiment. No SO<sub>2</sub> was detected when the experiment was repeated at 70 K.

- [1] D.V. Mifsud et al., *Space Sci. Rev.* **217** (2021) 14
- [2] D.E. Anderson et al., *Astrophys. J.* **779** (2013) 141
- [3] X.Y. Lv et al., *Mon. Not. R. Astron. Soc.* **438** (2014) 922
- [4] P. Boduch et al., *Icarus* **277** (2016) 424
- [5] P. Herczku et al., *Rev. Sci. Instrum.* **92** (2021) 084501
- [6] D.V. Mifsud et al., *Eur. Phys. J. D* **75** (2021) 182
- [7] J.J. Ding et al., *Icarus* **226** (2013) 860



## Electron interactions with HFC (R134a) refrigerant gas

Filipe Ferreira da Silva<sup>1,\*</sup>, J. Pereria-da-Silva<sup>1</sup>, M. Mendes<sup>1</sup>, J. M. M. Araújo<sup>2</sup>, L. M. Cornetta<sup>3</sup>

<sup>1</sup> CEFITEC, Departamento de Física, Faculdade de Ciências e Tecnologia, Universidade NOVA de Lisboa, Campus de Caparica 2829-516 Caparica, Portugal,

\*E-mail: f.ferreiradasilva@fct.unl.pt

<sup>2</sup> LAQV, REQUIMTE, Departamento de Química, Faculdade de Ciências e Tecnologia, Universidade NOVA de Lisboa, Campus de Caparica 2829-516 Caparica, Portugal

<sup>3</sup> Instituto de Física Gleb Wataghin de Universidade Estadual de Campinas, 13083-859 Campinas, Brazil

Montreal protocol [1] have imposed restrictions in the emission of chlorine containing gases to the atmosphere, as the case of chlorofluorocarbons (CFCs) and hydrochlorofluorocarbons (HCFCs). The absence of chlorine or bromine atoms in the molecular structure of hydrofluorocarbons (HFCs) makes such compounds good candidates in replacing CFC and HCFC, leading to an Ozone Depletion Potential value close to zero [2-3]. Tetrafluoroethane,  $\text{CF}_3\text{CH}_2\text{F}$  (R134a), a widely used refrigerant gas, has been recognized as a promising substitute for dichlorodifluoromethane,  $\text{CCl}_2\text{F}_2$  (R12). When R12 is replaced by R134a, the global warming potential drops from 8100 to 1430, the ozone depletion potential changes from 1 to 0, and the atmospheric lifetime decreases from 100 to 14 years [4].

Electron interactions in the gas phase play a fundamental role in the atmospheric sciences. Fragmentation pathways upon low energy electron interactions to  $\text{CF}_3\text{CH}_2\text{F}$  were investigated and the electron ionization and dissociative electron attachment processes have been described [5]. The measurements allow describe the ion efficiency curves for ion formation in the energy range of 0 up to 25 eV. For positive ion formation, R134a dissociates into a wide assortment of ions, in which  $\text{CF}_3^+$  is observed as the most abundant out of seven ions with a relative intensity above 2%. The results are supported by quantum chemical calculations based on bound state techniques, electron-impact ionization models, and electron-molecule scattering simulations, showing a good agreement. Moreover, the experimental first ionization potential was found at  $13.10 \pm 0.17$  eV and the second at around 14.25 eV. For negative ion formation,  $\text{C}_2\text{F}_3^-$  was detected as the only anion formed, above 8.3 eV. In the present communication is presented the role of electrons in the dissociation of R134a, which is relevant for an improvement of the refrigeration processes as well as in atmospheric chemistry and plasma sciences.

[1] *Montreal Protocol on Substances That Deplete the Ozone Layer Montreal C* (1989)

[2] A.R. Ravishankara, A.A. Turnipseed, N.R. Jensen, S. Barone, M. Mills, C.J. Howard, S. Solomon, *Science* **263** (1994) 71

[3] S.A. Montzka, R.C. Myers, J.H. Butler, J.W. Elkins, L.T. Lock, A.D. Clarke, A.H. Goldstein, *Geophys. Res. Lett.* **23** (1996) 169

[4] V. Morcelle, A. Medina, L.C. Ribeiro, I. Prazeres, R.R.T. Marinho, M.S. Arruda, L.A.V. Mendes, M.J. Santos, B.N.C. Tenório, A.B. Rocha, A.C.F. Santos, *J. Phys. Chem. A* **122** (2018) 9755

[5] J. Pereira-da-Silva, R. Rodrigues, J. Ramos, C. Brígido, A. Botnari, M. Silvestre, J. Ameixa, M. Mendes, F. Zappa, S. J. Mullock, J. M. M. Araújo, M. T. do N. Varella, L. M. Cornetta, F. Ferreira da Silva, *J. Am. Soc. Mass Spectrom.* **32** (2021) 1459

## Structural transitions in metal nanoparticles: equilibrium-driven processes in Au and AuPd

Cesare Roncaglia<sup>1</sup>, Diana Nelli<sup>1</sup>, El Yakout El Koraychy<sup>1</sup>, Chloé Minnai<sup>2</sup> and Riccardo Ferrando<sup>3</sup>

<sup>1</sup> Dipartimento di Fisica dell'Università di Genova,  
Via Dodecaneso 33, Genova 16146, Italy

E-mail: roncaglia@fisica.unige.it, nelli@fisica.unige.it, elkoraychy@fisica.unige.it

<sup>2</sup> Molecular Cryo-Electron Microscopy Unit, Okinawa Institute of Science and Technology Graduate  
University

1919-1 Tancha, Onna-son, Kunigami-gun, Okinawa, Japan 904-0495

E-mail: chloe.minnai@oist.jp

<sup>3</sup> Dipartimento di Fisica dell'Università di Genova and CNR-IMEM,  
Via Dodecaneso 33, Genova 16146, Italy

E-mail: ferrando@fisica.unige.it

The shape of AuPd nanoalloys grown in the gas phase can be changed by tuning their composition [1]. In pure Pd distributions the dominant structures are fcc truncated octahedra (TO), while increasing the Au content there is a transition to icosahedral (Ih) structures in which Au atoms are preferentially placed on the surface. Global optimization searches and free energy calculations confirm that Ih becomes the equilibrium structure for increasing Au content and atomic stress calculations demonstrate that the driving force of this shape change is the more efficient relaxation of anisotropic surface stress in Ih compared to TO.

Gold nanoparticles with  $N=300 \div 320$  atoms are studied with global optimizations and molecular dynamics simulations. Global optimizations allow to understand that in this range there are at least two competitive structural motifs: fcc and decahedral. In particular, for every size, some isomers for both families are collected near the global minimum, and thanks to the Harmonic Superposition Approximation the probabilities as a function of temperature for each motif are calculated. From these calculations it is evident that the two structural families are almost equal in probabilities at room temperature. Molecular dynamics eventually makes even more evident this close competition, as we record in our simulations a lot of solid-solid transitions between these two structural motifs.

[1] D. Nelli, C. Roncaglia, R. Ferrando and C. Minnai, *J. Phys. Chem. Lett.* **12** (2021) 4609

**Novel software based on artificial neural networks and deep learning for automatic analysis of ionizing radiation-induced foci (IRIFs) and advanced analysis of their micro-morphological and additional parameters**

Tomáš Vičar<sup>1\*</sup>, Martin Falk<sup>2\*</sup>, Iva Falková<sup>2</sup>, Jaromír Gumulec<sup>3,4</sup>, Radim Kolář<sup>1</sup>,  
Olga Kopečná<sup>2</sup>, Eva Pagáčová<sup>2</sup>

<sup>1</sup> Department of Biomedical Engineering, Faculty of Electrical Engineering and Communications, Brno University of Technology, Brno, Czech Republic

<sup>2</sup> Department of Cell Biology and Radiobiology, Institute of Biophysics of CAS, v.v.i., Královopolská 135, Brno, Czech Republic

<sup>3</sup> Department of Pathological Physiology, Faculty of Medicine, Masaryk University Kamenice 5, Brno, Czech Republic

<sup>4</sup> Central European Institute of Technology, Brno University of Technology Purkynova 123, Brno, Czech Republic

\*E-mail: Tomas Vicar, tomasvicar@gmail.com; Martin Falk, falk@ibp.cz

Presenting Author: Iva Falkova, ivafalk@seznam.cz

Double-strand breaks of the DNA molecule, visualized by Ionizing Radiation-Induced Foci (IRIF), are the most deleterious DNA lesions, hazardous to human health. IRIF scoring based on immunofluorescence confocal microscopy represents the most sensitive and gold standard method in radiation biodosimetry. It also allows research of DSB damage induction and repair at the molecular and a single-cell level. Manual counting of IRIFs is a very time-demanding and tiring process, while manual segmentation of individual IRIFs is almost impracticable. We have developed novel deep learning-based method for segmentation of cell nuclei and IRIFs, which is capable to analyze 3D microscopy images automatically, with a fidelity comparable to visual inspection by an experienced evaluator. This is critical both for biodosimetry in clinical or radiation protection practice and radiobiological research. Moreover, as the software provides 3D segmentation of individual IRIFs and nuclei, it allows extraction of micro-morphological IRIF parameters, such as the volume, solidity or volume of the nucleus, and other IRIF parameters, including the focus intensity and mutual colocalization between IRIFs of different repair proteins. Importantly, the software can be trained for different IRIF and cell types, which is critical when analyzing cancer cells, which often show diffuse, irregular and heterogeneous IRIFs, and a high background signal.

The proposed method for IRIF and nuclei segmentation is based on U-Net convolutional neural network and maximally stable extremal region method. Training of this method requires manual segmentation of nuclei and positional label of IRIFs, where whole method is described on Figure 1. Data were acquired using Leica DM RXA microscope, where the resulting images are  $90.0 \times 67.2 \times 15 \mu\text{m xyz}$  ( $1392 \times 1040 \times 50 \text{ px}$ ). The training dataset (270 fields of views (FOVs) for nucleus segmentation and 400 for IRIFs detection) was based on patient-derived primary cell cultures prepared from spinocellular tumors and morphologically normal tissues adjacent to the tumor taken from head and neck cancer patients. The method was applied on unseen data and several features were extracted to show its potential. Results of distinction tumor vs tumor-adjacent tissue and results of distinction of various post-radiation times (0.5 h 8 h and 24 h) are shown on Figure 2, where extracted parameters are shown with principal component analysis (PCA) biplot. Principal component analysis biplot shows the dependence between these parameters. Here we show that the separation of groups (tumor vs tumor-adjacent tissue, times post-irradiation) is better compared to a separation solely by the number of foci: As the dependence between these parameters can be complex, the separation of tumor tissue and tumor-adjacent tissue in a head and neck squamous cell cancer dataset was more precise when IRIF morphology was considered together with 53BP1 intensity. In this dataset, it was also shown that the separation of times post-irradiation groups was in addition to IRIF numbers further refined by gH2AX intensity. gH2AX and 53BP1 did not colocalize and degree of colocalization between these channels can be used to further refine the separation of such groups. The proposed deep learning-based method for IRIF and nuclei segmentation is able to achieve automatic 3D segmentation of individual IRIFs and nuclei. This segmentation can be used for extraction of

## “Structure and dynamics of molecules, clusters and nanoparticles”: Tue-IV-3

various parameters, which shown to be potential beneficial for biodosimetry and allows extraction of new information for further analysis.

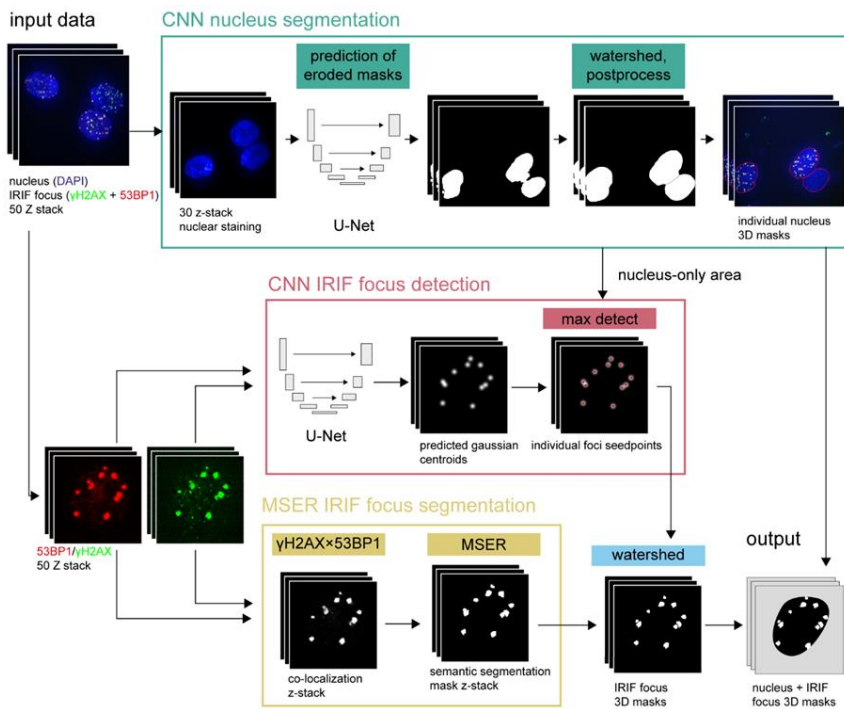


**Figure 1:** Block diagram of automatic IRIF segmentation. 3-channel images are used for a network input: one for nuclear staining and two for IRIF staining, as exemplified by DAPI staining of the nuclei (blue) and immunodetection of  $\gamma$ H2AX (green) and 53BP1 (red) IRIFs. The process is divided into three steps: First, 3D nuclei masks are created using U-Net convolutional neural network from the nucleus staining. Second, individual IRIF foci are detected using again U-Net. Third, individual foci are segmented from a multiplied z-stack composed of the two channels for IRIFs using a maximally stable extremal region method.

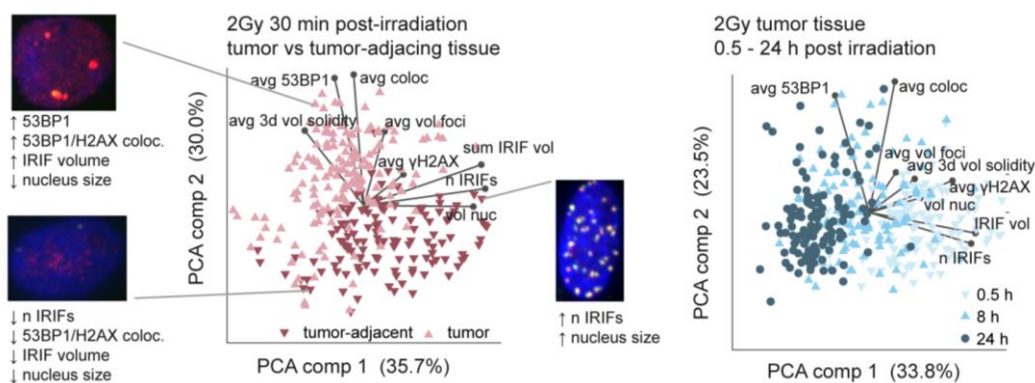


**Figure 2:** Principal component analysis biplot showing the separation of tumor-adjacent and tumor tissues and different post-irradiation times of tumor tissue and representative nuclei. Avg - average values for nuclei, n - number of, vol - volume, nuc – nucleus, 53BP1 and  $\gamma$ H2AX - average intensities of these signals.

- [1] Vicar et al., DeepFoci: Deep Learning-Based Algorithm for Fast Automatic Analysis of DNA Double Strand Break Ionizing Radiation-Induced Foci, *Bioinformatics* (2020) (bioRxiv, preprint)  
 [2] Vicar et al., Advanced Learning- Based Algorithm for Fast Automatic Analysis of DNA Double Strand Break (DSB) Repair Foci, *Comput. Struct. Biotechnol. J.* (2021) (in revision)

Projects support: GACR-20-04109J, GACR-19-09212S, Czech Government Plenipotentiary and 3 + 3 Projects, DAAD-19-03 and DFG grant H1601/16-1.

## Structural and dynamic traits of avian cryptochromes

Anders Frederiksen<sup>\*</sup>, Maja Hanić, Ilia A. Solov'yov

Department of Physics, Carl von Ossietzky University of Oldenburg,  
Carl-von-Ossietzky-Strasse 9-11, 26129, Oldenburg, Germany

<sup>\*</sup>E-mail: anders.frederiksen@uol.de

Cryptochrome (Cry) is a protein, which in the late 90s was shown to be part of the mammalian eye. It has been widely suggested as the protein responsible for the magnetoreception of birds [1-3]. Cryptochromes from different organisms have different primary amino acid sequences, hence different structures, that would result in different functional properties. Cryptochrome type 4 (Cry4) is found in migratory birds and is believed to be important for navigation during the migration period. Cryptochrome is however also found in non-migratory birds having slightly different primary sequence. The exact role of specific amino acids in cryptochrome is unknown. This study aims to unveil how certain amino acids could influence the dynamics of the protein. The investigation relies on mutating certain amino acids of interest, where mutations are done on residues which are either highly conserved or very different between migratory European robin (ErCry4) or non-migratory pigeon (ClCry4) Cryptochrome 4 [4].

The study features the results utilising documented computational methods such as analysis of the root mean square fluctuations [5] of the wild type proteins as well as their mutations, but also more original tools such as the interaction energy matrices between individual amino acid and planarity of a selected residues in the structure, see Fig. 1. The results give indications at how single amino acid mutations can influence the overall properties of the entire protein and thus could influence the functional properties of the protein.

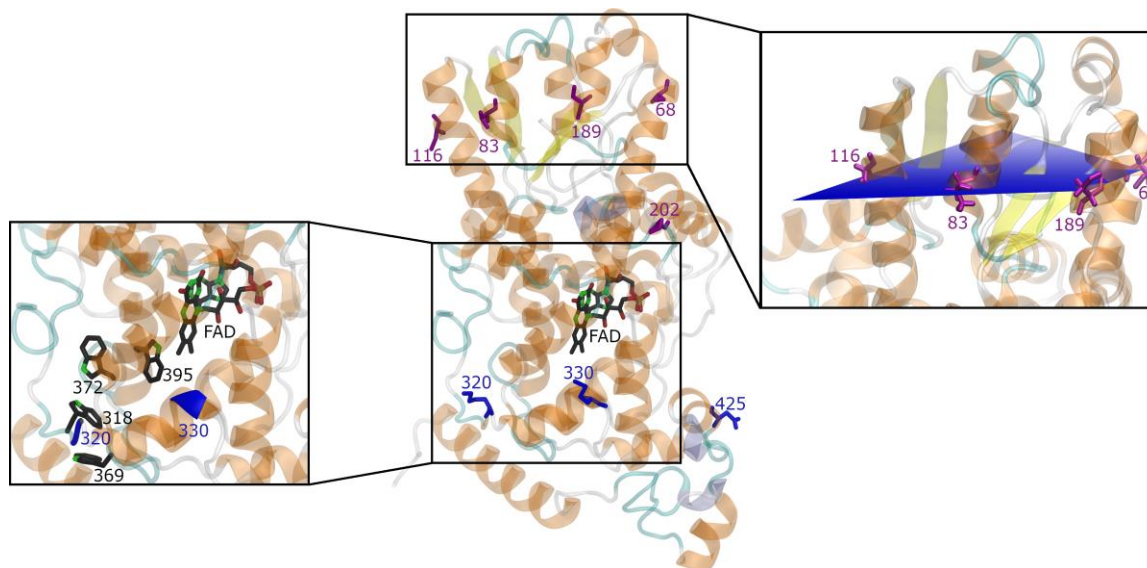


**Figure 1:** Exemplary European robin cryptochrome 4 with highlighted residues 68, 83, 116 and 189 that experience unusual planarity in the protein structure. The active site of the protein which includes the flavin adenine dinucleotide (FAD) cofactor and a chain of tryptophan residues 395, 372, 317 and 369 are also shown [6].

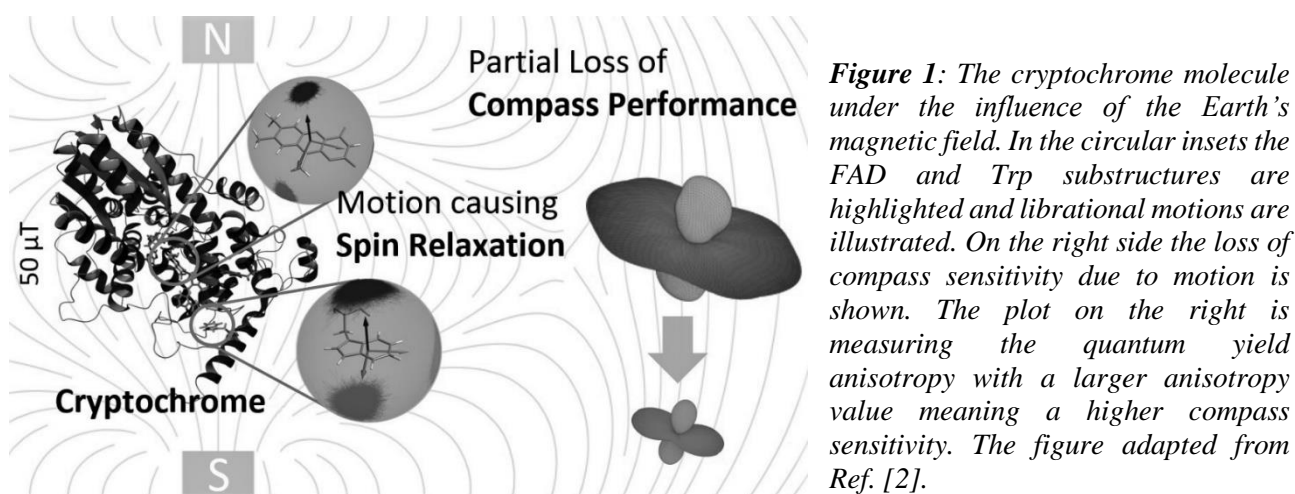
- [1] T. Ritz, S. Adem, K.A. Schulten, *Biophys. J.* **78** (2000) 707
- [2] I.A. Solov'yov, H. Mouritsen, K. Schulten, *Biophys. J.* **99** (2010) 40
- [3] P.J. Hore, H. Mouritsen, *Ann. Rev. Biophys.* **45** (2016) 299
- [4] B.D. Zoltowski et al., *Proc. Natl. Acad. Sci. U.S.A.*, **116** (2019) 19449
- [5] S. Zhang et al., ProDy 2.0: Increased scale and scope after 10 years of protein dynamics modelling with Python *Bioinformatics* (2021)
- [6] J. Xu et al., *Nature* **594**, (2021) 535

## The influence of dynamical degrees of freedom on spin relaxation in the European Robin cryptochrome

Gesa Grüning, Ilia A. Solov'yov

Department of Physics, Carl von Ossietzky University of Oldenburg,  
Carl-von Ossietzky Str. 9-11, 26129, Oldenburg, Germany  
E-mail: gesa.gruening@uol.de

The leading hypothesis how migratory birds can sense the magnetic field is based on the radical-pair mechanism [1]. To function as a compass sensor the radical pair in cryptochrome of migratory birds needs to be in a coherent state long enough for the Earth's magnetic field to have an influence. Several interactions weaken the coherence of the radical pair in a process called spin relaxation [2]. In this project we present a molecular dynamics simulation of the cryptochrome 4 protein of the European robin. Several dihedral and librational angles in the flavin adenine dinucleotide (FAD) and tryptophan (Trp) radical pair inside cryptochrome were chosen as degrees of freedom that could be responsible for subsequent spin relaxation [2] (Figure 1). Through analysis of time evolution of these parameters we have established their contribution to the coherence lifetimes of potential radical pairs inside cryptochrome. For this, the hyperfine coupling constants of the atoms in the FAD and Trp radicals were computed and their fluctuations were studied dependent on the chosen degrees of freedom. Next, the quantum yield anisotropy of the magneto-dependent reaction from the singlet state of the radical pair was calculated. The quantum yield anisotropy, which is a measure for the sensitivity of the birds' magnetic compass, was first determined without spin relaxation and then with spin relaxation by including the motion-dependent hyperfine interactions in the calculations.



The investigation allows us to conclude on the efficiency of spin relaxation in cryptochrome from a migratory bird species and allows to render an outlook if the radical pairs' coherence lifetime is sufficiently optimized by restrictions in the intraprotein dynamics to explain the magnetic sensing ability of migratory birds.

- [1] J. Xu, L.E. Jarocho, T. Zollitsch, M. Konowalczyk, K.B. Henbest, S. Richert, M.J. Golesworthy, J. Schmidt, V. Dejean, D.J.C. Sowood, et al., *Nature* **594** (2021) 535  
[2] D. Kattinig, I. A. Solov'yov, P.J. Hore, *Phys. Chem. Chem. Phys.* **18** (2016) 12443



## Ab initio informed Monte Carlo simulations of biologically relevant materials excitation spectra

Simone Taioli<sup>1,2,3</sup>, Paolo E. Trevisanutto<sup>1,2</sup>, Pablo de Vera<sup>1</sup>, Stefano Simonucci<sup>5,6</sup>, Isabel Abril<sup>7</sup>, Rafael Garcia-Molina<sup>4</sup>, Maurizio Dapor<sup>1,2</sup>

<sup>1</sup> European Centre for Theoretical Studies in Nuclear Physics and Related Areas (ECT\*-FBK), Trento, Italy

<sup>2</sup> Trento Institute for Fundamental Physics and Applications (TIFPA-INFN), Trento, Italy

<sup>3</sup> Peter the Great St. Petersburg Polytechnic University, Russia

<sup>4</sup> Departamento de Física, Centro de Investigación en Óptica y Nanofísica, Universidad de Murcia, Spain

<sup>5</sup> School of Science and Technology, University of Camerino, Italy

<sup>6</sup> INFN, Sezione di Perugia, Italy

<sup>7</sup> Departament de Física Aplicada, Universitat d'Alacant, Spain

The effective use of swift ion beams in cancer treatment (known as hadrontherapy) as well as an appropriate protection in manned space missions rely on the accurate understanding of energy delivery to cells damaging their genetic information [1]. The key ingredient characterizing the response of a medium to the perturbation induced by charged particles is its electronic excitation spectrum. By using linear response time-dependent density functional theory, we obtain the energy and momentum transfer excitation spectrum (the energy-loss function, ELF) of liquid water which is the main constituent of biological tissue, in excellent agreement with experimental data [2]. The inelastic scattering cross sections obtained from this ELF, together with the elastic scattering cross sections derived considering the condensed phase nature of the medium, are used to perform accurate Monte Carlo simulations of the energy deposited by swift carbon ions in liquid water and carried away by the generated secondary electrons producing inelastic events (ionization, excitation, and dissociative electron attachment), strongly correlated with cellular death, which are scored in sensitive volumes having the size of two DNA convolutions [2-4]. The sizes of clusters of damaging events for a wide range of carbon ion energies, from those relevant to hadrontherapy up to cosmic radiation, predict with unprecedented statistical accuracy the nature and relative magnitude of the main inelastic processes contributing to radiation biodamage, confirming that ionization accounts for the vast majority of complex damage, while DEA only adds up for a minor contribution. Applications to the calculation of the ELF and REEL spectra in radio enhancing ceria [5] and of beta-decay also in astrophysical scenarios will be shown in this talk [6,7].

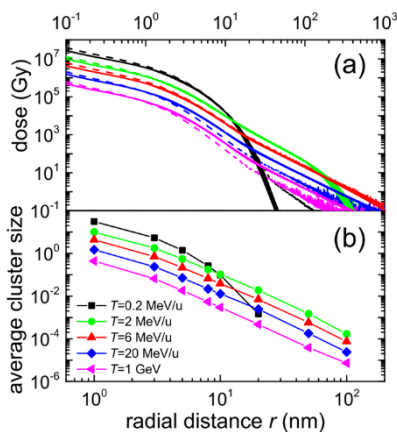


**Figure 1:** (a) Dose deposited by carbon ions in liquid water for several ion energies  $T$ . (b) Average cluster size

- [1] M. Dapor, I. Abril, P. de Vera, R. Garcia-Molina, *Phys. Rev. B* **96** (2017) 064113  
 [2] S. Taioli et al., *J. Phys. Chem. Lett.* **12** (2020) 487  
 [3] P. de Vera et al., *Cancers* (submitted, 2021)  
 [4] M. Dapor, *Transport of Energetic Electrons in Solids*, 3rd ed. (Springer, 2020)  
 [5] A. Pedrielli et al., *Phys. Chem. Chem. Phys.* **23** (2021) 19173  
 [6] T. Morresi, S. Taioli, S. Simonucci, *Adv. Theory Simul.* **1** (2018) 1870030  
 [7] S. Taioli, S. Simonucci, *Ann. Rep. Comput. Chem.* **17** (accepted, 2021)

## The change of DNA radiation damage upon hydration: In-situ observations by near-ambient-pressure XPS

Marc Benjamin Hahn<sup>1</sup>, Paul M. Dietrich<sup>2</sup>, Jörg Radnik<sup>1</sup>

<sup>1</sup>Bundesanstalt für Materialforschung und -prüfung, Berlin, Germany  
E-Mail: hahn@physik.fu-berlin.de

<sup>2</sup>SPECS Surface Nano Analysis GmbH, Berlin, Germany

X-ray photoelectron-spectroscopy (XPS) allows simultaneous irradiation and damage monitoring. Although water radiolysis is essential for radiation damage, all previous XPS studies were performed in vacuum. [1] Here we present near-ambient-pressure XPS experiments to directly measure DNA damage under water atmosphere. They permit in-situ monitoring of the effects of radicals on fully hydrated double-stranded DNA. Our results allow us to distinguish direct damage, by photons and secondary low-energy electrons (LEE), from damage by hydroxyl radicals or hydration induced modifications of damage pathways. The exposure of dry DNA to x-rays leads to strand-breaks at the sugar-phosphate backbone, while deoxyribose and nucleobases are less affected. In contrast, a strong increase of DNA damage is observed in water, where OH-radicals are produced. In consequence, base damage and base release become predominant, even though the number of strand-breaks increases further.

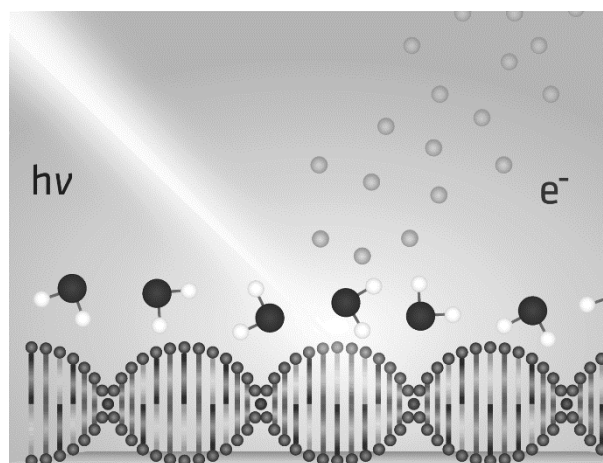


**Figure 1:** X-rays interact with hydrated DNA and eject photoelectrons. With permission from Ref. [1].

[1] M.B. Hahn, P.M. Dietrich, J. Radnik, *Commun. Chem.* **4**, (2021) 50



## Multiple valence electron detachment following Auger decay of inner-shell vacancies in gas-phase DNA

Thomas Schlathölter

University of Groningen, Zernike Institute for Advanced Materials,  
9747AG Groningen, Netherlands  
E-mail: t.a.schlatholter@rug.nl

Inner-shell ionization or excitation leading to core level vacancies is one of the first steps in many types of biological radiation damage. Therapeutic X-ray photons and electrons, protons and heavy ions at clinically relevant kinetic energies have the potential to create inner shell vacancies in DNA. In light elements such as carbon, nitrogen and oxygen,  $1s$  holes predominantly decay by Auger processes and in biological systems the interaction of Auger electrons with e.g. DNA play an important role in the evolution of radiation tracks.

The decay of inner-shell vacancies in DNA can be investigated in great detail in gas-phase studies. We have studied the interaction of soft X-rays and MeV ions at Bragg peak energies with gas-phase deprotonated DNA. We have brought  $[\text{dTGGGGT} - 2\text{H}]^{2-}$  anions into the gas-phase by means of electrospray ionization. The mass-selected oligonucleotides were then stored in a radiofrequency ion trap. The trapped ions were exposed to monochromatic soft X-rays from the U492/PGM1 beamline of the BESSY II synchrotron (Helmholtz Zentrum Berlin, Germany) or to MeV  $\text{C}^{q+}$  ions from the IRRSUD beamline of the GANIL facility (Caen, France). The interaction products were subsequently analyzed by means of high-resolution time-of-flight mass spectrometry.

The dominating decay mechanism of the X-ray induced inner shell vacancy was found to be Auger decay with detachment of at least three electrons, leading to charge reversal of the anionic precursor and the formation of positively charged photofragment ions. The same process is observed in heavy ion (12 MeV  $\text{C}^{4+}$ ) collisions with  $[\text{dTGGGGT} - 2\text{H}]^{2-}$  where inner shell vacancies are generated as well, but with smaller probability.

Auger decay of inner-shell vacancies in DNA that is not followed by single high-energy Auger electron emission but instead by removal of three or more low energy electrons has profound implications for DNA damage and damage modelling. Lower electron energies imply shorter mean free path and therefore more localized damage. Our findings therefore imply that secondary electron-induced DNA damage will be much more localized around the initial K-shell vacancy. The fragmentation channels triggered by triple electron detachment Auger decay are predominantly related to protonated guanine base loss and even loss of protonated guanine dimers is tentatively observed. The fragmentation is not a consequence of the initial K-shell vacancy but purely due to multiple detachment of valence electrons, as a very similar positive ion fragmentation pattern is observed in femtosecond laser-induced dissociation experiments.

[1] W. Li, O. Kavatsyuk, W. Douma, X. Wang, R. Hoekstra, D. Mayer, M. S. Robinson, M. Gühr, M. Lalande, M. Abdelmouleh, M. Ryszka, J.C. Poully, T. Schlathölter, Multiple valence electron detachment following Auger decay of inner-shell vacancies in gas-phase DNA, *Chemical Science* (2021) (advance article)

## **Repair focus micro- and nano architecture in DSB repair efficiency and pathway selection**

Elham Persimehr<sup>1</sup>, Lucie Dobesova<sup>1</sup>, Jiri Toufar<sup>1</sup>, Elizaveta Bobkova<sup>2</sup>, Hannes Hahn<sup>2</sup>, Charlotte Neitzel<sup>2</sup>, Ruth Winter<sup>2</sup>, Götz Pilarczyk<sup>2</sup>, Georg Hildenbrand<sup>2</sup>, Olga Kopečna<sup>1</sup>, Eva Pagacova<sup>1</sup>, Iva Falkova<sup>1</sup>, Alena Bacikova<sup>1</sup>, Tatiana Bulanova-Chramko<sup>3</sup>, Mariia Zadneprianetc<sup>3</sup>, Elena Kulikova<sup>3</sup>, Alla Boreyko<sup>3</sup>, Evgeny Krasavin<sup>3</sup>, Dieter W. Heermann<sup>4</sup>, Harry Scherthan<sup>5</sup>, Martin Falk<sup>1\*</sup>, Michael Hausmann<sup>2</sup>

<sup>1</sup> Czech Academy of Sciences, Institute of Biophysics, Brno, Czech Republic

<sup>2</sup> Kirchhoff-Institute for Physics, Heidelberg University, Heidelberg, Germany

<sup>3</sup> Joint Institute for Nuclear Research (JINR), Dubna, Russia

<sup>4</sup> Institute for Theoretical Physics, Heidelberg University, Heidelberg, Germany

<sup>5</sup> Bundeswehr Institute of Radiobiology, affiliated to the University of Ulm, Munich, Germany

\*E-mail: falk@ibp.cz

Ionizing radiation-induced foci (IRIFs) are a sensitive marker of DNA double strand break (DSB) induction and repair. A dramatic development in the field of microscopy techniques currently allows to study not only the spatio-temporal distribution and micro-morphology of IRIFs but also their internal composition and architecture at the nano-scale, i.e., molecular level. The architecture of IRIFs could be expected to be dependent on both, local chromatin architecture and ongoing repair processes at individual DSB sites. Hence, it could be hypothesized that the multi-scale IRIF nano-architecture reflects various aspects (e.g., the mechanism, efficiency, and fidelity) of DSB repair or even (co)determines repair processes, including the selection for the best repair pathway at each DSB site. The IRIF nano-architecture may thus represent a new layer in DSB repair regulation and an important aspect / marker of carcinogenesis (reviewed in [1]). In the present contribution, we were interested if the IRIF architecture depends on the DSB repair stage (i.e., post-irradiation time), local chromatin architecture at damage sites and type of the incidental radiation. As the radiosensitivity of cancer cells often differ from normal cells, we also investigated if there exist some differences in IRIF architecture, that could be correlated to differences in chromatin architecture, repair pathway activation, persistence of unrepaired DSBs and, in turn, the overall cell radiosensitivity. Combining advanced techniques of particle accelerators, 3D high-resolution immunofluorescence confocal microscopy and super-resolution microscopy (Single-Molecule Localization Microscopy, SMLM), we compared the micro- and nano-scale architecture of IRIFs in normal human skin fibroblasts (NHDF) and various cancer cells. U87 cells were involved into the study for the aggressiveness and high radioresistance of brain glioblastoma. MCF7 and SkBr3 cells were selected for the highest prevalence of mammary carcinoma in women. The cells were exposed to different doses of low-LET and high-LET radiation, respectively, and fixed at different times (5 min – 24 h) post-irradiation. Using novel mathematical approaches based on Ripley’s distance frequencies, cluster analyses, and persistence homology, we found that the nano-architecture of IRIFs formed by  $\gamma$ H2AX [2,3], 53BP1 [3-6], RAD51 and MRE11 [7,8] is protein-specific and follows the same principles in normal and cancer cells, with high mutual similarity of individual IRIFs. Interestingly, the topology was more similar for IRIFs associated with heterochromatin [9]. Together, this suggests that the internal architecture of IRIF has a functional role (reviewed in [1]). However, the IRIF assembly, extent of topological similarity and protein composition differed for normal and tumor cells [4,8], which could be correlated to repair differences and/or radiosensitivity of investigated cells.

[1] M. Falk, M. Hausmann, *Cancers* **13** (2021) 18

[2] M. Hausmann, M. Falk, C. Neitzel, A. Hofmann, A. Biswas, T. Gier, I. Falkova, D.W. Heermann, G. Hildenbrand, *Int. J. Mol. Sci.* **22** (2021) 3636

[3] M. Hausmann, C. Neitzel, E. Bobkova, D. Nagel, A. Hofmann, T. Chramko, E. Smirnova, O. Kopečná, E. Pagáčová, A. Boreyko, et al., *Front. Phys.* **8** (2020) 578662

[4] E. Bobkova, D. Depes, J.-H. Lee, L. Jezkova, I. Falkova, E. Pagacova, O. Kopečna, M. Zadneprianetc,

## “Interaction of radiation with bio-systems: mechanisms and applications”: Wed-II-1

- A. Bacikova, E. Kulikova, et al., *Int. J. Mol. Sci.* **19** (2018) 3713
- [5] D. Depes, J.-H. Lee, E. Bobkova, L. Jezkova, I. Falkova, F. Bestvater, E. Pagacova, O. Kopečna, M. Zadneprianetc, A. Bacikova, et al., *Eur. Phys. J. D* **72** (2018) 158
- [6] L. Jezkova, M. Zadneprianetc, E. Kulikova, E. Smirnova, T. Bulanova, D. Depes, I. Falkova, A. Boreyko, E. Krasavin, M. Davidkova, et al., *Nanoscale* **10** (2018) 1162
- [7] M. Eryilmaz, E. Schmitt, M. Krufczik, F. Theda, J.-H. Lee, C. Cremer, F. Bestvater, W. Schaufler, M. Hausmann, G. Hildenbrand, *Cancers* **10** (2018) 25
- [8] H. Hahn, C. Neitzel, O. Kopečná, D.W. Heermann, M. Falk, M. Hausmann, Topological Analysis of  $\gamma$ H2AX and MRE11 Clusters Detected by Localization Microscopy during X-Ray Induced DNA Double-Strand Break Repair, *Cancers* (2021)
- [9] M. Bach, C. Savini, M. Krufczik, C. Cremer, F. Rösl, M. Hausmann, *Int. J. Mol. Sci.* **18** (2017) 1726

### ACKNOWLEDGEMENT

The work was supported by the projects GACR 20-04109J, GACR 19-09212S and projects of the Czech Government Plenipotentiary and Project 3 + 3 for cooperation with JINR Dubna. The Czech-German collaboration was supported by the Heidelberg University Mobility Grant for International Research Cooperation within excellence initiative II of the Deutsche Forschungsgemeinschaft (DFG), project DAAD-19-03 and DFG grant H1601/16-1.

## Lethal DNA damage caused by heavy ion-induced shock waves in cells

Alexey Verkhovtsev<sup>1</sup>, Ida Friis<sup>2</sup>, Ilia A. Solov'yov<sup>3</sup>, Andrey V. Solov'yov<sup>1</sup>

<sup>1</sup>MBN Research Center, Altenhöferallee 3, 60438 Frankfurt am Main, Germany

<sup>2</sup>Department of Physics, Chemistry and Pharmacy, University of Southern Denmark, Campusvej 55, 5230 Odense M, Denmark

<sup>3</sup>Department of Physics, Carl von Ossietzky Universität Oldenburg, 26129 Oldenburg, Germany  
E-mail: verkhovtsev@mbnexplorer.com

The elucidation of fundamental mechanisms underlying ion-induced radiation damage of biological systems is crucial for advancing radiotherapy with ion beams and for radiation protection in space. The study of ion-induced biodamage using the phenomenon-based MultiScale Approach to the physics of radiation damage with ions (MSA) [1-3] has led to the prediction of nanoscale shock waves created by ions in a biological medium at the high linear energy transfer (LET) [4]. The high-LET regime corresponds to the keV and higher-energy losses by ions per nanometer, which is typical for ions heavier than carbon at the Bragg peak region in biological media.

The talk will overview the results of the recent study [5] that revealed that the thermomechanical stress of the DNA molecule caused by the ion-induced shock wave becomes the dominant mechanism of complex DNA damage at the high-LET ion irradiation. Damage of the DNA molecule in water caused by a projectile-ion-induced shock wave has been studied by means of reactive molecular dynamics simulations [6,7] using the MBN Explorer software package [8].

The simulations [5] have revealed that the shock-wave-induced thermomechanical stress by carbon and oxygen ions causes only a few isolated strand breaks within a DNA double twist containing 20 base pairs. Thus, the ion-induced shock wave affects the survival probabilities of cells irradiated with carbon and oxygen ions mainly via the transport of reactive species away from the ion track. At higher LET values (as in the case of irradiation with argon and especially iron ions) the thermomechanical stress induced by the shock wave becomes the dominant mechanism of DNA damage. The DNA damage produced in segments of such size leads to complex irreparable lesions in a cell [9]. This makes the shock-wave-induced thermomechanical stress the dominant mechanism of complex DNA damage at the high-LET ion irradiation. A detailed theory for evaluating the DNA damage caused by ions at high-LET has been formulated [5] and integrated into the existing MSA formalism [1-3].

The theoretical analysis [5] revealed that a single ion hitting a cell nucleus at high-LET is sufficient to produce highly complex, lethal damages to a cell by the shock-wave-induced thermomechanical stress. Accounting for the shock-wave-induced thermomechanical mechanism of DNA damage provides an explanation for the “overkill” effect observed experimentally in the dependence of cell survival probabilities on the radiation dose delivered with iron ions. This important observation provides strong experimental evidence of the ion-induced shock-wave effect [4] and the related mechanism of radiation damage in cells.

[1] E. Surdutovich and A. V. Solov'yov, *Eur. Phys. J. D* **68** (2014) 353

[2] A.V. Solov'yov (ed.), *Nanoscale Insights into Ion-Beam Cancer Therapy* (Springer International Publishing, Cham, 2017).

[3] E. Surdutovich and A. V. Solov'yov, *Cancer Nanotechnol.* **10** (2019) 6

[4] E. Surdutovich and A. V. Solov'yov, *Phys. Rev. E* **82** (2010) 051915

[5] I. Friis, A.V. Verkhovtsev, I.A. Solov'yov, and A.V. Solov'yov, Lethal DNA damage caused by ion-induced shock waves in cells, *Phys. Rev. E* (in print); see also arXiv:2103.10187 [physics.bio-ph]

[6] G. Sushko, I.A. Solov'yov, A. Verkhovtsev, S.N. Volkov, A.V. Solov'yov, *Eur. Phys. J. D* **70** (2016) 12

[7] I. Friis, A. Verkhovtsev, I.A. Solov'yov, and A.V. Solov'yov, *J. Comput. Chem.* **41** (2020) 2429

[8] I.A. Solov'yov, A.V. Yakubovich, P.V. Nikolaev, I. Volkovets, and A.V. Solov'yov, *J. Comput. Chem.* **33** (2012) 2412

[9] A. Schipler and G. Iliakis, *Nucleic Acids Res.* **41** (2013) 7589

## Realising the potential of particle therapy and nanoparticle enhanced radiotherapy

Kate Ricketts<sup>1</sup>, Gary Royle<sup>2</sup>

<sup>1</sup>Department of Targeted Intervention, UCL  
Gower Street, London WC1E 6BT  
E-mail: k.ricketts@ucl.ac.uk

<sup>2</sup>Department of Medical Physics and Bioengineering, UCL  
Gower Street, London WC1E 6BT  
E-mail: g.royle@ucl.ac.uk

Cancer particle radiotherapy is currently the fastest growing cancer treatment approach. The advantage of particles in radiotherapy, for example protons, is the healthy tissue sparing offered by their unique depth dose curves, and potential tumour dose escalation this brings. Despite the impressive results so far reported, there are still uncertainties on the delivered dose distribution owing to the impact of anatomical changes on Bragg peak position, with potential to lead to tumour underdosage or healthy tissue overdose. When you are given a weapon that demands such precision for delivery, you need to couple that with imaging techniques and delivery techniques to know exactly what you are aiming at. Additionally, the relationship between proton dose and biological effect within a complex treatment field in the patient is simply unknown at a detailed level. Current lack of theoretical and experimental data is forcing treatment plans to adopt broadly averaged parameters for estimating tumour cell killing. Ongoing research is aimed at reducing the uncertainties on proton therapy through image-guidance, adaptive radiotherapy, further study of biological properties of protons and the development of novel dose computation and optimization methods.

Nanoparticle enhanced radiotherapy (NERT) demonstrates great potential to enhance the therapeutic ratio in radiotherapy for improved patient outcomes and reduced side effects. A plethora of in vitro and in vivo studies demonstrate enhancement factors on the order of 10–100% at clinically feasible concentrations<sup>1</sup>. Despite the promising experimental results presented in the literature there has been limited clinical translation of this concept, with only two metal-based nanoformulations currently in NERT clinical trials. Lack of translation is largely due to an incohesive set of experimental parameters (unrelated broad spectra of cell lines, nanoparticle properties, nanoparticle coating, radiation characteristics) – each of which impact on radiation enhancement, and also poor consideration of in vivo factors. In order to accelerate clinical translation for patient benefit, barriers to translation must be identified in the first instance, and research driven to overcome those barriers. Mechanism discovery of NERT and standardisation of appropriate experimental methods is required to enable meaningful comparison of nanoparticle systems throughout the diverse research community. Understanding of mechanisms driving NERT will inform the correct experimental read-outs to enable comparison and mechanism-driven optimisation of nanosolutions. Monte Carlo simulations can be used to calculate the physical dose enhancement on the microscale stemming from photoelectrons and Auger electrons (the probability of these interactions increasing with atomic number of material, the original reason for using gold). However, physical models underestimate the observed biological enhancement in cellular systems.<sup>2</sup> Alternative mechanisms have been suggested including nanoparticle-induced cellular oxidative stress and enhanced production of reactive oxygen species, and modification of the cell cycle to radiosensitive phases. However, there is still no consensus nor significant evidence regarding the fundamental science governing these processes, and additional mechanisms may yet be at play. Therefore, mechanism discovery through introduction of more sophisticated methodologies not currently performed in this field such as genomics or proteomics is required and will be discussed in this talk.

[1] S. Her, D.A. Jaffray, C. Allen, *Adv. Drug Deliv. Rev.* **109** (2017) 84

[2] K.T. Butterworth et al., *Nanoscale* **4** (2012) 4830

## Crystal-based intensive gamma-ray light sources

Andrei V. Korol and Andrey V. Solov'yov

MBN Research Center,  
Altenhöferallee 3, 60438 Frankfurt am Main, Germany  
E-mail: korol@mbnexplorer.com  
E-mail: solovyov@mbnresearch.com

Possibilities and perspectives for designing and practical realization of novel gamma-ray Crystal-based Light Sources (CLS) operating at photon energies  $E_{\text{ph}} = 10^2$  keV and above (the corresponding wavelength are below 0.1 Å) that can be constructed through exposure of oriented crystals (linear, bent and periodically bent crystals) to beams of ultra-relativistic charged particles. CLSs include Channeling Radiation (ChR) emitters, crystalline synchrotron radiation emitters, crystalline Bremsstrahlung radiation emitters, Crystalline Undulators (CU) and stacks of CUs. This interdisciplinary research field combines theory, computational modeling, beam manipulation, design, manufacture and experimental verification of high-quality crystalline samples and subsequent characterization of their emitted radiation as novel LSs.

Examples of CLSs are shown in Figure 1 [1]. The synchrotron radiation is emitted by ultra-relativistic projectiles propagating in the channeling regime through a bent crystal, panel (a). A CU, panel (b), contains a periodically bent crystal and a beam of channeling particles which emit CUR following the periodicity of the bending [2]. A CU-based LS can generate photons of  $E_{\text{ph}} = 10^2$  keV– $10^1$  GeV range (corresponding to  $\lambda$  from 0.1 to  $10^{-6}$  Å). Under certain conditions, CU can become a source of the coherent light within the range  $\lambda = 10^{-2}$ – $10^{-1}$  Å. An LS based on a stack of CUs is shown in panel (c) [17].

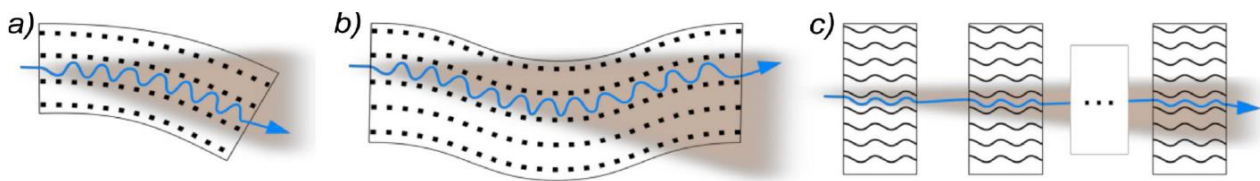


**Figure 1:** Selected examples of the novel CLSs: (a) bent crystal, (b) periodically bent crystal, (c) a stack of periodically bent crystals. Black circles and lines mark atoms of crystallographic planes, wavy curves show trajectories of the channeling particles, shadowed areas refer to the emitted radiation [1].

In an exemplary case study, the brilliance of radiation emitted in a CU-LS is estimated. Intensity of CU radiation in the photon energy range  $10^0$ – $10^1$  MeV, which is inaccessible to conventional synchrotrons, undulators and XFELs, greatly exceeds that of laser-Compton scattering LSs and can be higher than predicted in the Gamma Factory proposal to CERN [3]. The results of model approach will be compared with those of a rigorous all-atom relativistic molecular dynamics simulations carried out using the MBN Explorer software package [4,5].

[1] A.V. Korol and A.V. Solov'yov, *Eur. Phys. J. D* **74** (2020) 201

[2] A.V. Korol, A.V. Solov'yov, W. Greiner, *Channeling and Radiation in Periodically Bent Crystals*, 2nd edn. (Springer-Verlag, Berlin, Heidelberg, 2014)

[3] M. Krasny, The Gamma Factory proposal for CERN, *CERN Proc.* **1** (2018) 249

[4] I.A. Solov'yov, A. Yakubovich, P. Nikolaev, I. Volkovets, A.V. Solov'yov, *J. Comput. Chem.* **33** (2012) 2412

[5] <http://mbnresearch.com/get-mbn-explorer-software>

## Considerations on channeling of charged particles in diamond, based on experiments, simulations, and the Fokker-Planck equation

Hartmut Backe

Institute for Nuclear Physics, Johannes Gutenberg-University,  
Johann-Joachim-Becher-Weg 45, D-55128 Mainz, Germany  
E-mail: backe@uni-mainz.de

In this contribution I shall make extensive use of the continuum potential picture in the description of (110) planar channeling of  $pv = 855$  MeV electrons in a diamond single crystal. As already pointed out by Lindhard [1], this picture has some deficiencies since the electron may approach atoms comprising the plane at small impact parameters and may experience large deflections terminating the channeling process. Consequently, sophisticated simulation codes have been developed which trace the electron in the realistic atom potential [2, 3]. However, since this talk intends largely to explain channeling in a didactic way, I went this step back in comparison to modern state of the art treatments, and intend to present simulation results for the movement of channeled electron and positrons in the continuum potential picture.

In order to construct the continuum channeling potential, the electron scattering factor of carbon is required. There exist essentially the Molière [4] and the Doyle and Turner [5] approach. I stucked to the Molière approach since the scattering factor asymptotes to a Lorentzian rather than to a unrealistic Gaussians, however, with a modified parameter set which approximates the Doyle-Turner representation in the relevant region to better than 8 %. I mention that significant deviations of up to a factor 2.6 were found for small momentum transfers  $q = 4\pi s$ , with  $s < 0.2 \text{ \AA}^{-1}$  as compared with the original Molière parameters. The projected angular distribution  $p^{(at)}(\theta_x)$ , obtained after integration of the differential scattering cross-section  $d^2\sigma/d\theta_x d\theta_y$  over the vertical angular coordinate  $\theta_y$ , is shown in Fig. 1. With these ingredients the mean transverse energy increase for a homogenous medium is  $\overline{\Delta E_{\perp}/\Delta z} = (pv/2) \langle \theta_x^2 \rangle_{at} (\Delta n/\Delta z) = 0.743 \text{ eV}/\mu\text{m}$  with  $\Delta n/\Delta z = 4.31/\mu\text{m}$  the mean number of collisions per unit path length  $\Delta z$  in nominal beam direction. The latter results from the total scattering cross-section  $\sigma_{tot} = 0.00245 \text{ \AA}^2$ .

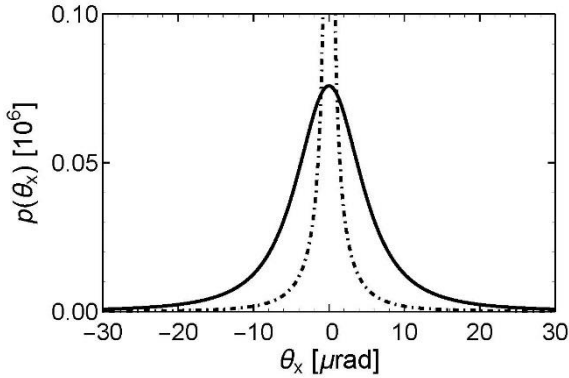


**Figure 1:** Normalized atomic (full) and electronic (dot-dashed) scattering distributions  $p^{(at)}(\theta_x)$  and  $p^{(el)}(\theta_x)$  for 855 MeV electrons at carbon. The electronic distribution is very narrow extending vertically a factor of 25.1 higher than depicted. Both distributions have long tails taken into account up to  $\pm 0.0345$  rad.

The distribution function for scattering of the particle at electrons of the atomic shell  $p^{(el)}(\theta_x)$ , has been calculated on basis of the relativistic extended Ashley model [6] making extensive use of Ref. [7]. With this model the required complex dielectric function  $\epsilon(q, \hbar\omega)$  can be constructed from the accessible optical constant  $\epsilon(q = 0, \hbar\omega)$  at momentum transfer  $q = 0$ . The very narrow distribution function  $p^{(el)}(\theta_x)$  is depicted also in Fig. 1. It is of crucial importance for de-channeling of positrons. The procedure described so far has been checked for an “amorphous” diamond foil with a thickness of 120  $\mu\text{m}$ . Good agreement with a Gaussian of a projected width parameter as taken from the Particle Data Group was found. Thus, the basic ingredients to describe scattering on carbon atoms seem to be appropriate to be applied also for channeling.



## “Propagation of particles through media”: Wed-III-2

At channeling, the electrical gradient force governs the dynamics of the particle in the potential wall, and also for the above barrier motion. Again, the particle interacts with the screened potential of the atomic nucleus as well as with the electrons of the atomic shell. A particle with transverse energy  $E_{\perp}$  at the position  $x$  experiences at moving from  $x$  to  $x + \Delta x$  a change of the transverse energy in the potential wall  $U(x)$  by

$$\Delta E_{\perp}(x) = \sqrt{2pv \cdot (E_{\perp} - U(x))} \Delta\theta_x(x) + \frac{pv}{2} (\Delta\theta_x(x))^2. \quad (1)$$

At constant step sizes  $\Delta x$  the particle moves in the longitudinal beam direction by a variable distance  $\Delta z(x) = \Delta t(x) \cdot v = \sqrt{\gamma m_e c^2} / \sqrt{2(E_{\perp} - U(x))} \Delta x$  which determines  $\Delta\theta_x(x)$  via the number of single scattering events occurring in the interval  $\Delta z(x)$ . This way  $E_{\perp}(x)$  can be traced at traversal of the electron through the crystal. Since in Eqn. (1) the quantity  $\Delta\theta_x$  has both signs, the first term results in fluctuations while the second one in a drift, i.e., both terms attribute to de-channeling while re-channeling is effected only by the first one.

Differential drift and diffusion coefficients can be define, entering as a mean over one oscillation period the Fokker-Planck equation. Both coefficients are proportional to  $(\Delta\theta_x(x))^2 / \Delta z(x)$ . The scattering angle  $\Delta\theta_x(x) = \Delta\theta_x^{(at)}(x) + \Delta\theta_x^{(el)}(x)$  has two contributions resulting from the scattering at the screened atomic potential and at the atomic shell electrons, respectively. It should be emphasized that the cross term  $2 \Delta\theta_x^{(at)}(x) \cdot \Delta\theta_x^{(el)}(x)$  has a significant impact at overlap of the corresponding atomic and electron densities although  $\Delta\theta_x^{(el)}(x)$  is small.

In the Fokker-Planck equation, the quantity  $\overline{\Delta E_{\perp} / \Delta z}$  is the relevant prefactor for the drift and diffusion coefficients. With the parametrization  $\overline{\Delta E_{\perp}^{FP} / \Delta z} = \frac{1}{2} E_S^2 / (pv X_0)$ ,  $X_0 = 12.13$  cm being the radiation length for diamond, an  $E_S = 12.4$  MeV is obtained from the above quoted value  $\overline{\Delta E_{\perp} / \Delta z} = 0.743$  eV/ $\mu\text{m}$  for the atomic interaction. It is significantly lower than 15.0 MeV as V.N. Baier et al. use in their textbook [8, p. 250], and larger than 10.6 MeV as used in our previous work [9]. It should be emphasized that this revised  $E_S$  is derived from the elementary atomic scattering cross section. It reduces the calculated de-channeling length by a factor  $(10.6/12.4)^2 = 0.73$ . Taking in addition scattering on the atomic shell electrons into account results in a further significant reduction of the de-channeling length to 21.4  $\mu\text{m}$  which deviates only by 25 % from the simulation result obtained on the basis of the MBN explorer [10].

- [1] J. Lindhard, *Mat. Fys. Medd. Dan. Vid. Selsk.* **34** (1965) 14
- [2] A.V. Korol, A.V. Solov'yov, W. Greiner, *Channeling and Radiation in Periodically Bent Crystals*, 2<sup>nd</sup> edn. (Springer Verlag, Berlin Heidelberg, 2014)
- [3] V.V. Tikhomirov, *Phys. Rev. Acc. Beams* **22** (2019) 054501 and references cited therein
- [4] G. Molière, *Z. Naturforschung* **2a** (1947) 133
- [5] P.A. Doyle and P.S. Turner, *Acta Crystall.* **A 24** (1968) 390
- [6] J.C. Ashley, *J. Electron Spectrosc. Rel. Phenom.* **28** (1982) 177
- [7] J.M. Fernández-Varea, F. Salvat, M. Dingfelder, D. Liljequist, *Nucl. Instrum. Meth. B* **229** (2005) 187
- [8] V.N. Baier, V.M. Katkov, V.M. Strakhovenko, *Electromagnetic processes at high energies in oriented single crystals*. World Scientific, Singapore (1998)
- [9] H. Backe, W. Lauth, T.N. Tran Thi, *Journal of Instrumentation (JINST)* **13** (2018) C04022
- [10] A.V. Pavlov, A.V. Korol, V.K. Ivanov, A.V. Solov'yov, *Eur. Phys. J. D* **72** (2020) 21

## Characterization of crystalline undulators at the Mainz Microtron MAMI

Werner Lauth, Hartmut Backe

Institut für Kernphysik, Johannes-Gutenberg-Universität, D-55099 Mainz, Germany

E-mail: Lauthw@uni-mainz.de

The Institute for Nuclear Physics of the University of Mainz operates the accelerator complex MAMI which supplies an electron beam with a maximum energy of 1.6 GeV and a beam current of up to 100  $\mu$ A. Outstanding qualities of MAMI is the continuous beam with an excellent beam quality of 4  $\pi$  nm rad emittance, a very low energy spread of less than  $10^{-4}$ , as well as its extremely high reliability. All kind of channeling experiments require such a high-quality beam with a divergence less than the Lindhard angle ( $< 0.3$  mrad at 1 GeV). The possibility to produce undulator-like radiation in the hundreds of keV up to the MeV region by means of channeling in periodically bent crystals is well known (see [1] for a review). In the last decade, experiments have been performed to explore the radiation emission from periodically bent  $\text{Si}_{1-x}\text{Ge}_x$  crystals and boron doped diamond crystals [2,3,4]. Due to the de-channeling length of electrons in Si of about 15  $\mu$ m at 1 GeV, only very thin crystalline undulators with short period lengths were investigated. The results will be discussed for several epitaxially grown strained layer  $\text{Si}_{1-x}\text{Ge}_x$  crystals and boron doped diamond crystals at electron beam energies between 270 and 855 MeV.

For positrons, the de-channeling length exceeds that for electrons by more than an order of magnitude allowing the use of thicker undulators with more periods. External continuous wave positron beams with the quality and intensity of the MAMI electron beam at energies of about 1 GeV are currently not available in Europe. The aim of a new project is the preparation of high-quality positron beam, which is suitable for the investigation of channeling phenomena. Generating high-energy positrons by means of Bremsstrahlung photons can be realized with high energy electrons from the MAMI accelerator. An existing beamline area with a high-current beam dump can be used to generate the positrons in a conversion target and separate them via a dipole magnet. With focusing and dispersive beam guiding elements and collimators, the beam quality can be improved. Preparatory calculations for the implementation of this project have already been carried out and will be discussed.

[1] A.V. Korol, A.V. Solov'yov, W. Greiner, *Channeling and Radiation in Periodically Bent Crystals*, 2<sup>nd</sup> edn. (Springer Verlag, Berlin Heidelberg, 2014)

[2] H. Backe, D. Krambrich, W. Lauth, K.K. Andersen, J. Lundsgaard Hansen, U.I. Uggerhøj, *J. Phys.: Conf. Ser.* **438** (2013) 012017

[3] H. Backe, D. Krambrich, W. Lauth, K.K. Andersen, J. Lundsgaard Hansen, U.I. Uggerhøj, *Nucl. Instrum. Meth. B* **309** (2013) 37

[4] H. Backe, W. Lauth and T.N. Tran Thi, *JINST* **13** (2018) C04022

Work supported by the European Commission (the PEARL Project within the H2020-MSCA-RISE-2015 call, GA 690991).

## Advancement of bent crystals technology in high-energy particle accelerators

M. Romagnoni<sup>1,2</sup>, A. Mazzolari<sup>2</sup>, L. Bandiera<sup>2</sup>, A. Sytov<sup>2</sup>, M. Soldani<sup>2,3</sup>, M. Tamisari<sup>3</sup>, V. Guidi<sup>2,3</sup>

<sup>1</sup> Università degli Studi di Milano,  
Via del Perdono 7, 20122, Milano, Italia  
E-mail: marco.romagnoni@unimi.it

<sup>2</sup> INFN Ferrara,  
Via Saragat 1, 44122, Ferrara, Italy

<sup>3</sup> Università degli Studi di Ferrara,  
Via Saragat 1, 44122, Ferrara, Italy  
E-mail: romagnoni@fe.infn.it

Bent crystals are a powerful mean for ultrarelativistic particles steering, achieving deflection equivalent to hundreds-tesla magnetic dipole in compact and zero-energy consumption devices. Currently, bent crystals are a candidate for the upgrade of LHC ion collimation.

Novel experimental setups are being proposed, especially in the field of spin precession. Indeed, the unparallel steering power of crystals enables magnetic and electric dipole moment studies on fast decaying particles like charmed baryons. Axial phenomena such as stochastic deflection and new materials such as Ge are also being tested as innovative solutions for future hadronic and leptonic accelerators (FCC, ILC and muon colliders). In the laboratories of the University of Ferrara and INFN, several prototypes for such applications have been developed.

Design of bending mechanisms and fabrication process for samples are described, as well as curvature and lattice quality measurements. Finally, results are presented regarding testbeams performed at H8 and H4 extracted beamline of SPS at CERN, where steering performances are tested on 180 GeV/c  $\pi^+$  and 120 GeV/c  $e^\pm$  beams.

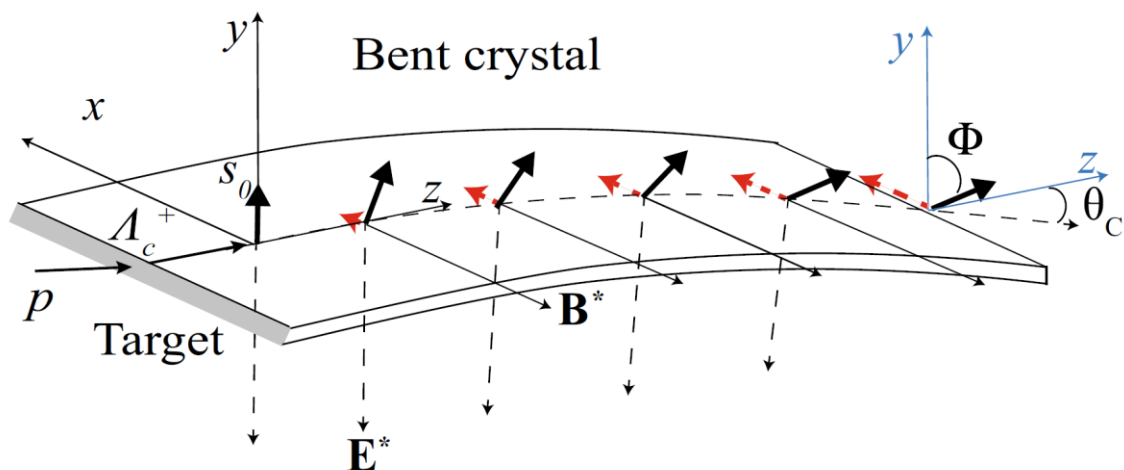


**Figure 1:** Scheme of spin precession of a charmed baryon  $A_c$  during planar channel in a bent crystal as proposed in the SELDOM project.

## Pulsed laser melting processes for nanoscale doping and strain control

D. De Salvador<sup>1,2</sup>, E. Napolitani<sup>1,2</sup>, C. Carraro<sup>1,2</sup>, F. Sgarbossa<sup>1,2</sup>, E. Di Russo<sup>1</sup>, G. Maggioni<sup>1,2</sup>, S. M. Carturan<sup>1,2</sup>, W. Raniero<sup>2</sup>, S. Bertoldo<sup>2</sup>, D.R. Napoli<sup>2</sup>

<sup>1</sup> Dipartimento di Fisica e Astronomia, Università di Padova, Via Marzolo 8, I-35131 Padova, Italy  
E-mail: [davide.desalvador@unipd.it](mailto:davide.desalvador@unipd.it)

<sup>2</sup> National Institute for Nuclear Physics INFN, Laboratori Nazionali di Legnaro, Viale dell'Università 2, 35020 Legnaro, Italy

The investigation of innovative dynamical processes for the fabrication of highly doped, strain-controlled Si and Ge layers is currently a hot topic in many applicative fields such as nanoelectronics, photonics, and radiation detectors and may furnish new tools for modulated crystal bending. Pulsed laser melting (PLM) is an out-of-equilibrium process that we currently investigate to activate a high number of foreign atoms in semiconductor crystals. PLM consists in the temporary melting of a single crystal to a depth from few nm to some microns by means of a high intensity UV laser pulse. During the following epitaxial growth that occurs in about 100ns during the sample cooling, foreign atoms deposited on the surface may diffuse and get incorporated into the layer.

Much research revealed different positive effects of such a technique. i) The out-of-equilibrium drop of segregation coefficient can bring to a very high electrical activation in narrow region both of p and n type. In conjunction with monolayer deposition of the dopant precursor, this can make the nanoscale doping procedure relevant for nanoelectronics [1]. Moreover, the high doping may transform germanium in a plasmonic material for sensor applications, or in an optical active material thanks to the direct gap transition that occurs at high doping and high strain. A high p-type dopant is demonstrated to induce a superconductive transition in germanium. ii) We demonstrated that PLM preserve the material purity during doping processes, due to the very rapid, low thermal budget process [2,3]. This aspect is relevant, especially when high purity germanium (HPGe) is used for gamma detector for nuclear spectroscopy and gamma imaging applications. iii) The high doping or alloying induced by PLM in surface layers demonstrated a strong effect on the strain [4]. In this talk we will propose some methods that could be used to induce a laterally modulated strain layer by combination of lithography and PLM. In principle the laser pulse of PLM can be laterally modulated by direct masking of the incoming beam with a lateral resolution of few tenths of microns. This resolution can be increased by patterning the dopant source reaching in principle micron resolution.

[1] F. Sgarbossa et al., *Nanotechnology* **29** (2018) 465702

[2] V. Boldrini et al., *J. Phys. D: Appl. Phys.* **52** (2018) 035104

[3] S. Bertoldo, *Eur. Phys. J. A* **57** (2021) 177

[4] C. Carraro et al., *Appl. Surf. Sci.* **509** (2020) 145229

## **Revealing single crystal quality by insight Diffraction Imaging technique**

Thu Nhi Tran Thi

European Synchrotron Radiation Facility, BP 220, 38043, Grenoble, France

E-mail: thu-nhi.tran-thi@esrf.fr

X-ray Bragg diffraction imaging (“topography”) entered into practical use when Lang<sup>1</sup> designed an “easy” technical setup to characterise the defects / distortions in the high perfection crystals produced for the microelectronics industry. The use of this technique extended to all kind of high-quality crystals, and deposited layers, and a series of publications explained, starting from the dynamical theory of diffraction, the contrast of the images of the defects.

A quantitative version of “monochromatic topography” known as “Rocking Curve Imaging” (RCI) was implemented, by using synchrotron light and taking advantage of the dramatic improvement of the 2D-detectors and computerised image processing. The rough data is constituted by a number (~ 300) of images recorded along the diffraction (“rocking”) curve. If the quality of the crystal is such that a one-to-one relation between a pixel of the detector and a voxel within the crystal can be established (this approximation is very well fulfilled if the local mosaic spread of the voxel is  $< 1$  mradian), a software we developed provides, from the each rocking curve recorded on each of the pixels of the detector, not only the “voxel” integrated intensity (the only data provided by the previous techniques), but also its “mosaic spread” (FWHM) and peak position. We will show, based on many examples, that this new data, never recorded before, open the field to a highly enhanced characterization of the crystal and deposited layers. These examples include the characterization of dislocations and twins occurring during silicon growth, various growth features in  $\text{Al}_2\text{O}_3$ , GaN and CdTe (where the diffraction displays the Borrmann anomalous absorption, which leads to new type of images), and the characterisation of the defects within deposited layers, or their effect on the substrate.

We could also observe (due to the very high sensitivity of the setup installed on BM05, which allows revealing these faint effects) that, when dealing with very perfect crystals, the Kato’s interference fringes predicted by dynamical theory are also associated with very small modifications of the local FWHM and peak position (of the order of the  $\mu$ radian). This rather unexpected (at least for us) result appears to be in keeping with preliminary dynamical theory calculations.

---

<sup>1</sup> A reference book for dynamical theory, Borrmann effect and diffraction topographic techniques (excluding RCI) is: André Authier, Dynamical Theory of X-Ray Diffraction, Oxford University Press (2001)

## Positronium collisions with molecules: Free-electron-gas model

I. I. Fabrikant<sup>1</sup>, R. S. Wilde<sup>2</sup>

<sup>1</sup>Department of Physics and Astronomy  
University of Nebraska-Lincoln, Lincoln, NE 68588, USA  
E-mail: ifabrikant@unl.edu

<sup>2</sup>Department of Natural Sciences  
Oregon Institute of Technology, Klamath Falls, OR 97601, USA  
E-mail: Robyn.Wilde@oit.edu

Since the discovery [1] of similarity between electron and positronium (Ps) scattering by atoms and molecules, a lot of theoretical effort has been directed at explaining this intriguing phenomenon. Since the static potential between Ps and neutral atom or molecule is zero, inclusion of exchange and correlation in these processes is particularly important. Exact inclusion of electron exchange in Ps collisions with atoms and molecules is a very challenging task and has been accomplished only for simple targets such as the hydrogen atom and rare-gas atoms [2]. An even more challenging problem is incorporation of short-range correlations in Ps-atom and Ps-molecule scattering. Using the pseudopotential method [3], we showed that the similarity between electron and Ps scattering can be explained by the dominance of the electron exchange interaction at intermediate energies. However, at lower energies, below the threshold of Ps ionization (break-up) results for Ps and electron scattering differ because of the difference in the long-range interactions: polarization interaction in the case of electron collisions and van der Waals interaction in the case of Ps collisions. In particular the theoretical cross sections for Ps collisions with rare-gas atoms do not exhibit the Ramsauer-Townsend minimum [4].

Recently we developed a method [5] of inclusion of electron exchange and correlations in Ps-atom and Ps-molecule collisions based on the free-electron-gas model for target electron. From the target charge density, we can use the Thomas-Fermi relation to obtain local exchange and correlation scattering potentials. The method allows us to obtain the resonance in Ps-N<sub>2</sub> scattering similar to the resonance in *e*-N<sub>2</sub> scattering [6]. The result agrees reasonably well with the experiment, but the position of the resonance is somewhat shifted towards lower energies, probably due to the fixed-nuclei approximation employed in the calculations. The partial-wave analysis of the resonant peak shows that its composition is more complex than in the case of *e*-N<sub>2</sub> scattering. We have also predicted resonances in Ps collisions with O<sub>2</sub> and CO<sub>2</sub> molecules [7]. Details of these calculations and their results will be discussed at the conference.

[1] S.J. Brawley, S. Armitage, J. Beale, D.E. Leslie, A.I. Williams, and G. Laricchia, *Science* **330**, (2010) 789

[2] G. Laricchia and H.R.J. Walters, *Riv. Nuovo Cimento* **35** (2012) 305

[3] I.I. Fabrikant and G.F. Gribakin, *Phys. Rev. A* **90** (2014) 052717

[4] R.S. Wilde and I.I. Fabrikant, *Phys. Rev. A* **98** (2018) 042703

[5] I.I. Fabrikant and R.S. Wilde, *Phys. Rev. A* **97** (2018) 052707

[6] R.S. Wilde and I.I. Fabrikant, *Phys. Rev. A* **97** (2018) 052708

[7] R.S. Wilde, H.B. Ambalampitiya and I.I. Fabrikant, *Phys. Rev. A* **104** (2021) 012810

## Soft X-ray spectroscopy of peptides and porphyrins

Lucas Schwob, Kaja Schubert, Simon Dörner, Amir Kotobi, Sadia Bari

Deutsches Elektronen-Synchrotron DESY,  
Notkestr. 85, 22607, Hamburg, Germany  
E-mail: [sadia.bari@desy.de](mailto:sadia.bari@desy.de)

Peptides and Protein are the basis of life. Metalloporphyrins, composed of a porphyrin ring coordinating metal ion in the ring cavity center, are widely found in nature as well, e.g. in metalloproteins. To gain new insights into the properties of those biomolecules, soft X-ray absorption spectroscopy experiments have been carried out at synchrotron facilities, offering a large photon energy range and a high photon flux. In particular, near-edge X-ray absorption mass spectrometry (NEXAMS), which is an action-spectroscopy technique based on the resonant photoexcitation of core atomic levels, has been of growing interest in recent years for investigating the spatial and electronic structure of biomolecules. It has been used successfully to unravel different aspects of the photodissociation of peptides and to probe conformational features of proteins. The experiments are carried out in the gas phase, thus allowing for control over the chemical state and molecular environment of the molecules. Comparison between NEXAMS spectra and quantum mechanical calculations reveal indeed further insights into the electronic and spatial structures of peptides [1] and metalloporphyrins [2].

[1] S. Dörner, L. Schwob, K. Atak, K. Schubert, R. Boll, T. Schlathölter, M. Timm, C. Bülow, V. Zamudio-Bayer, B. von Issendorff, J. T. Lau, S. Techert, S. Bari, *J. Am. Soc. Mass Spectrom.* **32** (2021) 670

[2] K. Schubert, M. Guo, K. Atak, S. Dörner, C. Bülow, B. von Issendorff, S. Klumpp, J. T. Lau, P. S. Miedema, T. Schlathölter, S. Techert, M. Timm, X. Wang, V. Zamudio-Bayer, L. Schwob, S. Bari, *Chem. Sci.* **12** (2021) 3966



## Towards the analysis of attosecond dynamics in complex systems

P.-G. Reinhard<sup>1</sup> and E. Suraud<sup>2,3</sup>

<sup>1</sup>Institut für Theoretische Physik, Universität Erlangen, Staudtstr.7, D-91058 Erlangen, Germany

<sup>2</sup>Laboratoire de Physique Théorique, UMR 5152, Université Paul Sabatier,  
118 route de Narbonne, F-31062 Toulouse Cedex, France

<sup>3</sup>School of Chemistry and Chemical Engineering, Queen’s University Belfast,  
Belfast BT7 1NN, United Kingdom

The progress in laser technology over the last decades has opened up new avenues for the exploration of properties of clusters and molecules. A laser pulse is characterized by its frequency but also by the laser intensity as well as the laser time profile. The latter can now be tailored up to time scales of the order of magnitude of electronic motion and even below. This allows the follow up of the detail of electronic dynamics at its own “natural” time. We shall focus in this presentation on the recent explorations of electron dynamics down to the attosecond time scale. Some experimental cases can be well reproduced by time dependent microscopic theories. For accessing a detailed explanation of observed trends, we introduce a schematic model which surprisingly enough provides a remarkable account of experimental trends. It shows in particular that the response of the system is heavily biased by properties of the laser used for exciting and testing the system, especially its IR component. Using the ideas developed in the schematic model we can reanalyze former computed data and show how much one can attain system's properties.

We then focus on a specific pump and probe setup. By recording observables of electron emission, we analyze the response of small metal clusters and organic molecules to a pump probe setup using an IR fs laser pulse as pump followed by an attosecond XUV pulse as probe. As observables, we consider total ionization, average kinetic energy from Photo Electron Spectra (PES) and anisotropy parameters from Photo-electron Angular Distributions (PAD). We show that these signals can provide a map of the system's dynamical properties. The connection is especially simple for metal clusters in which the response is dominated by the Mie surface plasmon. The case of organic molecules is more involved due to the considerable spectral fragmentation of the underlying dipole response. But at least the dipole anisotropy from PAD provides a clean and robust signal which can be directly associated to system's properties even reproducing non-linear effects such as the change of spectra with excitation strength [6].

[1] U. Saalman, C. Siedschlag, J. M. Rost, *J. Phys. B* **39** (2006) R39

[2] Th. Fennel et al., *Rev. Mod. Phys.* **82** (2010) 1793

[3] C. Neidel et al., *Phys. Rev. Lett.* **111** (2013) 033001

[4] C.-Z. Gao et al., *Phys. Chem. Chem. Phys.* **19** (2017) 19784

[5] T. Brabec et al., *Eur. Phys. J. D* **73** (2019) 212

[6] P.G. Reinhard, E. Suraud, *Eur. Phys. J. D* **74** (2020) 162

## Statistical vs. non-statistical emission of electrons from hot anions

Juraj Fedor

J. Heyrovský Institute of Physical Chemistry, Czech Academy of Sciences,  
Dolejškova 3, 18223 Prague, Czech Republic  
E-mail: juraj.fedor@jh-inst.cas.cz

We address a question of the decay dynamics of resonances formed in electron molecule collisions. Typically, a lifetime of such resonance towards electron detachment lies in a femto- to pico-second time domain. However, in polyatomic molecules an efficient intramolecular vibrational redistribution (IVR) prior to the electron detachment can lead to the electronic stabilization of the resonance and create a vibrationally hot molecular anion. The total energy of such complex lies in the continuum and it can decay via competing statistical processes.

Our main experimental tool is a 2D electron energy loss spectroscopy, where we control energy of the incident electrons, collide them with the molecular target and monitor the residual energy of scattered electrons. Such 2D map provides a complete picture of the inelastic scattering processes. I will focus on processes involving IVR and slow-electron emission. This is observed in number of molecules and can be described by the Weisskopf model for particle emission which is based on the detailed balance principle.

However, in addition to the thermal signal, in very few molecules we have observed emission of electrons with preference for finite non-zero residual energies. This is a signature of a mode-specific electron autodetachment, most probably happening on the timescale longer than IVR. We suggest a mechanism for this process involving electron emission via non-valence anion states [1].

[1] C. S. Anstöter et al., *Phys. Rev. Lett.* **124** (2020) 203401

## Ultrafast relaxation of photoexcited “hot” electrons in fullerene materials

Himadri Chakraborty<sup>1</sup>, Mohamed Madjet<sup>1,2</sup>, Esam Ali<sup>1</sup>, Ruma De<sup>1</sup>

<sup>1</sup> Department of Natural Sciences, D. L. Hubbard Center for Innovation, Northwest Missouri State University  
Maryville, Missouri 64468, USA  
E-mail: himadri@nwmissouri.edu

<sup>2</sup> Bremen Center for Computational Materials Science, University of Bremen  
2835 Bremen, Germany

Ultrafast studies of the dynamics of photoinduced “hot” electron relaxation in fullerenes and endofullerenes are valuable in organic photovoltaics that use these materials [1], besides their fundamental scopes. With the possibility of easy production of gas-phase C<sub>60</sub> and with remarkable advances in synthesis methods of endohedral C<sub>60</sub> in gas phase, in solution or as thin films [2], these systems render eminent natural laboratories to probe the relaxation process. First, they can support surgical level-to-level excitations. Second, they can showcase the pristine decay and charge transfer or even charge oscillation dynamics between atom and C<sub>60</sub>. Third, the details of the transient intermediate state populations can potentially map out excited state structures. Therefore, these molecules can be of particular appeal for both ultrafast transient absorption spectroscopy and time-resolved photoelectron spectroscopy.

We consider two rather attractive endofullerene systems: Mg@C<sub>60</sub> and Li@C<sub>60</sub>. For the former, we follow the electron relaxation after an initial localized photoexcitation in Mg by nonadiabatic molecular dynamics simulations. This leads to an ultrafast decay and charge transfer from Mg to C<sub>60</sub> – the formation of a nonlocal atom-to-fullerene excitonic state. The result further elicits a transient trap of the transferred electron that can delay the electron-hole recombination. Figure 1 depicts a cartoon of Mg 3s→3p photoexcitation in Mg@C<sub>60</sub>. It also presents simulated energy-time spectrogram of the decay of the initial excited state and the subsequent population dynamics during the relaxation including the charge transfer and transient captures [3]. In general, the decay and transfer times are found to be in ten’s of femtoseconds (fs) while that for transient events to be longer than 100 fs.

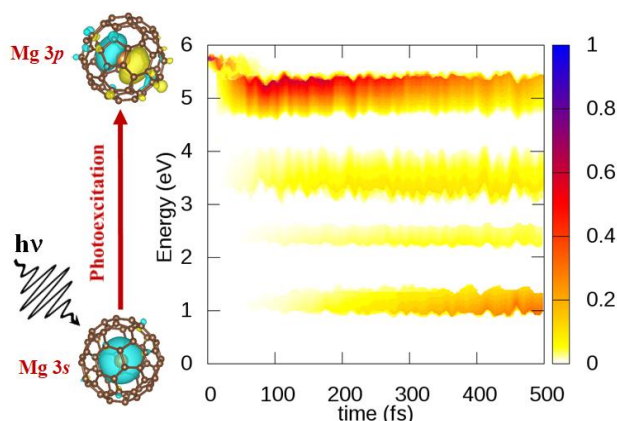


**Figure 1:** Energy-time map of Mg@C<sub>60</sub> transient excited electronic state population from DFT/B3LYP level.

For Li@C<sub>60</sub> on the other hand, the lone Li electron is found to transfer to C<sub>60</sub> already at the ground state. However, after inducing a photoexcitation in C<sub>60</sub>, the electron transfers in ultrafast scale to Li and to latch on to the empty Li 2s state to form a fullerene-to-atom *reverse* exciton. The simulation reveals that, remarkably, for Li@C<sub>60</sub> this excitonic state is very long-lived. I will present some of these results in the talk.

The research is supported by the US National Science Foundation grant PHY-1806206, PHY-2135107, and Bartik High-Performance Cluster under National Science Foundation Grant CNS-1624416, NWMSU.

[1] S. Collovini and J. S. Delgado, *Sust. En. Fuels* **2** (2018) 2480

[2] A. Popov, *Nanostruc. Sc. Tech. Ser. (Springer)* (2017)

[3] M. Madjet, E. Ali, M. Carignano, O. Vendrell, and H.S. Chakraborty, *Phys. Rev. Lett.* **126** (2021) 183002

## Reaction in selected molecular films induced by low energy electrons

Hassan Abdoul-Carime

Université de Lyon, Université Lyon 1, F-69003 Lyon, France  
E-mail: hcarime@ipnl.in2p3.fr

The last two decade has seen the emergence of applications in various fields of research [1] (e.g., radiation biology and radiotherapy, astrochemistry or nano-lithography) involving low energy ( $< 20$  eV) electrons. The gas phase experiments provide valuable information on the intrinsic collision process (Dissociative Electron Attachment, DEA) which is now well established theoretically [2] and a very large number of molecules in relation to the potential applications have been studied. In DEA process, the formed temporary anion by electron attachment to the target molecule undergoes dissociation into a negative fragment and at least one neutral counterpart.

In condensed media or cluster of molecules, DEA may change (e.g., shift in the resonance positions, suppression or enhancement) since the presence of the environment. Most of all, the negative ion fragment as well as the neutral counterparts may undergo subsequent reaction leading to new products [3]. It is this “chemical synthesis” aspect that will be discussed through some examples [4].

[1] I. Fabrikant et al., *Adv. Atomic, Mol. Optical Phys.* **66** (2017) 545 (2017); O. Ingolfsson (ed.), *Low Energy Electron, Fundamentals and Applications* (Pan Stanford Publishing, 2019)

[2] I.I. Fabrikant, *EPJ Web Conf.* **84** (2015) 07001

[3] E. Bölher, J. Warneke, P. Swiderek, *Chem. Soc. Rev.* **42** (2013) 9219

[4] H. Abdoul-Carime et al., *J. Phys. Chem. C* **122** (2018) 24137; G. Thiam et al., *J. Phys. Chem. C* **124** (2020) 20874

## An operando FTIR to monitor the reaction mechanism of adsorbed molecular species in chemoresistive devices

Vincenzo Guidi<sup>1</sup>, Matteo Valt<sup>1</sup>, Michele Della Ciana<sup>2</sup>, Barbara Fabbri<sup>1</sup>, Andrea Gaiardo<sup>3</sup>,  
Elena Spagnoli<sup>1</sup>

<sup>1</sup> Department of Physics and Earth Sciences, University of Ferrara, Via G. Saragat 1/C, 44122, Ferrara, Italy  
E-mail: [guidi@fe.infn.it](mailto:guidi@fe.infn.it); [matteo.valt@unife.it](mailto:matteo.valt@unife.it); [barbara.fabbri@unife.it](mailto:barbara.fabbri@unife.it)

<sup>2</sup> Institute for Microelectronics and Microsystems IMM-CNR, via Gobetti 101, 40129, Bologna, Italy  
E-mail: [dellaciana@bo.imm.cnr.it](mailto:dellaciana@bo.imm.cnr.it)

<sup>3</sup> MNF - Micro Nano Facility unit, Sensors and Devices center, Bruno Kessler Foundation,  
Via Sommarive 18, 38123, Trento, Italy  
E-mail: [gaiardo@fbk.eu](mailto:gaiardo@fbk.eu)

The increasing demand for precise detection of gaseous molecules towards diverse applications, such as air quality monitoring, breath and health analyses or precision agriculture, has led to expanding research for high-performance semiconductor-based chemical sensors. Indeed, although these devices suffer from several unsolved drawbacks, such as the not well-defined selectivity, lack of stability and cross-sensitivity to humidity, they reach popularity thanks to their low cost of production, small size and ability to be easily integrated into microelectronic platforms. Besides, the employment of nanostructured materials in thick or thin sensing films has stimulated the development of chemiresistive gas sensors during the last two decades. Indeed, it has been demonstrated that a change of morphological characteristics in nanostructured materials, such as particle or crystallite size, leads to a change of active surface area and ultimately to the gas sensor sensitivity. Therefore, in the case of nanostructured materials, it becomes fundamental to deeply investigate the chemical phenomena occurring at the sensing film surfaces while analyzing the connected variations of the electronic structure and sensing characteristics. This correlation between surface chemistry and electronic properties has become critical in chemical sensors since it represents the core of the gas-detection mechanism.

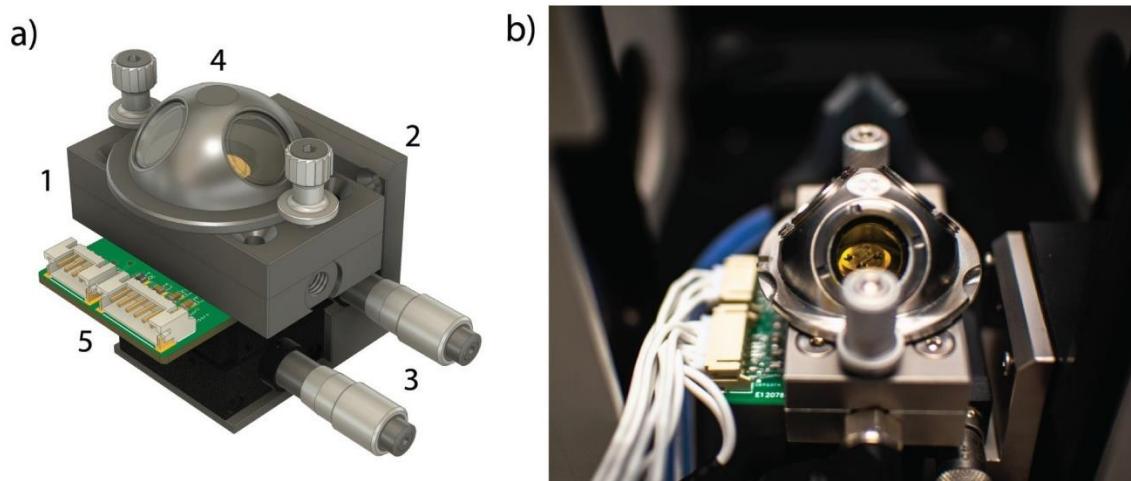


**Figure 1:** (a) 3D drawing and (b) photograph of the operando test chamber. The chamber is composed by three parts: the main cell body (1 in Fig. 1a), a cell support (2 in Fig. 1a) and a vacuum compatible precision XY micro-stage (Standa) (3 in Fig. 1a). Two Viton O-ring provide a seal between each of the two cell body components and the IR dome (4 in Fig. 1a). Connections for electrical measurements, sensor heating and T/RH% measurements are established via JST connector (5 in Fig. 1a).

Among the arsenal of characterization tools available to support mechanistic proposals, Fourier-transform infrared spectroscopy (FTIR) spectroscopy has been known for several years for the investigation of surface chemistry of nanostructured materials. Accordingly, a variety of cells for in situ and operando spectroscopy have been developed over the years for transient catalytic investigations. However, efforts from

## “Cluster-molecule interactions, reactivity and nanocatalysis”: Thu-III-1

a few research groups have been devoted to the development of a dedicated and optimized chemiresistive gas sensor testing chamber.

Thus, a reliable sensing chamber must fulfil some basic requirements: it must be able to read-out the sensor as well as to heat the film, the electrical connections for the sensing electrodes and the heating element should not interfere with the simultaneous spectroscopic characterization and the chamber must allow direct treatments and high-temperature spectroscopy measurements in controllable gas atmospheres. We designed, fabricated, and validate a new gas sensing system that is easy to use and maintain (Figure 1) [1, 2]. This can be employed with solid-state gas sensors with operating temperatures up to 650 °C, it is equipped with a precision stage for the alignment of the sample, and it is fully compatible with Harrick Scientific's diffuse reflection optics.

[1] M. Valt, M. Della Ciana, B. Fabbri, D. Sali, A. Gaiardo, and V. Guidi, *Sensors and Actuators B* **341** (2021) 130012

[2] M. Della Ciana, M. Valt, B. Fabbri, P. Bernardoni, V. Morandi and V. Guidi, *Rev. Sci. Instrum.* **92** (2021) 074702

## On the potential of immobilizing active species for energy and sensing applications

A.E.H. Wheatley, K.J. Jenkinson, A. Wagner, N. Kornienko, E. Reisner

Yusuf Hamied Department of Chemistry, University of Cambridge,  
Lensfield Road, Cambridge, CB2 1EW, UK  
E-mail: aehw2@cam.ac.uk

**Introduction.** Anisotropic nanoparticles (NPs) show asymmetric morphology; one recently presented subset boasting relatively high surface areas being nanopods [1]. These exhibit branched morphologies. For example, octopods (OPs) are cube-based nanopods overgrown at the vertices to give eight branches [2]. Considering the wealth of desirable properties of Pt and its alloys, they are ideal targets for morphology development aimed at yielding catalytically active and potentially magnetically recyclable nanopods.

Prior art has shown that the efficacy of Pt for promoting the oxygen reduction reaction (ORR) can be improved by forming mixed bimetallic NPs such as (Fe/Ni/Co)Pt or Pt-Fe<sub>3</sub>O<sub>4</sub> dumbbell architectures [3]. Moreover, composition and structure-driven improvements in catalytic activity have inspired a new generation of catalysts with branched architectures, e.g. FePt OPs. However, simultaneous control of composition *and* morphology in one synthetic step is essential for the formation of advanced nanoarchitectures, and this remains elusive [4].

This presentation outlines efforts to make complex heterobimetallic NPs by simultaneous reduction of Pt(II) and decomposition of an Fe(0) complex [3]. Control will be exerted over faceting and alloying in heterodimeric nanodumbbells. Notably, this one-pot method will avoid the need for etching or additives to induce anisotropic particles. The approach offers selective generation of a faceted heterostructure, compositional control and systematic morphology variation.

**Faceted dumbbell structure.** Given the ease of faceted NP formation achievable with equimolar oleic acid (OA) and oleylamine (OAm) [4], FePt alloys were targeted with various surfactant ratios. Simultaneous reaction of Pt(II) and Fe(0) in 1:1 OA:OAm gave the expected Pt-rich particles. However, using excess OAm gave remarkable faceted heterodimer dumbbells. Scanning TEM-high angle annular dark field (STEM HAADF) imaging (Figure 1) reveals retention of a bright OP morphology and the addition of a darker cubic phase (octopod cubic dumbbell, OPD<sub>c</sub>).

Consistent with prior art [2], data suggest an OA and OAm mixture promotes overgrowth at the cube corners of a cuboctahedral FePt seed. However, the current work also shows that varying OA:OAm allows OPD<sub>c</sub> composition to be manipulated; excess OAm appears to promote an iron oxide phase. EDX confirms that this cubic lobe is Pt-free and suggests that the OP lobe comprises equimolar Fe and Pt. The OPD<sub>c</sub> particles are therefore considered to comprise an FePt octopod, and a cube of Fe, which oxidizes. This understanding made it possible to fabricate pure, equimolar FePt OP (OP<sub>FePt</sub>) NPs using 25:75 OA:OAm and half as much Fe(0). Meanwhile, the isolation of dendrite-dumbbell, DD<sub>c</sub>, where the OP lobe is replaced by a Pt-rich dendrite, occurs if lower temperatures are used – again since Fe reagent levels are depleted. Overall, these data point to the selective manipulation of the FePt component of a dumbbell [5].

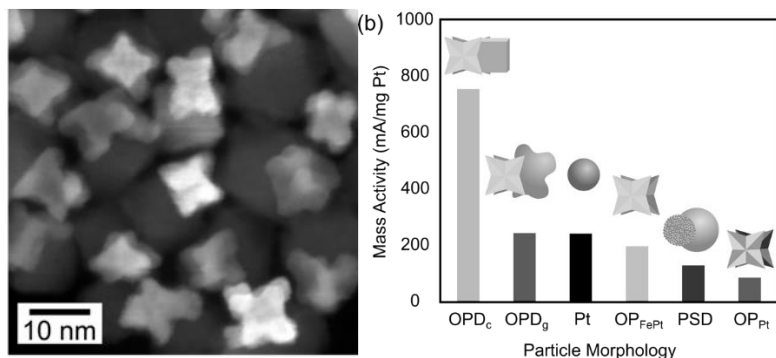


**Figure 1:** OPD<sub>c</sub> structures imaged by STEM HAADF (left). Mass activity of various immobilized FePt and FePt-Fe<sub>3</sub>O<sub>4</sub> NPs and of a Pt standard in ORR at -0.2 V (right).



## “Cluster-molecule interactions, reactivity and nanocatalysis”: Thu-III-2

**ORR performance.** OPD<sub>c</sub> NPs demonstrate three traits of interest in catalytic ORR; selective faceting, high surface area, and heterojunctions offering unique active sites. They have therefore been tested for electrocatalytic ORR in alkaline media. Their activity has been compared with those of structures exhibiting only one of the three traits (e.g. pseudospherical dumbbell, PSD, and octopod globular dumbbell, OPD<sub>g</sub>) as well as with industry standard Pt. To conduct electrocatalysis, (Fe)Pt/C inks were created and then immobilized on a rotating-ring disk working electrode. At -0.06 V, the onset potential of the OPD<sub>c</sub> sample is competitive with the Pt standard, and more positive than for other samples [5]. Figure 1 shows mass activity normalized for Pt content at -0.2 V vs. SCE. The OPD<sub>c</sub> performs significantly best. Lastly, ORR can proceed via a 2e<sup>-</sup> or 4e<sup>-</sup> reduction to yield H<sub>2</sub>O<sub>2</sub> or H<sub>2</sub>O respectively. At -0.2 V, there is little difference between the selectivity of each morphology for a 4e<sup>-</sup> reduction.

**Summary.** OPD<sub>c</sub> NPs prepared by our one-pot technique, ensuring good reproducibility and atom efficiency, show very superior activity to industry standard Pt with a minimal compromise in selectivity for H<sub>2</sub>O. Given the combination of morphology and composition control demonstrated, and the benefits of incorporating targeted faceting, high surface area and intermetallic junctions, other multimetallic combinations are now being investigated.

- [1] J. Watt, S. Cheong, R.D. Tilley, *Nano Today* **8** (2013) 198
- [2] S. Chou, C. Zhu, S. Neeleshwar, C. Chen, Y. Chen, C. Chen, *Chem. Mater.* **21** (2009) 4955
- [3] C. Wang, H. Daimon, S. Sun, *Nano Lett.* **9** (2009) 1493
- [4] N. Pazos-Pérez, B. Rodríguez-González, M. Hilgendorff, M. Giersig, L. M. Liz-Marzán, *J. Mater. Chem.* **20** (2010) 61
- [5] K.J. Jenkinson, A. Wagner, N. Kornienko, E. Reisner, A.E.H. Wheatley, *Adv. Funct. Mater.* 2002633 (2020)

**Metal-chalcogenide superatoms for nano p- n- junction with tunable band gaps, adjustable band alignment, and light harvesting**

S. N. Khanna, D. Bista, A. C. Reber, T. Sengupta

Physics Department, Virginia Commonwealth University, Richmond VA 23284-2000, USA  
E-mail: snkhanna@vcu.edu

Organic ligands that protect the surfaces of clusters and nanoparticles against reactions and control the rate of growth are generally considered to be inert passive coatings. I will first demonstrate that ligands can also strongly affect redox properties of clusters. Attaching phosphine ligands to simple metal, noble metal, semiconducting, metal-oxide, and metal-chalcogen clusters is shown to severely reduce ionization energies in all classes of clusters. Several of the simple and noble metal-ligated clusters are transformed into super donors with ionization energies nearly half that of cesium atoms and extremely low second and third ionization energies. The reduction in ionization energy can be split into initial and final state effects. The initial state effect derives in part from the surface dipole but primarily through the formation of bonding/antibonding orbitals that shifts the highest occupied molecular orbital. The final state effect derives from the enhanced binding of the donor ligand to the charged cluster. An opposite effect is observed if the donor ligands are replaced by acceptor ligands including CO. Ligation is shown to be an outstanding strategy for the formation of multiple electron donors/acceptors.

I will then describe how this strategy can be used to develop a new class of p-n junctions. Traditional p-n junctions used for photovoltaics require an interface where a light induced electron-hole pair is separated by an electric field. Developing alternative strategies for forming strong internal electric fields for electron-hole pair separation offers the possibility for better performance. We demonstrate that fusing two superatomic clusters with donor/acceptor ligands on opposite sides of the cluster leads to such a strong internal electric field. In two fused metal-chalcogenide  $\text{Re}_6\text{S}_8\text{Cl}_2(\text{L})_4$  clusters with donor  $\text{PMe}_3$  ligands and acceptor CO ligands on the opposite sides of the fused clusters, the electronic levels undergo shifts analogous to band bending in traditional p-n junctions. The fused cluster has a large dipole moment, and an optical spectrum that strongly absorbs excitation above the HOMO-LUMO gap of the fused clusters, but is optically very weak for the lowest energy excitation that can lead to electron-hole pair recombination. This is because the electron is localized on the CO portion of the fused cluster, while the electron-hole pair is localized on the  $\text{PMe}_3$  side of the cluster. It is shown that the electronic states localized on each side of the cluster can be aligned/misaligned by applying a voltage in different directions, offering diode like characteristics.

Work supported by the US Air Force Office of Scientific Research (AFOSR) under Grant No. FA 9550-18-1-0511 and by US Department of Energy (DOE) under the award DE-SC0006420.

## Probing ultrafast nanoscale dynamics by femtosecond electron imaging

Sascha Schäfer

Institute of Physics, Carl-von-Ossietzky University Oldenburg,  
Carl-von-Ossietzky-Straße 9-11, 26129 Oldenburg, Germany  
E-mail: sascha.schaefer@uni-oldenburg.de

Ultrafast transmission electron microscopy (UTEM) is a highly promising technique which provides access to ultrafast dynamics on nanometer length scales [1]. In UTEM, a pulsed electron beam with sub-picosecond bunch duration is utilized to stroboscopically probe optically triggered processes. Dynamics in structural, electronic and spin degrees of freedom are generally accessible in UTEM by utilizing the versatile imaging and diffraction capabilities of state-of-the-art electron microscopes. However, up to now, the broad applicability of UTEM was limited by the coherence properties of available pulsed electron sources.

In the talk, I will initially focus on the instrumental aspects which allow for the generation of highly coherent electron pulses, achieving electron focal spot sizes down to below one nanometer and pulse durations of about 200 fs [2].

In the second part of the talk, I will provide a brief overview on the broad range of applications accessible by UTEM, including the mapping of ultrafast structural dynamics by local diffractive probing [3], the imaging of ultrafast magnetic dynamics by time-resolved Lorentz microscopy [4,5], and the investigation of coherent interactions of free-electron states with localized optical near-fields and resonant modes [6-8]. Finally, I will address some of the future challenges in the field of ultrafast transmission electron microscopy.

- [1] A. H. Zewail, *Science* **328** (2010) 187
- [2] A. Feist, N. Bach, N. Rubiano da Silva, Th. Danz, M. Möller, K.E. Priebe, T. Domröse, J.G. Gatzmann, S. Rost, J. Schauss, S. Strauch, R. Bormann, M. Sivils, S. Schäfer, C. Ropers, *Ultramicroscopy* **176** (2017) 63
- [3] A. Feist, N. Rubiano da Silva, W. Liang, C. Ropers, S. Schäfer, *Struct. Dynamics* **5** (2018) 014302
- [4] N. Rubiano da Silva, M. Möller, A. Feist, H. Ulrichs, C. Ropers, S. Schäfer, *Phys. Rev. X* **8** (2018) 031052
- [5] M. Möller, J.H. Gaida, S. Schäfer, C. Ropers, *Comm. Phys.* **3** (2020) 1
- [6] A. Feist, K.E. Echternkamp, J. Schauss, S.V. Yalunin, S. Schäfer, C. Ropers, *Nature* **521** (2015) 200
- [7] K.E. Priebe, C. Rathje, S.V. Yalunin, Th. Hohage, A. Feist, S. Schäfer, C. Ropers, *Nature Photonics* **11** (2017) 793
- [8] N. Müller, V. Hock, C. Rathje, H. Koch and S. Schäfer, *ACS Photonics* **8** (2021) 1569

## Laser-generated ultrafast and coherent X-ray sources and their application in nanoscopy

N. A. Papadogiannis<sup>1,2</sup>, S. Petrakis<sup>1,3</sup>, A. Grigoriadis<sup>1,3</sup>, G. Andrianaki<sup>1,4</sup>, I. Tazes<sup>1,5</sup>, A. Skoulakis<sup>1</sup>, Y. Orphanos<sup>1,2</sup>, M. Bakarezos<sup>1,2</sup>, V. Dimitriou<sup>1,2</sup>, E. P. Benis<sup>1,3</sup>, M. Tatarakis<sup>1,5</sup>

<sup>1</sup> Institute of Plasma Physics and Lasers, Hellenic Mediterranean University Research Centre, 74100 Rethymno, Greece

<sup>2</sup> Physical Acoustics and Optoacoustics Laboratory, Department of Music Technology and Acoustics, Hellenic Mediterranean University, 74133 Rethymnon, Greece

<sup>3</sup> Department of Physics, University of Ioannina, 45110 Ioannina, Greece

<sup>4</sup> School of Production Engineering and Management, Technical University of Crete, 73100 Chania, Greece

<sup>5</sup> Department of Electronic Engineering, Hellenic Mediterranean University, 73133, Chania, Greece

E-mails: npapadogiannis@hmu.gr, spetak@hmu.gr, agrigoriadis@hmu.gr, gandrianaki@hmu.gr; g.tazes@hmu.gr; skoulakis@hmu.gr; yorpahnos@hmu.gr; bakarezos@hmu.gr; dimvasi@hmu.gr; mbenis@uoi.gr; mictat@hmu.gr

Although ultrafast laser technology provides today electromagnetic sources in the visible and near-infrared region of spectrum (ultra-short lasers technology), their spatial resolution to probe dynamics in the nanoscale of materials is often very low and the observation capacity is limited by their wavelength. The probe of ultrafast excitation phenomena that occur on the surface or inside the bulk of nano-structured materials, at proper spatial and time scales, requires the development of coherent laser-based secondary sources in the Extreme Ultraviolet (XUV) or (even) in the X-Ray region of spectrum (see Fig. 1 and Fig. 2). These sources offer the ability of monitoring the matter at extremely small spatiotemporal windows.

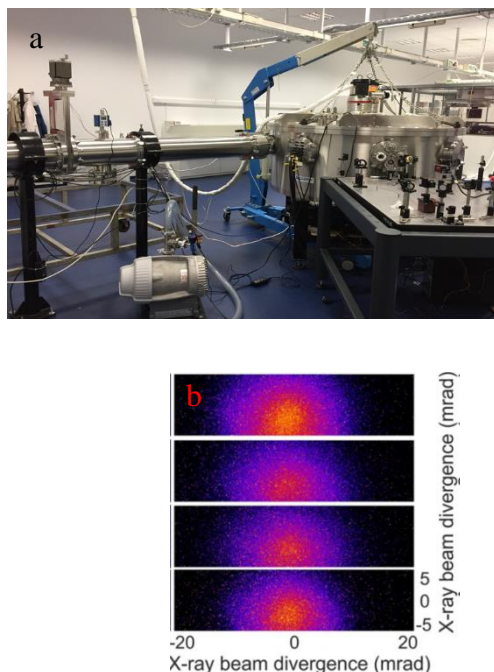


**Figure 1:** (a) The 1m diameter interaction chamber at IPPL laser facility that is used for the generation of coherent betatron-type X-rays and (b) geometrical characteristics of the generated X-rays after the appropriate filtering observed with a X-ray CCD camera.

## “Structure and dynamics of molecules, clusters and nanoparticles”: Fri-I-2

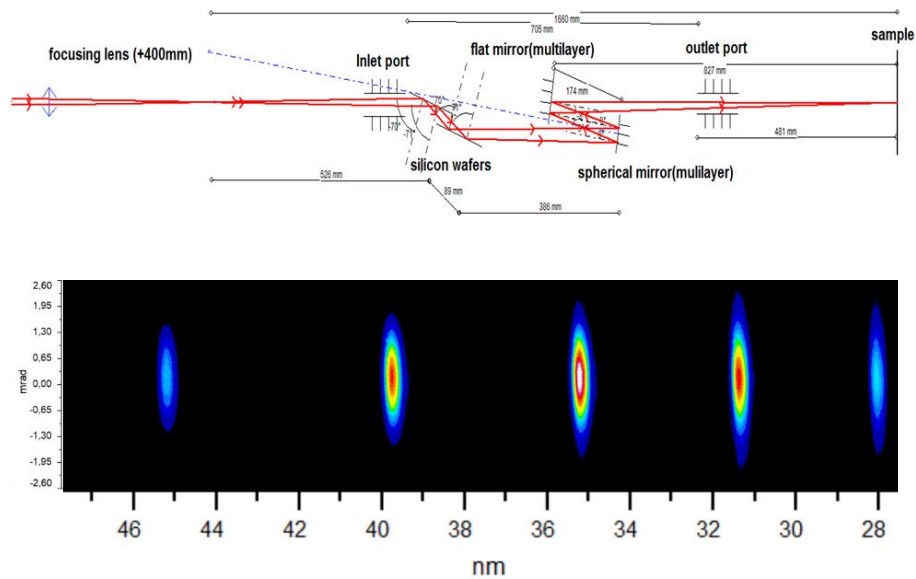


**Figure 2:** The optical set-up for femtosecond high harmonic generation (upper part) and XUV filtering for imaging and the initial measured spectrum of the corresponding XUV harmonic lines (lower part)

Here we present the physics and technology of soft-X-ray novel coherent sources that will be, in our opinion, the future of dynamic imaging of nanostructured materials at small spatial dimensions, much less than a micrometer, and at very short time scales, in the order of femtoseconds or less. These sources are the ultrafast laser XUV high harmonics [1-3] and the laser-plasma betatron-type X-rays generated by relativistic electrons [4,7].

This research has been co-financed by the European Regional Development Fund of the European Union and Greek national funds through the Operational Program Competitiveness, Entrepreneurship and Innovation, under the call RESEARCH –CREATE – INNOVATE (project code: T1EDK-04549, project title: Development of a coherent X-ray multispectral microscopy system) and the Internal Program ELKE/HMU, Institute of Plasma Physics and Laser (project code: 70002).

- [1] N.A. Papadogiannis et al., *Appl. Phys. B* **73** (2001) 687
- [2] A. Willner et al., *New J. Phys.* **13** (2011) 113001
- [3] S. Petrakis et al., *Preprint from Research Square*, 04 Aug 2021, DOI: 10.21203/rs.3.rs-764431/v1
- [4] G. Andrianaki et al., The 22nd International Conference on Ultrafast Phenomena 2020, *OSA Technical Digest*, paper Tu4A.12 (2020)
- [5] I. Tazes et al., *Plasma Phys. Controlled Fusion* **62** (2020) 094005
- [6] A. Grigoriadis et al., *Appl. Phys. Lett.* **118** (2021) 131110
- [7] E.L. Clark et al., *High Power Laser Science and Engineering* (published online by Cambridge University Press: 02 September 2021); DOI: 10.1017/hpl.2021.38

## What happens if phenol meets toluene?

Małgorzata A. Śmiałek

Institute of Naval Architecture and Ocean Engineering  
Faculty of Mechanical Engineering and Ship Technology  
Gdansk University of Technology  
Gabriela Narutowicza 11/12  
80-233 Gdansk, Poland  
E-mail: smialek@pg.edu.pl

Both phenol [1] and toluene [2] are well-known and broadly described in the literature. It is also a well-known fact that characteristic features in the molecular spectra can serve as molecular fingerprints and aid their identification. Hence the idea to measure and to analyse the photoelectron and photoabsorption spectra of the related *o*-, *m*- and *p*-cresol isomers (shown in Fig. 1), also known as methylphenols or hydroxytoluenes. These are toxic compounds, widely used throughout industry as raw materials or in the chlorinated and nitrated forms to yield compounds with herbicidal and insecticidal properties. In other fields of application, *o*-cresol is used in the synthesis of epoxy resins, precursors of dye intermediates, pharmaceuticals and adducts for various synthetic purposes. They are also the basis of fragrance and flavour substances as well as disinfectants, preservatives, explosives and light-resistant antioxidants and dyes. Mixtures of cresols are used as lubricant additives, fire-resistant hydraulic fluids, and plastic additives. They are also formed by biotic and abiotic transformation of pesticides in agriculture. From there they readily contribute to the pollution of ground waters and the atmosphere. In the atmosphere in the presence of NO<sub>x</sub> radicals, the degradation of these compounds in the troposphere contributes substantially to the ozone and photo-oxidant burden and also the formation of secondary organic aerosol. Cresol isomers have been reported to account for 15–42% of the products from the OH + toluene reaction with the level of about 20%.

Thus, obtaining a detailed information on the electronic structure throughout the photoionization measurements of these compounds is desired. To date there is no such information coming from the gas phase studies of cresols. Together with photoabsorption and photoelectron data and support from quantum chemical calculations, it was possible to provide detailed information regarding the electronic structure of these compounds. It is reasonable to expect that the different ring substituents and their position will affect the ionization energy values and electronic structure of both the valence and inner shell electrons of the different species. This in turn will determine their chemical reactivity which involve the frontier orbitals, as well as their subsequent fragmentation [3] and chemical properties due to the interplay between the competing electron-donor and electron-acceptor effects of the hydroxyl- and methyl-substituents. This was recently demonstrated for the nitrotoluene isomers [4], where the correlation patterns between ab-initio calculated proton affinities and core ionization energies has been used to predict site-specific reactivities of polysubstituted molecules. Indeed, core ionization energies measured by X-ray photoelectron spectroscopy (XPS) represent a direct probe of local environment of the different specific site. A similar situation is expected to arise for the cresols isomers, opening up the possibility to extend the approach developed in Ref. [4] and to provide new information on the chemical reactivity of these important molecules.

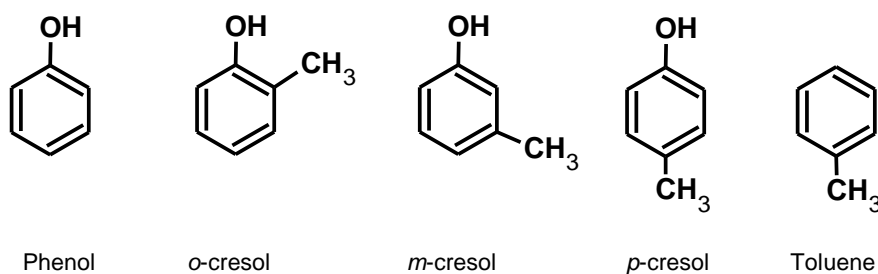


**Figure 1:** Structures of: phenol, toluene and *o*-, *m*- and *p*-cresols.

**“Structure and dynamics of molecules, clusters and nanoparticles”: Fri-I-3**

[1] P. Limao-Vieira et al., *J. Chem. Phys.* **145** (2016) 034302

[2] C. Serralheiro et al., *J. Phys. Chem. A* **119** (2015) 9059

[3] P. Bolognesi et al., *J. Chem. Phys.* **145** (2016) 191102

[4] F. Rondino et al., *RSC Adv.* **4** (2014) 5272

## Phase transition of alanine polypeptides in water

Jonathan Hungerland, Iliia A. Solov'yov

Department of Physics, Carl von Ossietzky Universität Oldenburg  
 Carl-von-Ossietzky Str. 9-11, 26129, Oldenburg, Germany  
 E-mail: jonathan.hungerland@uol.de

Alanine has been shown to have a high helix-propensity [1] and the helix $\leftrightarrow$ coil phase-transition of polyalanine has been thoroughly studied in vacuum [2-5]. In this study, we focus on the effect of solvent on the helix-stability (see Fig. 1) and potential energy surfaces (see Fig. 2) in the scope of molecular dynamics. Similar to previous studies [4], our results show features of a first-order phase-transition. However, studies in vacuum have predicted chain-length-dependend transition-temperatures of about 600 K and above. This is in contrast to typically much lower temperatures for thriving life [6] and also to the limits of even the best adapted organisms, that can only withstand temperatures of nearly 400 K under 400 bar pressure [7]. In other words, protein structures and thus their functionality are expected to be destroyed way below 600 K. Our findings show indeed, that the introduction of water into our system goes along with much lower transition-temperatures of around 360 K for 1 bar and around 420 K for 400 bar (see Fig. 1).

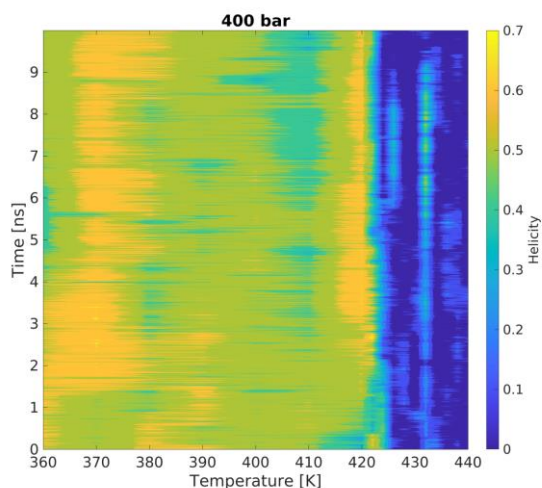


**Fig. 1:** Solvated  $(A)_{40}$  starting as a stable  $\alpha$ -helix-rich structure was simulated with increasing temperature for a total of 170ns at 400bar. From 360K to 420K the temperature was increased by 10K every 10ns, after that by 2K every 10ns. Backbone dihedral angles and hydrogen bonds allow the systematic assignment of helicity to residues. Their number is divided by the total number of residues and the resulting helicity is plotted against simulation-time and temperature.

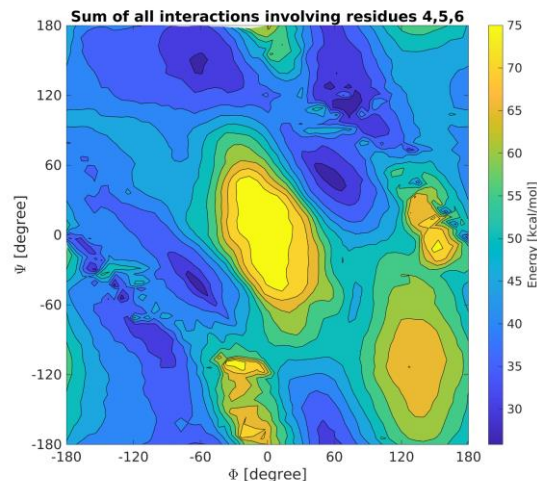


**Fig. 2:** Solvated  $(A)_9$  was simulated with constrained backbone dihedrals  $\Phi$  and  $\Psi$  on the residues 3 to 7. Perturbing either  $\Phi$  or  $\Psi$  by  $6^\circ$  every 2ns for a total of 7200ns simulation time allows the calculation of a statistical potential energy surface describing the twisting motion of the polypeptide. The sum of all bonded and non-bonded interactions involving the atoms of the residues 4,5 and 6 is plotted against the respective dihedral angles.

- [1] K. Fujiwara, H. Toda, M. Ikeguchi, *BMC Structural Biology* **12** (2012) 18
- [2] A. Yakubovich, I.A. Solov'yov, A.V. Solov'yov et al., *Eur. Phys. J. D* **40** (2006) 363
- [3] A. Yakubovich, I.A. Solov'yov, A.V. Solov'yov et al., *Eur. Phys. J. D* **46** (2008) 215
- [4] I.A. Solov'yov, A.V. Yakubovich, A.V. Solov'yov et al., *Eur. Phys. J. D* **46** (2008) 227
- [5] I.A. Solov'yov, A.V. Yakubovich, A.V. Solov'yov, W. Greiner. *Phys. Rev. E* **73** (2006) 021916
- [6] A. Stolz, *Extremophile Mikroorganismen* (Springer Verlag GmbH, 2017)
- [7] K. Takai, K. Nakamura et al., *PNAS* **105** (2008) 10949



## Structural and dynamic characterization of avian cryptochrome 4

Maja Hanić<sup>1</sup>, Anders Frederiksen<sup>1</sup>, Fabian Schuhmann<sup>1</sup>, Corinna Langebrake<sup>2</sup>, Miriam Liedvogel<sup>2</sup>, Jingjing Xu<sup>3</sup>, Henrik Mouritsen<sup>3,4</sup>, and Ilia A. Solov'yov<sup>1</sup>

<sup>1</sup> Department of Physics, Carl von Ossietzky University of Oldenburg, Oldenburg, Germany

<sup>2</sup> Institute of Avian Research, Wilhelmshaven, Germany

<sup>3</sup> Department of Biology and Environmental Sciences, Carl von Ossietzky University of Oldenburg, Oldenburg, Germany

<sup>4</sup> Research Centre for Neurosensory Sciences, Carl von Ossietzky University of Oldenburg, Oldenburg, Germany

Carl-von Ossietzky Str. 9-11, 26129, Oldenburg, Germany

E-mail: maja.hanic@uol.de

In order to migrate migratory animals need to rely on stable cues such as celestial and/or geomagnetic information. It is remarkable that the inclination angle of the Earth's magnetic field vector can be used by birds as a source of a geomagnetic compass. Since the geomagnetic field penetrates biological materials the sensor for the magnetic field could be located anywhere inside an animal's body [1]. Protein that is believed to be involved in magnetic field sensing is called cryptochrome (Cry) [2,3]. Crys are photoreceptors that are known to regulate the entrainment of the circadian clock in plants and animals. The structure of the protein also includes a chromophore cofactor, a flavin adenine dinucleotide (FAD) that triggers its functioning [4]. There are four types of cryptochromes – Cry1a, Cry1b, Cry2 and Cry4 that have been found in the eyes of birds [5,6]. Cry4 in particular was found in the outer segment of double cone cells and long wavelength single cones of birds' eye and was shown to possess unique biochemical properties, unlike other members of the cryptochrome family, making it the best candidate for a magnetic field receptor in migratory birds [6].

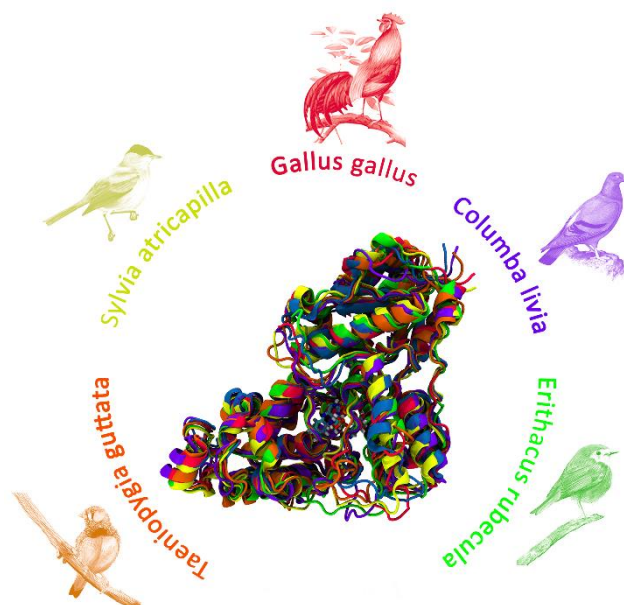


**Figure 1:** Overlaid secondary structures of the Cry4s of the avian species that were modelled: zebra finch (*Taeniopygia guttata*), chicken (*Gallus gallus*), blackcap (*Sylvia atricapilla*), European robin (*Erithacus rubecula*) and a crystal structure of a pigeon (*Columba livia*) [6].

To understand the foundation of cryptochrome magnetic field sensing and unravel its biophysics it is imperative to have the structure of the protein. Currently the only Cry4 crystal structure available is that of a non-migratory bird, pigeon (*Columba livia*) [7]. It is fortunate that in order to elucidate the molecular sensory biology behind the magnetic field sensing in migratory birds, homology models can be used. Homology modeling is a computational process in which a 3D protein structure can be constructed by using

## “Structure and dynamics of nanosystems”: Fri-II-2

the structure of another, similar protein, as a template [8]. In this investigation homology models of birds' Cry4 from migratory birds (European robin and Blackcap) and non-migratory bird species (Chicken and Zebra finch) have been constructed and studied (Fig 1. shows an overlay of all the mentioned structures). With thorough molecular dynamics simulation and structural analysis we justify the correctness of the obtained structures and perform a detailed structural comparison of Cry4 from different bird species. The comparison reveals little structural difference of various Cry4. With this investigation we hope to get a deeper insight into protein dynamics that is important for magnetic sensing in migratory birds vs. non-migratory birds.

- [1] H. Mouritsen, *Nature* **558** (2018) 50
- [2] D.R. Kattinig, J.K. Sowa, I.A. Solov'yov, and P.J. Hore, *New J. Phys.* **18** (2016) 063007
- [3] J. Xu, L.E. Jarocha, T. Zollitsch et al., *Nature* **594** (2021) 535
- [4] E. Sjulstok and I.A. Solov'yov, *J. Phys. Chem. Lett.* **11** (2020) 3866
- [5] R. Wiltshko, W. Wiltshko, *J. R. Soc. Interface* (2019)
- [6] A. Günther et al., *Current Biology* **28** (2018) 211
- [7] B.D. Zoltowski et al., *PNAS* **116** (2019) 19449
- [8] T. Schwede, J. Kopp, N. Guex, M.C. Peitsch, *Nucl. Acids Res.* **31** (2003) 3381

## From kinetic trapping to equilibration in the coalescence of elemental and bimetallic nanoparticles

Diana Nelli<sup>1</sup>, Giulia Rossi<sup>1</sup>, Zhiwei Wang<sup>2</sup>, Richard E. Palmer<sup>2</sup>, Manuella Cerbelaud<sup>3</sup>,  
Chloé Minnai<sup>4</sup> and Riccardo Ferrando<sup>1</sup>

<sup>1</sup>Physics Department, Università di Genova,  
via Dodecaneso 33, 16146, Genova, Italy  
E-mail: nelli@fisica.unige.it

<sup>2</sup>College of Engineering, Swansea University,  
Bay Campus, Fabian Way, SA1 8EN, Swansea, UK

<sup>3</sup>CNRS IRCER, Université de Limoges,  
UMR 7315, F-87000, Limoges, France

<sup>4</sup>Okinawa Institute of Science and Technology Graduate University,  
1919-1 Tancha, 904-0495, Onna-son, Kunigami-gun, Okinawa, Japan

Coalescence is often an important step in the growth of nanoparticles, both in liquid and in the gas phase. In coalescence, two preformed clusters collide and merge to form a larger aggregate, whose shape evolves from an initial configuration, which is strongly out of equilibrium, towards more compact structures. This kind of equilibration process is often rather complex: the coalescence velocity and final outcome are influenced by the initial features of the colliding units, such as their geometric structure and relative size; in addition, kinetic trapping effects can take place, so that peculiar out-of-equilibrium structures can be observed in the experiments. Here molecular dynamics simulations are employed to shed light on the key aspects of coalescence, in the case of both elemental and bimetallic nanoparticles.

In the first case, we simulate the coalescence of pure Au clusters in vacuum. The two colliding units have the same size (147 atoms) and different geometric structures: decahedron (Dh), truncated octahedron (TO) and icosahedron (Ih). All possible types of collision are considered, and, in the case of Dh-TO and TO-TO collisions, we also consider different mutual orientation of the colliding clusters. Our simulations reveal a persistent influence of the structure and relative orientation of the colliding clusters on the final coalesced aggregate: while a compact shape is always achieved at the end of the simulations, the obtained geometric structure depends on the type of collision in a statistically significant way [1].

In the second case, we study the coalescence of PtPd nanoalloys. The colliding units are a pure Pd nanoparticle and a core@shell (PtPd)@Pd nanoparticle of similar size; both nanoparticles have truncated octahedral shape. Our simulations allow us to distinguish four different steps through which coalescence proceeds towards equilibrium, occurring at well-separated time scales: (i) alignment of the atomic columns of the two subunits; (ii) alignment of close-packed atomic planes; (iii) equilibration of the shape of the coalesced aggregate; (iv) equilibration of chemical ordering. Due to the slower equilibration of chemical ordering compared to geometric shape, peculiar configurations are obtained, with compact quasi-spherical shape and off-centered PtPd core, which are unlikely to be formed during atom-by-atom growth. The results of our molecular dynamics simulations are in agreement with experimental observations of PtPd nanoalloys grown in the gas phase [2].

[1] D. Nelli, G. Rossi, Z. Wang, R. E. Palmer and R. Ferrando, *Nanoscale* **12** (2020) 7688

[2] D. Nelli, M. Cerbelaud, R. Ferrando and C. Minnai, *Nanoscale Advances* **3** (2021) 836

## On structure prediction of proteins with alphafold and traditional methods

Georg Manthey, Ilia A. Solov'yov

Institute for Physics, University of Oldenburg  
Carl-von-Ossietzky-Str. 9-11, 26129, Oldenburg, Germany  
E-mail: georg.manthey@uni-oldenburg.de

Deepmind has recently released a new version of Alphafold, which was presented during CASP14 showing unprecedented accuracy on protein structure prediction tasks [1]. Alphafold roots upon the machine learning approach and has learned the protein structures prediction task using hundreds of thousands of proteins from the protein data bank [2]. We have evaluated the performance of Alphafold on a specific class of photoreceptors called Cryptochromes. Cryptochromes are seen as potential candidates for endowing migratory birds with the magnetic compass sense [3]. While some structures are available in the protein data bank, some others so far were generated by classical homology modelling.

We used Alphafold to predict the structure of different Cryptochromes from European robin and Rock dove and compared the output to structures generated by X-ray crystallography where available and homology models where crystal structures are lacking. While Alphafold predicts a global structure similar to classical methods, it shows some deviations in the local structure, especially when compared to homology models. A short molecular dynamics simulation of the structures obtained using Alphafold and conventional homology modelling revealed that the structure predicted by Alphafold was more stable, as indicated through lower values of the root mean square displacement (RMSD) of the protein backbone when excluding the C-Terminus (see Fig. 1). This part of the protein is absent in the homology model and is expected to be very flexible, which was also observed during the simulation.

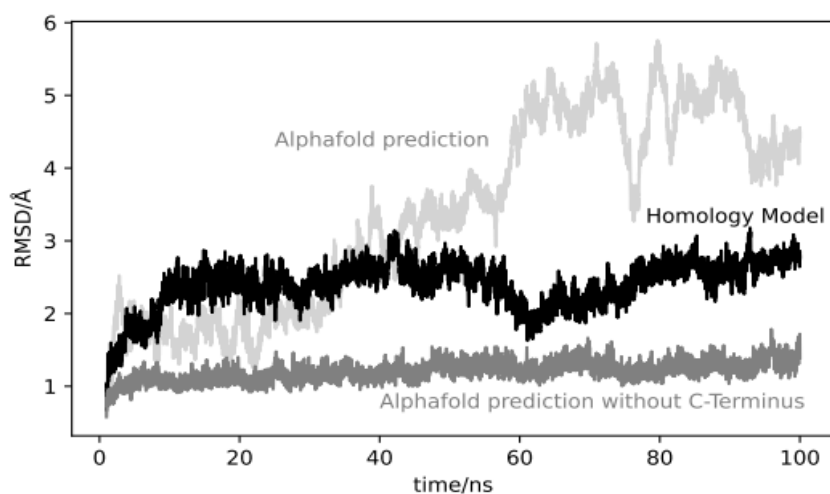


**Figure 1:** Root mean square displacement (RMSD) of Cryptochrome 4 of the European robin from different structure predictors. The structure predicted by Alphafold (light grey) shows higher RMSD values, but when removing the C-Terminus from the calculation (grey) the RMSD values are lower than the structure generated by the Homology Model (black).

With this work we show that Alphafold can provide stable structures for a system where some homologs are available, outperforming conventional homology models. At the same time Alphafold can give insights to structural parts that are absent in crystal structures, as for example the C-Terminus in Cryptochrome 4.

[1] J. Jumper et al., *Nature* **595** (2021) 583

[2] Protein Data Bank: the single global archive for 3D macromolecular structure data. wwPDB consortium, *Nucl. Acids Res.* **47** (2019) 520

[3] P.J. Hore and H. Mouritsen, *Annu. Rev. Biophys.* **45** (2016) 299

## Microscopic formation mechanisms of multiply twinned gold nanoparticles from tetrahedral seed

E. El Koraychy<sup>1</sup>, Cesare Roncaglia<sup>1</sup>, Diana Nelli<sup>1</sup>, Manuella Cerbelaud<sup>2</sup>, and Riccardo Ferrando<sup>3</sup>

<sup>1</sup>Dipartimento di Fisica dell’Università di Genova, via Dodecaneso 33, 16146 Genova, Italy,

<sup>2</sup>Université de Limoges, CNRS, IRCER, UMR 7315, F-87000 Limoges, France

<sup>3</sup>Dipartimento di Fisica dell’Università di Genova and CNR-IMEM, via Dodecaneso 33, Genova 16146, Italy

E-mail: elkoraychy@fisica.unige.it

Gold nanoparticles have a variety of current and potential applications in areas such as catalysis, bio-sensing and drug-delivery. Both the size and structure of these particles influence their properties; therefore, it is important to understand their microscopic formation mechanisms. It is believed that gold nanoparticle can form crystalline structures and noncrystalline structures such as Icosahedra and Decahedra, which are known as multiply twinned structures [1]. The synthesis of these multiply twinned structures, with precise control over the shape and morphology, remains quite challenging due to their complex growth and multiple competitive growth pathways. Despite previous successes, however, several issues in the detailed growth pathway of multiple twinned nanoparticles remain incomplete [2]. To gain further insight in this framework, a quantitative study using computer simulations is required since they allow to obtain a more comprehensive understanding of the formation mechanisms. In this work, we study the growth process of multiply twinned gold nanoparticles starting from tetrahedral seeds, in particular decahedra and icosahedra, in the gas phase through molecular dynamics simulations. Nucleation of clusters of atoms and subsequent growth to form multiply twinned nanoparticles are analyzed. Our analysis shows that the transition from tetrahedral structure to decahedral or icosahedral shape requires the formation of metastable defects on the (111) tetrahedral facets and their stabilization. However, the finale shape of twinned nanoparticles is strongly dependent on the number of stable defects on the preexisting (111) surfaces of tetrahedral seed and their relative growth rates.

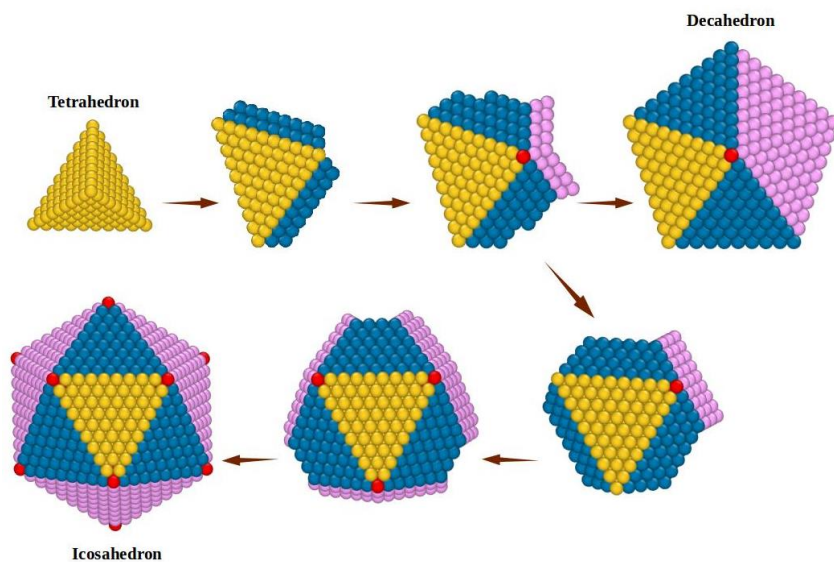


**Figure 1:** Cartoons showing the stepwise evolution of multiply twinned gold nanoparticles from tetrahedral seeds

[1] D. Bochicchio and R. Ferrando, *Nano Lett.* **10** (2010) 4211

[2] J.S. Du, W. Zhou, S.M. Rupich, C.A. Mirkin, *Angew. Chem. Int. Ed.* **60** (2021) 6858

## Computational approach for 3D reconstruction of missing protein fragments

Fabian Schuhmann, Ilia A. Solov'yov

Department of Physics, Carl von Ossietzky Universität Oldenburg  
Carl-von-Ossietzky Str. 9-11, 26129, Oldenburg, Germany  
E-mail: fabian.schuhmann@uol.de

A brief inspection of several randomly chosen crystal structures of proteins deposited in the protein data bank (PDB) reveals that often proteins are crystallized with certain fragments missing, while the sequence of these proteins are well characterized. For instance, the recently published pigeon cryptochrome 4 structure [1], is missing residues 228 to 244 as well as the C-terminal tail (residues 498 to 527). Similarly, the european robin cryptochrome 4 [2] is missing 28 of its residues at the end. This particular latter protein is yet to be crystallized, but can nevertheless be constructed through homology modeling. It is striking however, that even in that case, the N-terminal and the C-terminal of the protein could not be reconstructed due to the missing molecular template. Some other examples include the cattle rhodopsin [3] which is missing the last 26 amino acid residues from the crystal structure, the zebra fish RNase5 [4] which is missing the last eight residues or the fruit fly eukaryotic origin recognition complex [5] which is missing 399 residues spread over all crystallized chains. Naturally, one has to assume that those missing parts have a role in the biophysical function of the proteins. One can provide a long list of further examples, as missing fragments in protein structures appear frequently.

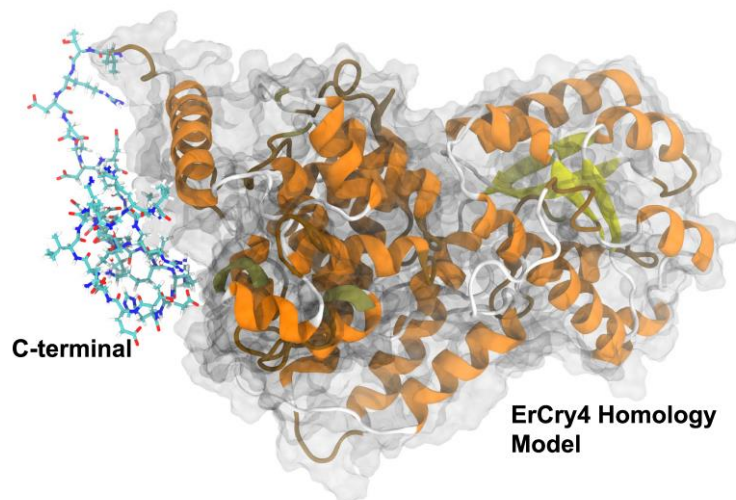


**Figure 1:** A european robin cryptochrome 4 homology model [8] with a computationally reconstructed c-terminal.

The dilemma could partially be addressed computationally. In order to make suggestions about the structure of the missing protein parts, they need to be constructed according to biochemical rules which can be a complex task, because it is necessary to guess the correct positions of the individual amino acid residues as well as to consider possible folding motifs and avoid steric collisions between atoms. Here, we present a program that utilizes a Monte-Carlo algorithm to construct 3D structures of polypeptide chains which could then be studied as stand-alone macro-molecules, or compliment the structure of known proteins. Using an algorithm to avoid steric clashes, the proposed approach allows to create multiple structures for the same predefined primary sequence of amino acids. These structures could then effectively be used for further analysis and investigation. We will illustrate the algorithm and describe its user-friendly approach that was made possible through the VIKING online platform [6]. Finally, we will provide several highlight examples where the program was used to predict the structure of the C-terminal of a known protein, generate a missing bit of already crystallized protein structures and simply generate short polypeptide chains [7], see Figure 1.

## “Structure and dynamics of nanosystems”: Fri-II-6

- [1] B. Zoltowski, Y. Chelliah, A. Wickramaratne, L. Jarocho, N. Karki, W. Xu, H. Mouritsen, P. Hore, R. Hibbs, C. Green, and J.S. Takahashi, *PNAS* **116** (2019) 19499
- [2] A. Günther, A. Einwich, E. Sjulstok, R. Feederle, P. Bolte, K. Koch, I.A. Solov'yov, and H. Mouritsen, *Current Biology* **28** (2018) 211
- [3] J. Park, P. Scheerer, K. Hofmann, H.W. Choe, and O. Ernst, *Nature* **454** (2008) 183
- [4] E. Pizzo, A. Merlino, M. Turano, I. Krauss Russo, F. Coscia, A. Zanfardino, M. Varcamonti, A. Furia, C. Giancola, L. Mazarella, F. Sica, and G. D'Alessio, *Biochem. J.* **433** (2010) 345
- [5] F. Bleichert, M. Botchan, and J. Berger, *Nature* **519** (2015) 321
- [6] V. Korol, P. Husen, E. Sjulstok, C. Nielsen, A. Frederiksen, A. Bogh Salo, I.A. Solov'yov, *ACS Omega* **5** (2020) 1254
- [7] F. Schuhmann, V. Korol, I.A. Solov'yov, *J. Comput. Chem.* **42** (2021) 572

## Cryptochrome magnetoreception: Four tryptophans could be better than three

Siu Ying Wong<sup>1</sup>, Yujing Wei<sup>2</sup>, Henrik Mouritsen<sup>3</sup>, Iliia A. Solov'yov<sup>1</sup> and P. J. Hore<sup>2</sup>

<sup>1</sup> Institut für Physik, Carl-von-Ossietzky Universität Oldenburg,  
26129 Oldenburg, Germany  
E-mail: siu.ying.wong@uni-oldenburg.de

<sup>2</sup> Department of Chemistry, University of Oxford,  
Oxford OX1 3QZ, United Kingdom

<sup>3</sup> Institut für Biologie und Umweltwissenschaften, Carl-von-Ossietzky Universität Oldenburg,  
26111 Oldenburg, Germany

The biophysical mechanism of the magnetic compass sensor in migratory songbirds is thought to involve photo-induced radical pairs formed in cryptochrome (Cry) flavoproteins located in photoreceptor cells in the eyes [1]. In Cry4a, the most likely of the six known avian cryptochromes to have a magnetic sensing function, four radical pair states are formed sequentially by the stepwise transfer of an electron along a chain of four tryptophan residues to the photo-excited flavin. In purified Cry4a from the migratory European robin, the third of these flavin-tryptophan radical pairs is more magnetically sensitive than the fourth, consistent with the shorter radical-radical separation of the former [2]. Here, we explore the idea that these two radical pair forms of Cry4a could exist in rapid dynamic equilibrium such that the key magnetic and kinetic properties are weighted averages of the two states. Spin dynamics simulations suggest that the third radical pair is largely responsible for magnetic sensing while the fourth is better placed to initiate magnetic signalling, especially if the terminal tryptophan radical is reduced by a nearby tyrosine. Such an arrangement could have allowed independent optimisation of the essential sensing and signalling functions of the protein. It might also rationalise why avian Cry4a has four tryptophans while cryptochromes from plants have only three.

[1] P.J. Hore and H. Mouritsen, *Annu. Rev. Biophys.* **45** (2016) 299

[2] J. Xu, L.E. Jarocha, T. Zollitsch, M. Konowalczyk, K.B. Henbest, S. Richert, M.J. Golesworthy, J. Schmidt, V. Déjean, D.J.C. Sowood, et al., *Nature* **594** (2021) 535



## List of Participants

	<b>Surname</b>	<b>Name</b>	<b>Affiliation</b>	<b>E-mail</b>
1	Abdoul-Carime	Hassan	Université Université Lyon 1, Lyon, France	hcarime@ipnl.in2p3.fr
2	Antoine	Rodolphe	Institut Lumière Matière & Université Lyon 1, Villeurbanne cedex, France	rodolphe.antoine@univ-lyon1.fr
3	Backe	Hartmut	Institute for Nuclear Physics, Johannes Gutenberg-University, Mainz, Germany	backe@uni-mainz.de
4	Bald	Ilko	Institute of Chemistry, University of Potsdam, Potsdam, Germany	bald@uni-potsdam.de
5	Bari	Sadia	Deutsches Elektronen-Synchrotron DESY, Hamburg, Germany	sadia.bari@desy.de
6	Beleggia	Marco	DTU Nanolab, Technical University of Denmark, Kgs. Lyngby, Denmark	mabele@dtu.dk
7	Bromley	Stefan	Dept. Materials Science and Physical Chemistry, Univ. Barcelona, Spain	s.bromley@ub.edu
8	Campbell	Eleanor	School of Chemistry, University of Edinburgh, Edinburgh, Scotland	eleanor.campbell@ed.ac.uk
9	Chakraborty	Himadri	Northwest Missouri State University, Maryville, Missouri, USA	himadri@nwmissouri.edu
10	De Salvador	Davide	Dipartimento di Fisica e Astronomia, Università di Padova, Italy	davide.desalvador@unipd.it
11	de Vera	Pablo	European Centre for Theoretical Studies in Nuclear Physics and Related Areas (ECT*-FBK), Trento, Italy	pdeveragomis@ectstar.eu
12	El Koraychy	El Yakout	Department of Physics, University of Genoa, Genoa, Italy	elkoraychy@fisica.unige.it
13	Fabrikant	Ilya	University of Nebraska-Lincoln, Lincoln, Nebraska, USA	ifabrikant@unl.edu
14	Falk	Martin	Institute of Biophysics of CAS, Brno, Czech Republic	falk@ibp.cz
15	Falková	Iva	Institute of Biophysics of CAS, Brno, Czech Republic	ivafalk@seznam.cz
16	Fedor	Juraj	J. Heyrovský Institute of Physical Chemistry, Prague, Czech Republic	juraj.fedor@jh-inst.cas.cz
17	Ferrando	Riccardo	Department of Physics, University of Genoa, Genoa, Italy	ferrando@fisica.unige.it
18	Ferreira da Silva	Filipe	Universidade NOVA de Lisboa, Caparica, Portugal	f.ferreiradasilva@fct.unl.pt
19	Frederiksen	Anders	Carl von Ossietzky University of Oldenburg, Oldenburg, Germany	anders.frederiksen@uol.de
20	Grüning	Gesa	Carl von Ossietzky University of Oldenburg, Oldenburg, Germany	gesa.gruening@uol.de
21	Guidi	Vincenzo	Department of Physics and Earth Sciences, University of Ferrara, Italy	guidi@fe.infn.it
22	Hahn	Marc Benjamin	Bundesanstalt für Materialforschung und -prüfung (BAM), Berlin, Germany	marc-benjamin.hahn@bam.de
23	Hailey	Perry	University of Kent, Canterbury, United Kingdom	pah35@kent.ac.uk
24	Hanić	Maja	Carl von Ossietzky University of Oldenburg, Oldenburg, Germany	maja.hanic@uol.de
25	Hungerland	Jonathan	Carl von Ossietzky University of Oldenburg, Oldenburg, Germany	jonathan.hungerland@uol.de
26	Khanna	Shiv	Virginia Commonwealth University, Richmond, VA, USA	snkhanna@vcu.edu
27	Korol	Andrei	MBN Research Center, Frankfurt am Main, Germany	korol@mbnexplorer.com

28	Kretschmer	Katarina	Carl von Ossietzky University of Oldenburg, Oldenburg, Germany	katarina.kretschmer@uni-oldenburg.de
29	Lauth	Werner	Institute for Nuclear Physics, Johannes Gutenberg-University, Mainz, Germany	Lauthw@uni-mainz.de
30	Manthey	Georg	Carl von Ossietzky University of Oldenburg, Oldenburg, Germany	georg.manthey@uni-oldenburg.de
31	Mason	Nigel	University of Kent, Canterbury, United Kingdom	N.J.Mason@kent.ac.uk
32	Mertig	Michael	Institute of Physical Chemistry, TU Dresden, Germany	michael.mertig@tu-dresden.de
33	Mifsud	Duncan	University of Kent, Canterbury, United Kingdom	duncanvmifsud@gmail.com
34	Nelli	Diana	Department of Physics, University of Genoa, Genoa, Italy	nelly@fisica.unige.it
35	Papadogiannis	Nektarios	Hellenic Mediterranean University Research Centre, Rethymno, Greece	npapadogiannis@hmu.gr
36	Plank	Harald	Institute of Electron Microscopy and Nanoanalysis, TU Graz, Austria	harald.plank@felmi-zfe.at
37	Prosvetov	Alexey	MBN Research Center, Frankfurt am Main, Germany	prosvetov@mbnexplorer.com
38	Ricketts	Kate	University College London, United Kingdom	k.ricketts@ucl.ac.uk
39	Romagnoni	Marco	Università degli Studi di Milano, Milan & INFN, Ferrara, Italy	marco.romagnoni@unimi.it
40	Roncaglia	Cesare	Department of Physics, University of Genoa, Genoa, Italy	roncaglia@fisica.unige.it
41	Schlathölter	Thomas	University of Groningen, Zernike Institute for Advanced Materials, Groningen, The Netherlands	t.a.schlatholter@rug.nl
42	Schuhmann	Fabian	Carl von Ossietzky University of Oldenburg, Oldenburg, Germany	fabian.schuhmann@uol.de
43	Schäfer	Sascha	Carl von Ossietzky University of Oldenburg, Oldenburg, Germany	sascha.schaefer@uni-oldenburg.de
44	Śmiałek-Telega	Małgorzata	Gdansk University of Technology, Gdansk, Poland	smialek@pg.edu.pl
45	Solov'yov	Andrey	MBN Research Center, Frankfurt am Main, Germany	solovyov@mbnresearch.com
46	Solov'yov	Iliia	Carl von Ossietzky University of Oldenburg, Oldenburg, Germany	ilia.solovyov@uni-oldenburg.de
47	Solovyeva	Irina	MBN Research Center, Frankfurt am Main, Germany	irina@mbnexplorer.com
48	Surraud	Eric	Université Paul Sabatier, Toulouse, France	surraud@irsamc.ups-tlse.fr
49	Taioli	Simone	European Centre for Theoretical Studies in Nuclear Physics and Related Areas (ECT*-FBK), Trento, Italy	taioli@ectstar.eu
50	Teusch	Thomas	Carl von Ossietzky University of Oldenburg, Oldenburg, Germany	thomas.teusch@uol.de
51	Tran Thi	Thu Nhi	European Synchrotron Radiation Facility, Grenoble, France	thu-nhi.tran-thi@esrf.fr
52	Verkhovtsev	Alexey	MBN Research Center, Frankfurt am Main, Germany	verkhovtsev@mbnexplorer.com
53	Wheatley	Andrew	Dept. of Chemistry, University of Cambridge, United Kingdom	aehw2@cam.ac.uk
54	Wong	Siu Ying	Carl von Ossietzky University of Oldenburg, Oldenburg, Germany	siu.ying.wong@uni-oldenburg.de
55	Ziaja-Motyka	Beata	Center for Free-Electron Laser Science, DESY, Hamburg, Germany	ziaja@mail.desy.de

**For notes**

**Monday, October 18 (DySoN-related sessions)**

10 <sup>00</sup> – 14 <sup>00</sup>	Participants registration
14 <sup>00</sup> – 14 <sup>15</sup>	<b>DySoN-ISACC 2021 Opening</b> <b>V. Guidi, N.J. Mason, A.V. Solov'yov</b>
14 <sup>15</sup> – 15 <sup>45</sup>	<u>Afternoon session I: Dynamics of systems on the nanoscale</u> <b>Andrey Solov'yov / Eleanor Campbell / Beata Ziaja-Motyka</b>
15 <sup>45</sup> – 16 <sup>15</sup>	<b>Coffee break</b>
16 <sup>15</sup> – 17 <sup>45</sup>	<u>Afternoon session II: Structure and dynamics of molecules, clusters and nanoparticles</u> <b>Riccardo Ferrando / Rodolphe Antoine / Stefan Bromley</b>
19 <sup>00</sup> – 22 <sup>00</sup>	<b>Welcome reception</b>

**Tuesday, October 19 (DySoN-related sessions)**

9 <sup>30</sup> – 11 <sup>00</sup>	<u>Morning session I: Cluster and biomolecular ensembles, composite systems</u> <b>Ilko Bald / Michael Mertig / Ilia Solov'yov</b>
11 <sup>00</sup> – 11 <sup>30</sup>	<b>Coffee break</b>
11 <sup>30</sup> – 13 <sup>00</sup>	<u>Morning session II: Irradiation-driven processes and technologies involving Meso-Bio-Nano systems</u> <b>Nigel Mason &amp; Perry Hailey / Marco Beleggia / Harald Plank</b>
13 <sup>00</sup> – 14 <sup>30</sup>	<b>Lunch</b>
14 <sup>30</sup> – 16 <sup>00</sup>	<u>Afternoon Session I: Radiation-induced chemistry</u> <b>Pablo de Vera / Alexey Prosvetov / Duncan Mifsud</b>
16 <sup>00</sup> – 16 <sup>30</sup>	<b>Coffee break</b>
16 <sup>30</sup> – 18 <sup>00</sup>	<u>Afternoon Session II: Structure and dynamics of molecules, clusters and nanoparticles</u> <b>Filipe Ferreira da Silva / Cesare Roncaglia / Iva Falková / Anders Frederiksen / Gesa Grüning</b>

**Wednesday, October 20 (DySoN-related sessions)**

9 <sup>30</sup> – 11 <sup>00</sup>	<u>Morning session I: Interaction of radiation with biomolecular systems: mechanisms and applications</u> <b>Simone Taioli / Marc Benjamin Hahn / Thomas Schlathölter</b>
11 <sup>00</sup> – 11 <sup>30</sup>	<b>Coffee break</b>
11 <sup>30</sup> – 13 <sup>00</sup>	<u>Morning session II: Interaction of radiation with bio-systems: mechanisms and applications</u> <b>Martin Falk / Alexey Verkhovtsev / Kate Ricketts</b>

13 <sup>00</sup> – 13 <sup>15</sup>	<b>Conference photo</b>
13 <sup>15</sup> – 14 <sup>30</sup>	<b>Lunch</b>
14 <sup>30</sup> – 16 <sup>00</sup>	<u>Afternoon session I: Propagation of particles through media</u> <b>Andrei Korol / Hartmut Backe / Werner Lauth</b>
16 <sup>00</sup> – 16 <sup>30</sup>	<b>Coffee break</b>
16 <sup>30</sup> – 18 <sup>00</sup>	<u>Afternoon session II: Design and practical realization of novel gamma-ray crystal-based light sources</u> <b>Marco Romagnoni / Davide De Salvador / Thu Nhi Tran Thi</b>
19 <sup>00</sup> – 22 <sup>30</sup>	<b>Conference dinner</b>

**Thursday, October 21 (ISACC-related sessions)**

9 <sup>30</sup> – 11 <sup>00</sup>	<u>Morning session I: Collision and radiation-induced processes</u> <b>Ilya Fabrikant / Sadia Bari / Eric Suraud</b>
11 <sup>00</sup> – 11 <sup>30</sup>	<b>Coffee break</b>
11 <sup>30</sup> – 13 <sup>00</sup>	<u>Morning session II: Electron and photon cluster collisions</u> <b>Juraj Fedor / Himadri Chakraborty / Hassan Abdoul-Carime</b>
13 <sup>00</sup> – 14 <sup>30</sup>	<b>Lunch</b>
14 <sup>30</sup> – 16 <sup>00</sup>	<b>Free time / Conference walk through SML</b>
16 <sup>00</sup> – 16 <sup>30</sup>	<b>Coffee break</b>
16 <sup>30</sup> – 18 <sup>00</sup>	<u>Afternoon Session I: Cluster-molecule interactions, reactivity and nanocatalysis</u> <b>Vincenzo Guidi / Andrew Wheatley / Shiv Khanna</b>

**Friday, October 22 (ISACC-related sessions)**

9 <sup>30</sup> – 11 <sup>00</sup>	<u>Morning session I: Structure and dynamics of molecules, clusters and nanoparticles</u> <b>Sascha Schäfer / Nektarios Papadogiannis / Malgorzata Smialek-Telega</b>
11 <sup>00</sup> – 11 <sup>30</sup>	<b>Coffee break</b>
11 <sup>30</sup> – 13 <sup>15</sup>	<u>Morning session II: Structure and dynamics of nanosystems</u> <b>Jonathan Hungerland / Maja Hanić / Diana Nelli / Georg Manthey / El Yakout El Koraychy / Fabian Schuhmann / Siu Ying Wong</b>
13 <sup>15</sup> – 13 <sup>30</sup>	<b>DySoN-ISACC 2021 Closing</b>